VOT 74173

DEVELOPMENT OF ASYMMETRIC CARBON HOLLOW FIBER MEMBRANE FOR GAS SEPARATION.

(PEMBANGUNAN MEMBRAN GENTIAN GERONGGANG KARBON ASIMETRIK UNTUK PEMISAHAN GAS)

AZEMAN MUSTAFA. et. al

RESEARCH VOT NO : 74173

MEMBRANE RESEARCH UNIT
FACULTY OF CHEMICAL AND NATURAL RESOURCES ENGINEERING, UNIVERSITI TEKNOLOGI MALAYSIA

2006

DEDICATION

Thanks to all members in MRU and FKKKSA staff who have given me a substantial assistance and moral support in completing this project.

ACKNOWLEDMENT

I would like to express my grateful thanks for the help and advice given to me by Research Management Centre especially to Prof. Dr. Ariffin Samsuri and to all staff at RMC.

Special thanks to all the members of Membrane Research Unit (MRU) and FKKKSA staff who have given me a substantial assistance and moral support in completing this project. Gratitude is due to all the lecturers who have given me their opinion and advice. Without their encouragement and faith, this project might have remained just another dream.

Last but not least, thanks go to MOSTI for financial support through the IRPA funding and also in providing me such good environment for this project.

ABSTRAK

Objektif penyelidikan ini ialah membangunkan membran gentian geronggang karbon asimetrik yang baru dan mencirikan prestasi pemisahan gas serta morfologi membran karbon yang terhasil. Poliackrylonitril (PAN) telah dipilih sebagai bahan mentah membran karbon. Membran gentian geronggang dihasilkan melalui proses pemintalan kering/basah. Proses pirolisis dengan gas lengai digunakan untuk penghasilan membran karbon gentian geronggang daripada membran gentian geronggang PAN. Pencirian membran karbon dijalankan dengan pengukuran kebolehtelapan gas tulen, Mikroskopi Imbasan Electron (SEM), Spektroskopi Inframerah Transformasi Fourier (FTIR) dan Analisis Termogravimetri (TGA). Pengaruh keadaan pirolisis ke atas prestasi membran karbon telah dikaji. Parameter pirolisis yang telah dikaji termasuk suhu pirolisis, jangka masa pemanasan dan kadar alir gas cucikan. Keputusan ujikaji menunjukkan bahawa suhu pirolisis pada 700°C dan 800°C boleh meningkatkan kememilihan O_2/N_2 daripada 1.1 kepada 1.85 manakala kebolehtelapan tertinggi O_2 iaitu 480 GPU dicapai pada suhu 600°C. Walaupun kememilihan sebanyak 3.1 dicapai pada suhu 250°C, membran tersebut masih bukan membran karbon yang tulen. Jangka masa pemanasan yang lebih panjang meningkatkan kememilihan daripada 1.1 kepada 1.8 dengan peningkatan kebolehtelapan pada peringkat awal. Penurunan kebolehtelapan berlaku apabila masa pemanasan 180 minit digunakan. Membran yang dipanaskan selama 10 minit menunjukkan kememilihan yang tinggi iaitu 3.7 dengan kebolehtelapan yang lebih rendah daripada membran PAN. Walaupun, kadar alir gas cucikan yang tinggi meningkatkan kebolehtelapan O_2 dan N_2 dalam julat daripada 50 hingga 130 GPU kepada 150 hingga 730 GPU tanpa mempengaruhi kememilihannya. Oleh itu, keadaan pirolisis mempunyai pengaruh yang ketara terhadap membran gentian geronggang karbon asimetrik untuk pemisahan gas.

ABSTRACT

The objective of this research is to develop a novel asymmetric carbon hollow fiber membrane and to characterize it's gas separation performance and morphology. Polyacrylonitrile (PAN) was chosen as the precursor for carbon membranes. The hollow fiber membranes were produced using the dry/wet spinning process. PAN hollow fiber membranes were converted to carbon hollow fiber membranes with inert gas pyrolysis process. Carbon hollow fiber membranes were characterized by pure gas permeation measurement, Scanning Electron Microscopy (SEM), Fourier Transform Infrared Spectroscopy (FTIR) and Thermogravimetry Analysis (TGA). The influence of the pyrolysis conditions on carbon membrane performance was investigated. Pyrolysis parameters including pyrolysis temperature, heating duration (soak time) and purge gas flow rate were studied. The results showed that pyrolysis temperatures of 700°C to 800°C increased O_2/N_2 selectivity from 1.1 to 1.85 and the maximum O_2 permeability was achieved at 600°C with 480 GPU. Although the selectivity of 3.1 was achieved at 250°C, the membrane was not a pure carbon membrane. Longer duration of heating improved the selectivity from 1.1 to 1.8 with an increased in permeability at the initial stage. A decreased in permeability occurred at 180 min heating duration. Carbonized membrane with 10 min heating duration exhibited high selectivity of 3.7 with poorer permeability compared to PAN membranes. However, high purge gas flowrate gave an increase for O_2 and N_2 permeability from the original 50 – 130 GPU to 150 – 730 GPU without influencing it's selectivity. Therefore, pyrolysis condition has pronounced influence on asymmetric carbon hollow fiber membranes for gas separation.

TABLE OF CONTENTS

LIST OF TABLES

LIST OF FIGURES

LIST OF SYMBOLS

$(P/l)_i$	-	Permeability of gas i
Q_i	-	Volumetric flow rate of gas i at standard temperature and pressure
Δp	-	Transmembrane pressure drop
A	-	Membrane surface area
$\alpha_{A/B}$	-	Ideal separation factor/selectivity of gas mixture A and B
ID	-	Inner diameter
L_c	-	Crystalline thickness

LIST OF APPENDICES

CHAPTER I

INTRODUCTION

1.1 Membrane Separation Processes

There are numerous membrane definitions proposed in the literature [G10]. A general definition of membrane is a selective barrier between two phases [B3-1] and can be classified into biological and synthetic membranes. The synthetic membranes can be subclassified into organic (polymer or liquid) and inorganic membranes. Furthermore, membranes can be classified according to its structure or morphology, configurations as well as applications [G10,B3-1] as tabulated in Table 1.1. A process which using membrane to achieve particular separation is known as membrane process. Membrane can be considered as a heart of a membrane process. Membrane processes can be classified according to the driving force [G7] as shown in Table 1.2.

Table 1.1: Classification of membranes

Classification	**Types of Membranes**
Structure	-Asymmetric/anisotropic (porous with dense top layer, porous, composite) -Symmetric/isotropic (dense, porous, cylindrical porous)
Configuration	Hollow fiber, film, tube, plate & frame, spiral wound
Application	Microfiltration, ultrafiltration, pervaporation, reverse osmosis dialysis, electrodialysis, gas separation

Table 1.3 presents worldwide sales of various membrane processes in the industry and their growth per annual. Table 1.4 shows the worldwide sales of membrane for different applications and the sales of membrane products would most likely continue to grow at an annual rate more than 8%. Among those processes, membrane gas separation process has the highest growth percentages of 15%. In this century, membrane systems process more than 4000 million cubic meters of gas annually [F3]. Hence, the future of membrane gas separation process is tremendous and it has a great potential to sustain as an important process in the industry in new millennium.

Table 1.2: Classification of membrane processes

Driving force	**Type of membrane process**
Pressure	Microfiltration, ultrafiltration, reverse osmosis, gas separation
Concentration	Dialysis, controlled release and Donnan dialysis
Partial pressure	Pervaporation, vapor separation
Electrical potential	Electrolysis, electrodialysis, energy conversion

Table 1.3: Worldwide sales of membranes and modules for various membrane processes [G7]

Membrane Process	**Sales in 1998, US$ million**	**Growth, % p.a.**
Dialysis	1900	10
Microfiltration	900	8
Ultrafiltration	500	10
Reverse osmosis	400	10
Gas exchange	250	2
Gas separation	230	15
Electrodialysis	110	5
Electrolysis	70	5
Pervaporation	> 10	-
Miscellaneous	30	10
Total	4400	> 8

Table 1.4:Worldwide sales of membranes and modules for various applications [G7]

Market segment	Sales in 1998, US$ million	Growth, % p.a.
Haemodialysis/filtration	2200	8
Blood oxygenator	350	2
Water desalination	350	10
(Waste) water purification	400	10
Oxygen/nitrogen purification	100	8
Food processing	200	10
(Bio)chemical industry	150	15
Electrochemical industry	150	8
Analytical/diagnostic	150	10
Miscellaneous	350	10
Total	4400	> 8

1.2 Membrane for Gas Separation Applications

In 1830, Mitchell discovered that rubber membranes (film) are selectively permeable for gases [T7,T8]. Graham found that gas separation in nonporous polymer membranes (natural rubber films) is by solution diffusion mechanism and the gas mixtures could be partially separated by permeation through microporous membranes owing to the difference in the molecular weights of the gases (Graham's law) [T2]. Those finding is essentially important as an initiator for the development of today's membrane technology.

The first large-scale use of membranes to separate gases was developed in the 1940s for the "gaseous diffusion" process [G8] for the separation of uranium isotopes by utilizing microporous ceramic membranes. Nevertheless, Loeb and Sourirajan achieved a breakthrough in membrane technology with an invention of high flux asymmetric cellulose acetate membranes for water desalination in 1960s [T6] and thus boosted and stimulated both commercial and academic interest.

Membrane-based gas separation was introduced commercially in 1979 when Monsanto Co. installed the first large-scale membrane separation plant based on

polymer membranes (polysulfone/polysiloxane membrane) for the recovery of H_2 in refinery or petrochemical streams [T4].

Presently, membrane gas separation process has become an accepted new separation process in chemical industry. Gas separation membranes complement as well as compete with older separation technology such as cryogenic distillation, selective adsorption and absorption processes. Membrane technology has been applied in a wide range of gas separation processes such as the production of N_2 from air, oxygen enrichment, H_2 recovery from refinery, petrochemical and ammonia-purge streams, CO_2 and H_2S removal from natural gas, CO_2 removal from mixtures with hydrocarbons in enhanced oil recovery operation (EOR), enrichment of CH_4 from landfill gas and dehydration of air or natural gas streams [G3,G4,G8].

1.3 Advantages of Membrane Technology

Membrane technology is broadly applied in the gas separation industry as it offers advantages such as listed below [G4,G8,B3-1]:

(a) Ease of operation
(b) Continuous separation
(c) Membrane properties are variable and adjustable
(d) Economic viability for small unit operations
(e) Low energy cost
(f) Portability
(g) Simplicity
(h) Compactness
(i) Reliability
(j) Can easily be scaled up
(k) Can operate at partial capacity
(l) Environmental Friendly

1.4 Polymeric Membranes

The foundation for today's commercial gas-separation membranes was established in the 1960s & 1970s, primarily by the major chemical/plastics companies (e.g. Dupont, Monsanto, General Electric, Dow). The widely application of polymers as membrane materials is due to the simplicity of polymer processing into efficient membranes with small effective thickness, high area/volume ratio and relatively low material and processing cost [G3].

In membrane technology, glassy and amorphous polymers have been recognized as the most suitable membrane material. Organic, glassy polymer films have been well known as the major membrane candidates in the gas separation industry as glassy polymers offer improved permeability/selectivity combination for specific gas pair separation. The glassy state offers a more structured sieving matrix than the rubbery state, good mechanical properties as well as higher load bearing properties allowing for high pressure drop across the membrane. [G4,G8,B1-4].

The glassy polymers stand between the crystalline polymers, which are essentially impervious to gases and the rubbery polymers, which are highly permeable for all permanent gases as well as for many organic vapors with poor selectivity. Although the intrinsic gas permeability of glassy polymers are much lower than rubbery polymer, the development of high flux asymmetric membranes has eliminated this weakness [G8].

Porous solids are another class of media, which are known to have gas separation capability [C36]. Nowadays, porous inorganic membranes have become another alternative membranes in gas separation industry due to the limitation of the polymeric membranes.

1.5 Limitation and Disadvantages of Polymeric Membranes

For the past decade, the separation factor for gas pairs varies inversely with the permeability of the more permeable gas. An analysis of literature data reveals an upper bound relationship for these gas pairs [G9]. Over the last 40 years, polymer scientists have tried to push the limits of the upper bound of polymer membranes performance. However, significant advances in conventional polymeric membranes will be difficult to attain as currently, the direction is close to the limit of the technology. For instance, improvement of O_2/N_2 selectivity from the current level of 5 – 6.5 to 10 at 25°C requires breaking through the upper bound barriers for polymers. It is expected that inorganic materials with higher specificity towards O_2 such as carbon can achieve higher performance [G3].

Growth in traditional membrane markets has also been driven by technology developed in the 1970s and 1980s by the major chemical companies with intense membrane innovation. The ‘90s represents the industrialization and growth phase of the life cycle. At this period, membrane technology was implemented and driven by the industrial gas companies. However, the demands of the market have now changed and new technology is needed to spawn further expansion. It is owing to polymeric membranes are not as competitive (relative to cryogenic distillation or adsorption) for large units or where high purity is required. Therefore, membranes with improved selectivity, higher temperature and pressure capability as well as higher chemical resistance will spawn a new growth [G3,G4].

In the last decade, a lot of effort has been concentrated on membrane development especially to improve membrane efficiency and reduce membrane-manufacturing costs. Most of the improvements came from gains in cost or in membrane thickness/geometry or in bundle efficiency. Hence, next generation membranes will have to be similarity inexpensive in final module form to be commercially attractive [G3].

1.6 Potential of Inorganic Membranes

Increasing interest in gas separation by organic membranes has led to exploitation of inorganic membranes for high temperature or corrosive gas separation applications [C33]. Inorganic membrane producers are generally in the start-up and technology push stage. Meanwhile, the end-user industries have exhibited a “wait-and-see” attitude when they come to adopting advanced inorganic membrane applications. Industries currently have a major interest in basic quantitative knowledge of inorganic membranes and are interest to know the performance of inorganic membranes in separation process and their stability in aggressive environment [C32].

Gas separation inorganic membranes can be categorized into 3 types including microporous, amorphous membranes; microporous, crystalline membranes and dense, high temperature membranes. A lot of attention will be focused on realizing complex, well-defined porous architectures and all these 3 types of membranes will be combined to new separation properties with improved long-term stability in these few years. In the future, a gradual shift will take place from the exploration of new membrane concepts toward better control of membrane preparation and understanding of performance, long-term stability and process integration in the applications [C32].

Commercialized inorganic membranes exist in 3 types of configurations: disks or sheets, tubes and multichannels/honeycombs. Usually, flat disks or sheets are limited to small-scale industrial, medical and laboratory applications. They used almost exclusively in flow-through filtration in contrast to cross-flow filtration in tubes and multichannel monoliths. Meanwhile, tubes and monoliths are used for various industrial applications [C42,C33].

Today, 20 firms are involving in the inorganic membranes manufacturing; most of them were emerged in the market over the last five to ten years. The inorganic membranes produced by these firms are presented in the Table 1.5. The oldest inorganic porous membranes manufacturers, SCT/US Filter and TECH-SEP are now dominating the inorganic membranes market [C42].

Table 1.5: Commercial porous inorganic membranes [C42]

Manufacturer	**Trade Name**	**Material**	**Pore**	**Geometry**
USF/SCT	MEMBRALOX®	ZrO_2/Al_2O_3	20-100nm	Monolith
		$Al_2O_3/Al_2/O_3$	5nm-12μm	
	CERAFLO®	Al_2O_3/AL_2O_3	0.2-1.0μm	Monolith
TECH-SEP	CARBOSEP®	ZrO_2/C	10-300kD	Tube
		TiO_2/C	0.14μm	
	KERASEP®	$TiO_2/Al_2O_3 + TiO_2$	0.1-0.45μm	
		$ZrO_2/Al_2O_3 + TiO_2$	15-300kD	Monolith
Le Carbone Lorraine		C/C	0.1-1.4μm	Tube
CERASIV		$Al_2O_3/Al_2/O_3$	0.1-1.2μm	Tube/Monolith
		$+TiO_2/ZrO_2/Al_2O_3$	5-100nm	
NGK		$Al_2O_3/Al_2O_3+SiO_2$	0.2-5μm	Tube/Monolith
Whatman	ANOPORE®	Al_2O_3	20nm-0.2μm	Disk
Gaston Country	UCARSEP®	ZrO_2/C	4nm	Tube
Du Pont/Carre		$Zr(OH)_4$/SS	0.2-0.5μm	Tube
TDK	DYNACERAM®	ZrO_2/Al_2O_3	≈10nm	Tube
		Al_2O_3/Al_2O_3	50nm	
ATECH		SiC/SiC	0.05-1.0μm	Tube/Monolith
		Al_2O_3		
Asahi Glass		Glass	0.1-1.4μm	Tube
Fuji Filters		Glass	4-90nm	Tube
		Glass	0.25-1.2μm	
Fairey	STRATA-PORE®	Ceramics/Ceramics	1-10μm	Tube/Plate
	MICROFILTREX®	SS	0.2-1μm	Tube/Plate
Osmonics	HYTREX®	Ag/None	0.2-5μm	Tube/Plate
	CERATREX®	Ceramics/Ceramics	0.1μm	
Ceramen		Ceramics/Cordierite	0.05-0.5μm	Honeycomb
Trideltafiltration		Al_2O_3/Al_2O_3	0.1-7μm	Tube/Monolith
Hoogovens		Al_2O_3/Al_2O_3	0.1-1μm	Tube
Steenecker		Al_2O_3	0.4μm	Tube
NOK		Al_2O_3/Al_2O_3	0.2-6μm	Tube
TOTO		Al_2O_3/Al_2O_3	0.1-0.2μm	Tube/
		ZrO_2/Al_2O_3	5-30nm	Monolith
Carre		ZrO_2/SS		Tube

Currently, typical and prevalent inorganic membranes are Vycor glass, silica, alumina, zirconia and porous ceramic membranes. However the application of these materials is limited to their lower selectivities due to their relatively larger average pore size (more than 2.0nm). The selectivity for the O_2/N_2 is less than 1 [C42,C37].

1.7 Unique of Carbon Membrane

Selectivities of the carbon membranes are much larger than those of the inorganic membranes and the polymeric membranes. The selectivities of typical highly selective carbon membranes are 10 to 20 times larger than Vycor glass and silicon rubber membranes. In addition, the average permeabilities are one order of magnitude higher than that of Vycor glass [C37].

Meanwhile, Koros and Mahajan summarized three main challenges faced by the current membrane technology which are achieving higher permselectivity with acceptable productivity, maintaining these properties in the presence of complex and aggressive feeds and preventing the need for recompression of the desired product [G1]. Carbon membranes have the potential to overcome these three challenges with its advantages compared with polymeric membranes.

1.8 Advantages of Carbon Membrane Compare with Polymeric Membrane

Attention and interest in the developing of carbon membrane technology has risen since there are numerous advantages of carbon membranes as reported by previous researchers.

(a) Carbon membranes display superior permeabilities-selectivity combination than polymeric membranes [C1,C18,C22,C31,C36,C54,G1].
(b) Carbon membranes are effective to separate gas mixtures with similar molecular sizes such as O_2/N_2, CO_2/CH_4 and CO_2/N_2 [C57].

(c) Carbon membranes have stronger mechanical strength and withstand higher pressure differences for a given wall thickness [C36]. Carbon membranes have higher elastic modulus and lower breaking elongation than the polymeric membranes [C1].

(d) Feed pressure does not affected much on the permeation properties of carbon membranes [C1,C5] due to the structural stability of carbon membranes, which do not have compaction and swelling problems [C33].

(e) The permeation properties of carbon membranes will not be time dependent [C1]. It means that the operating life of carbon membrane is much longer than organic membrane [C59].

(f) Requirement of activation energies for the diffusion through carbon membranes are smaller than those in the polymer membranes. It means that the diffusing gas (especially with large molecule size) is much influenced by the activation energies when it diffuses in the polymer membranes compared with carbon membranes. Therefore, the selectivity of polymeric membrane decreases when the measurement temperature increases [C2]. This situation was absent with carbon membranes.

(g) Carbon membranes offer the advantage of operation in environments prohibitive to polymeric materials and have superior stability in the presence of organic vapor or solvent and non-oxidizing acids or bases environments [C1,C22,C31,C36]. They can perform well with high purity and dry feeds [C10]. They are ideal for corrosive applications [C43] and are not much affected by the aggressive feeds [G1]. They are much more resistance toward radiation, chemicals and microbiological attack [C32,C33].

(h) Carbon membranes have higher thermal stability than polymeric membranes. They are appropriate for the application in the high temperature separation processes with temperatures in the range of 500-900^{o}C. In contrast, organic polymer membranes cannot resist very high temperature and begin to decompose or react with certain components. [C12,C18,C22,C36,C43].

(i) The same starting material can be used to develop membranes of different permeation properties for different gas mixtures [C36].

(j) The pore dimension and distribution of the carbon membranes can be finely adjusted by simple thermochemical treatment to meet different separation needs and objectives [C31,C36].

(k) Carbon membranes have a superior adsorptivity for some specific gases, thus enhancing its gas separation capacity [C31].

(l) Carbon membranes have the ability to be back flushed, steam sterilized or autoclaved. This may encourage more developments and application of carbon membranes in biotechnology [C33].

1.9 Disadvantages of Carbon Membranes

Carbon membrane is very brittle and fragile and is difficult to process. It requires careful handling [C31,C36,G1].

Carbon membranes also require a pre-purifier for removing traces of strongly adsorbing vapors, which can clog up the pores due to the transport is through a pore system rather than through the bulk system. This is typical of many industrial adsorption separators. This problem may be avoided by operating at sufficiently high temperatures [C36].

Carbon membranes only demonstrated selectivities for certain gas mixture, limited to gases with molecular sizes smaller than 4.0 – 4.5 ⊕. Carbon membranes are not suitable to separate gas mixtures, such as iso-butane/n-butane and gas-vapour mixtures, for instance air/hydrocarbons, H_2/hydrocarbon [C57].

However, the advantages of carbon membrane are apparently much more than its disadvantages. This unique characteristic of carbon membranes has accounts for the wide application of this new technology in recent industry.

1.10 Application of Carbon Membranes

The most important application of carbon membrane is in the production of low cost and high purity nitrogen from air. Membrane can produce N_2 with purity up

to 99.5%. It is estimated that membranes currently produce 30% of all gaseous N_2 because many industrial and commercial applications do not require ultra-high purity nitrogen [G1,G3]. It is expected that carbon membrane would continuously to be an effective way for the production of N_2.

Other separation processes include purification of methane as well as recovery of carbon dioxide in oil fields [C3,C59]. Besides that, it is useful in the removal of acid gases from natural gas because it can operate in severe environment [C59]. Currently, the world market for natural gas is estimated at about US$22 billion annually. Although polymeric membranes are able to compete successfully with other technologies such as amine scrubbing, carbon membranes still has a broad market opportunity. This is due to some glassy polymeric membranes losing its selectivity and productivity in the presence of trace quantities of condensable heavy hydrocarbon. Furthermore, extremely high partial pressure of carbon dioxide can cause the plasticization in the skin layer of membrane [G1].

Membrane compete with cryogenic, catalytic and pressure swing adsorption processes in the hydrogen recovery process [G1]. Carbon membrane can be applied to recover a valuable chemical (H_2) from a waste gas or recovery of hydrogen from gasification gas without further compression of the feed gas while rejecting a substantial portion of the hydrocarbons [C17]. Conventional/polymeric membranes required adding recompression costs because H_2 as a fast gas exits the unit at the lower pressure permeate side [G1,G2].

Carbon membranes are promising candidates for the separation of light alkenes/alkanes especially propene/propane separation as carbon molecular sieve membranes possess excellent propene/propane permselectivities. They are expected to be superior to other methods such as distillation, adsorption and absorption based on energy consumption. Separation of light alkenes/alkanes has been recognized to be a key technology in the petrochemical industry [C48].

Carbon membranes are also implemented for the separation of olefins and paraffins, another important process in petrochemical industries especially for 1,3-butadiene/n-butane separation [C49]. A recent study estimated that about 10,000

BTU of energy is used annually for olefin-paraffin distillation. Distillation process is commercially used in this separation process. However, membrane separation with low energy consumption and simple operation can give a significant competition to distillation process [G1]. Therefore, the carbon membrane can give a great contribution to petrochemical industry.

The combination of reaction and separation at high temperature in a membrane reactor offers interesting new possibilities. In a carbon membrane reactor, the separate product and feed compartments allow more ways to optimize both selectivity and conversion [C32,C59].

In this research, attention only focused on the application in the air separation or oxygen enrichment application. The fundamental observation and findings obtained from this research can also implemented for other gas separation process such CO_2/CH_4 separation, CO_2/N_2 separation and others.

1.11 Air Separation Membrane Process

As reported, the 3rd and 5th largest bulk chemicals produced worldwide are O_2 and N_2 respectively. However, air separation membranes are still competing with conventional processes such as cryogenic distillation since those processes promise to give high purity of products. Currently, the gaseous O_2 market is dominated by distillation (99.999 % purity) and vacuum swing adsorption (95 % purity). Polymeric membranes only served for a limited number of applications that using low purity (25 – 50 %) O_2 [G1] because some nitrogen always permeates through the membrane with the oxygen, producing oxygen-enriched air rather than pure oxygen [G11].

Nevertheless, Stern evaluated O_2 enrichment of air as a developing and potential membrane process [G8]. Therefore, the crucial important task at present is to improve the O_2/N_2 separation factor of the membrane (without sacrificing the permeability) in order to ensure that membrane technology can be an attractive and competitive technology in the air separation industry. Additionally, the production

costs and selective layer thicknesses should be similar to the current generation of polymeric membranes [G1,G7]. With the economically competitive production, the oxygen enrichment process can find a significant market, especially in combustion applications [G8]. Oxygen-enriched air can be applied in FCC catalyst regeneration in refineries or to burn methane more efficiently in high-temperature furnace or cement kilns [G11]. One of the appropriate ways to overcome the current limitation and hurdles of the membrane technology is to develop carbon membrane, which has higher separation factor and higher productivity than polymeric membrane.

1.12 Problem Statement

Carbon membrane technology has been focus in this century. In the effort to develop carbon membrane, the main problem that must be overcome before broader application of carbon membrane technology is the fabrication of these materials in a manner that is both reproducible and scalable for manufacturing.

From Table 1.1, there are only a few manufacturers involved in the production of carbon membranes. It is because greater expenses in producing and packaging these carbon membranes in modules have prevented their use in large-scale membrane modules [G2]. The cost of carbon membrane is reported to be higher between one and three orders of magnitude per unit of membrane area compared to polymeric membrane [G1].

Since carbon membranes involve high production costs, permeability and permselectivity of carbonized membranes require further refinements and improvements before they can be used on a large industrial scale [C45]. High permeability membrane requires small membrane area that lower the capital cost of the membrane system. In addition, high selectivity membrane promises to give more efficient separation. Thereby, reducing the operating cost because lower driving force (pressure ratio) is required [G1]. A lot of research should be carried out to study the optimum way for the production of carbon membrane with excellent

performance in order to render the carbon membrane becomes an important separation tool in the industry.

Moreover, investigation on material selection of more suitable precursor should be done. Finding a more economical material than polyimide, which mainly used by other researchers as the carbon membrane precursors, is another necessary task in carbon membrane production at Malaysia. This indicates that discovering ways to provide excellent separation properties of carbon membrane without losing the economical processability of polymeric membrane materials would be a major breakthrough in this field.

This has given the inspiration and incentive for the development of polyacrylonitrile carbon hollow fiber membranes for oxygen/nitrogen separation. It is hoped that such fundamental knowledge will lead to the development of tailor-made carbon membrane in this century. The following section describes the objectives and the scopes of this research.

1.13 Objective of the Research

Based on the research background and problem statement describe above, the objective of the research is to develop a novel asymmetric carbon hollow fiber membrane and characterize the separation performance as well as morphology of the carbon membrane.

1.14 Scope of the Research

To accomplish the above objectives, the following scope of works has been drawn.

1. Prepare suitable polymer solution as precursor for the production of carbon membranes.
2. Fabrication of polymeric hollow fibers by using dry/wet-spinning process.

3. Set up an inert gas pyrolysis system for the production of carbon hollow fiber membranes.
4. Fabricate and set up a pure gas permeation testing system for the measurement of carbon membranes' performance.
5. Study the effect of pyrolysis condition on the carbon membranes's permeation properties (permeability and selectivity).
6. Study the effect of pyrolysis condition on the physical properties (structure and morphology) and chemistry properties (elemental content) of carbon membrane by using various characterization methods.

CHAPTER III

RESEARCH METHODOLOGY

3.0 Research Design

The fabrication method of carbon hollow fiber membrane is quite similar with the fabrication of carbon fiber. The carbon fibers technology has been long developed since it has been known as filaments for lamps for nearly a century, discovered by Edison. Modern carbon fibers were first developed by Shindo in 1961 when he pyrolysed polyacrylonitrile fiber [C62]. Furthermore, the control of structure and the interaction between the structure and properties have been extensively studied since high performance carbon fibers were first commercialized by Union Carbide in the 1960s [C67].

Manufacture of carbon fiber typically involves 4 major processes: preparation of precursor solution, fiber spinning, stabilization of fiber and carbonization of fiber. Hence, the production of carbon hollow fiber membrane also involves these four processes. By using these four processes, a carbonaceous precursor (polymer) will change into hollow fiber form and thereby become crosslinked hollow fiber. Finally the hollow fiber converted into carbon hollow fiber.

The major factors that determine the performance of carbon molecular sieve membrane including the nature of the precursor, solution formulation, spinning process and pyrolysis process as shown in Figure 3.1. The Figure 3.2 shows the experimental stages involved in the production of carbon membrane. Although post-treatment after pyrolysis process and surface modification will influence the

performance of carbon membranes [C80], it was neglect in this research. This research was emphasis on the investigation of pyrolysis process. The effect of different pyrolysis process conditions on the performance of carbon membrane was studied.

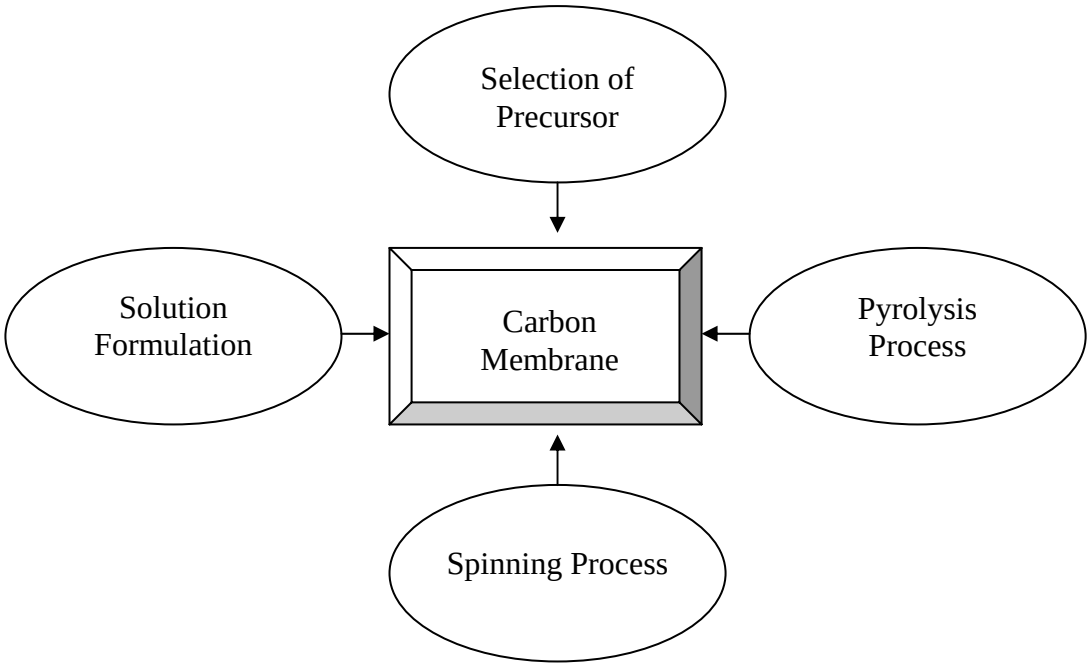

Figure 3.1: Factors influencing the performance of carbon membrane

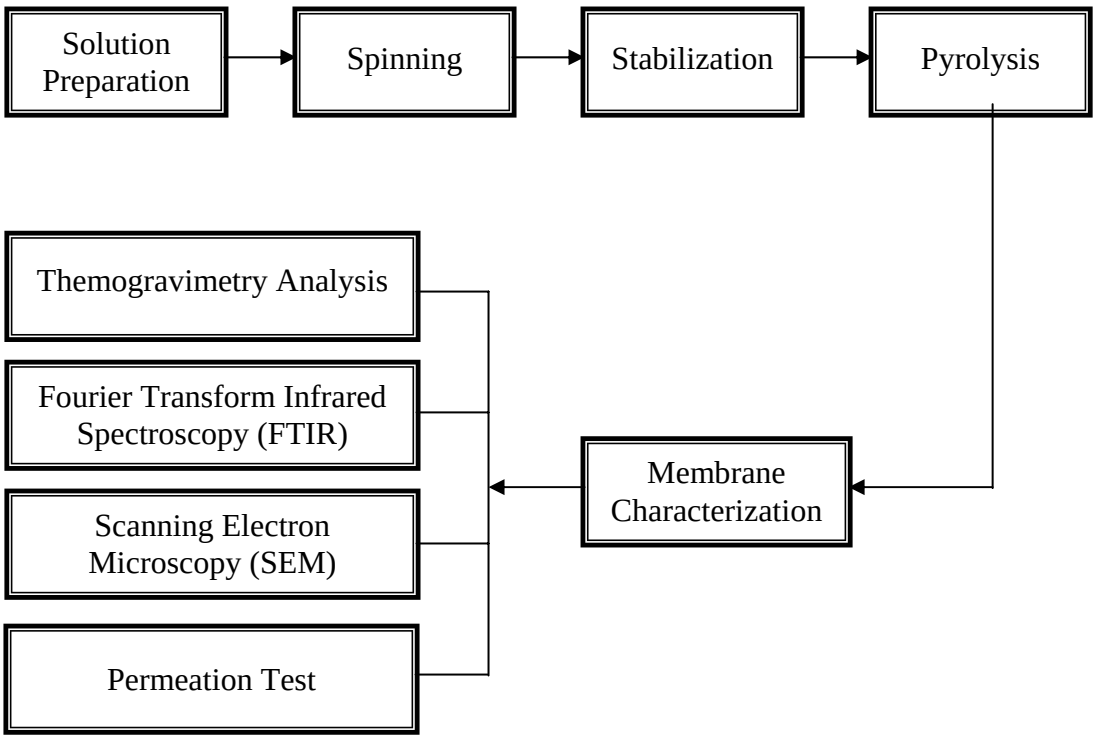

Figure 3.2: Experimental stages in this research

3.1 Precursor Selection

Carbon membranes may contain pores of very diversified dimensions depending on the morphology of the organic precursor and the chemistry of pyrolysis. Precursor must yield no pores larger than those of molecular dimensions after pyrolysis process. Thermosetting polymers usually do not liquefy or soften during any stage of the pyrolysis process. The porosity, which is due to morphology of precursor, is coarse macroporosity. In order to obtain a membrane free from pores larger than those of molecular dimension, one should start from an even, flawless, thermosetting polymers membrane as a precursor for pyrolysis. Many thermosetting polymers preserve their morphology upon pyrolysis is the basis of the art of producing high strength and high modulus graphite fibers utilized in composite material production [C35]. It is noteworthy that the thermosetting polymers are suitable to be chosen as precursor for carbon molecular sieve membrane. The Table 3.1 shows the various precursors used in the previous research.

Although polysulfone is a conventional commercial polymer for membrane fabrication [B18], it is a thermoplastic polymer, which cannot withstand very high temperature during carbonization process. Another classic polymer for membrane production -- cellulose acetate (thermoplastic polymer) also cannot withstand heat at high temperature. In both cases, the fibers were either melt and stuck together or broken into many parts and even disappeared. Therefore, a lot of weight loss occurs and the carbon yield is very low. Cellulosic precursors are no longer an important source of carbon fibers. Although the pitch-based carbon fibers have the advantages of low cost and high carbon yield, it has poor strength properties, nonuniformity and nonreproducibility of their properties [B21-1.1].

Polyimide, one of the thermosetting polymers has been proved to be a suitable precursor for the production of carbon membranes. Table 3.1 shows that numerous researchers are using the polyimide-based polymers to produce carbon molecular sieve membranes. Most of them use their own laboratory-synthesized polyimide. Polyimides are very expensive material compared with other polymers and most of them only available on the laboratory scale production. Furthermore, most of the commercial polyimides are not available in Malaysia. The possibility to

Table 3.1: Carbon membranes precursors used in the previous research

No	Precursor	Supplier	Trade Name	Reference(s)
1	Matrimid ®5218	Ciba Specialty Chemicals		C38
2	PMDA-ODA	Synthesis Synthesis/Dupont Inc. Dupont Inc. Synthesis Dupont Inc. Synthesis	 --/Kapton Kapton Kapton 	C12,C41 C20,C21 C4,C40,C48 C38 C50 C24,C53
3	Polyacrylonitrile (PAN)	Sythesis		C14
4	Polyvinylidene Chloride (PVDC)	-- --		C16,C17,C46 C71,C69,C79
5	Polyfurfuryl alcohol (PFA)	-- Occidental. Chemical. Corp -- Aldrich --	 Durez Resin 	C26 C15 C25 C56 C55,C70
6	Cellulosic	--		C35
7	Polyetherimide (PEI)	Polyscience	Ultem ®1000	C7
8	Phenolic Resins	-- --		C5,C57,C68 C23
9	Phenol formaldehyde	Synthesis --		C13,C37 C77
10	Poly(vinylidene chloride-co-vinyl chloride) (PVDC-PVC)	Aldrich (43038-2)	Saran	C39
11	Condensed polynuclear aromatic (COPNA)	Synthesis		C8
12	Polypyrrolones	Synthesis		C47
13	6FDA/BPDA	Synthesis Synthesis		C10,C22,C34 C44
14	BPDA-pPDA	Synthesis		C3, C6
15	BPDA-pp'-ODA	Synthesis Synthesis		C9,C30,C45,T5 C28
16	BPDA-ODA/DAT	Synthesis		C29
17	BPDA-DDBT	Synthesis		C49
18	BPDA-aromatic diamines	UBE UBE		C1 C2
19	Coal tar pitch	Dalian Gas Company		C31
20	Graphite	--		T1
21	AP	E. I. Dupont de Nemours		C54

synthesis a new polymer or polyimide in this research is not practical because it is another area of study.

Therefore, the selection of commercially available polymer instead of high cost polyimide or polyimides synthesized at the laboratory scale will ultimately contribute to the development of carbon membranes in Malaysia. The polymer used in this research is Polyacrylonitrile (Aldrich 18131-5). Polyacrylonitrile-based carbon fiber is one of the major carbon fiber produced and used in the industry. These commercial PAN-based carbon fibers have been available for over 25 years. Currently, PAN-based carbon fibers are recognized as the most important and promising precursor for the present manufacture of carbon fibers and dominate consumption, accounting for nearly 90 % of all sales worldwide [B21-1.2,C65].

Besides that, the numerous advantages of PAN fibers including a high degree of molecular orientation, higher melting point and a greater yield of the carbon fiber. Table 3.2 presents the weight loss of different fibers with heating at 1000°C in Helium [B21-1.1]. As seen in table 3.2, the carbon yield of the oxidized PAN fiber is very high compared with other precusor-based fibers. PAN fibers form a thermally stable, highly oriented molecular structure when subjected to a low temperature heat treatment, which is not significantly disrupted during the carbonization treatment at higher temperatures. This means that the resulting carbon fibers have good mechanical properties [B21-1.2]. It is noteworthy that PAN is a suitable polymer for the production of carbon hollow fiber membranes.

Table 3.2: Weight loss of different fibers at 1000°C in Helium [B21-1.1]

Polymer Type	Total Weight Loss (%)
Pitch	≈ 30
Oxidized Polyacrylonitrile	38
Polyacrylonitrile	60, 67
PRD-14	52
X-101	53
Saran	74
Rayons	87 – 89
Ramie	91
Poly(vinyl alcohol)	93

3.1.1 Structure of PAN

The acrylonitrile molecule has a nitril group, which is highly polar so that polymerization can take place in the presence of free radicals or negative initiators, leading to the production of polyacrylonitrile as seen in Figure 3.3 [B21-1.2]. Polyacrylonitrile (PAN) is often considered to be a “laterally ordered” polymer, with no c-axis order. It is generally believed that PAN forms relatively stiff, rod-like molecules due to the intramolecular dipole repulsions of its nitriles. Disordered or “amorphous” regions between crystalline domains consist of entanglements, chain-ends, defects, co-monomer sequence and tie-chains [C65]. The highly polar character of the nitrile group causes strong dipole-dipole forces which act as crosslinks, making the polymers soluble only in highly ionizing solvents, increasing its melting point and making it more suitable as a carbon fiber precursor [B21-1.2].

Acrylonitrile

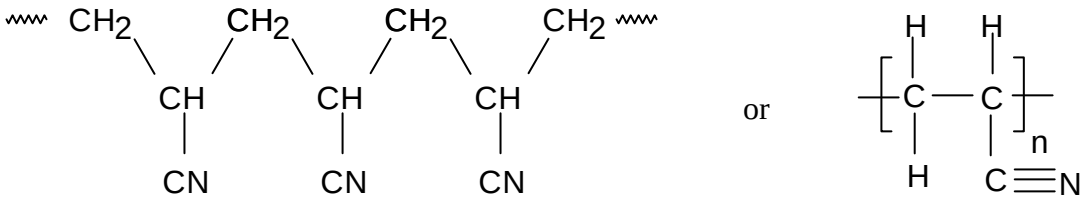

Polyacrylonitrile

Figure 3.3: Chemical structure of polyacrylonitrile (PAN)

3.2 Dope Formulation

In previous research, 10-30% by weight of PAN or (PAN copolymer) dissolved in a highly polar solvent were used [C67]. In this research, 15% by weight

of PAN was used for the polymer solution preparation as followed the composition used by previous researchers [Th1,F12].

There are a few requirements for the choice of solvents in an aqueous quenched membrane formation system [F4,F6]:

(a) The solvent must be miscible with the water (coagulant).
(b) The solvent must sufficiently strong for the dissolution of high polymer concentrations.
(c) The solvent must have sufficient volatility to allow ample evaporation from the membrane.
(d) The solvent must provide good mechanical properties to the formed yarn upon quenching.

Most of the solvents that interact strongly with water have relatively low volatilities. This is one of the severe limitations in the solvent selection [F6]. Polyacrylonitrile (PAN) is an atactic (amorphous), linear polymer containing highly polar nitrile pendant groups. Pure PAN tends to decompose before it melts due to its highly polar nature. Therefore, polyacrylonitrile (PAN) precursor fibers must be produced by either wet or dry spinning processes using a highly polar solvent. Among the suitable solvents for polyacrylonitrile (PAN) are sodium thiocyanate [C65,C66], dimethylsulfoxide (DMSO) [C14], nitric acid, dimethylacetamide (DMAc) and dimethylformamide (DMF) [C67].

In this study, dimethylformamide (DMF) was used as solvent for the polymer solution due to it is a good polar solvent for PAN as well as having high boiling point. Good solvent has the power to open and solvate the polymeric chains [F4]. DMF is commonly used as the solvent for PAN membranes production by researchers [F12,F13,Th1]. Furthermore, Cabasso et al. [F4] proposed that DMF is suitable solvent for the spinning process if water quenching is applied.

3.3 Solution Preparation

Figure 3.4 shows the solution mixing vessel and all necessary laboratory tools required to prepare a polymer solution. Round bottom solution vessel was used to prepare the solution. The function of stirrer is to make sure that the polymer and solvent can mix well in order to form a homogeneous solution. The thermometer measured the temperature during the mixing process. The processing temperature should be controlled in a suitable and optimum temperature range by the heater and the condenser. In order to remove all the water vapor from the polymer and equipment, they had been heated in the vacuum oven and air oven (Thelco Oven) respectively for 1 day before the solution being prepared. The existence of water in the polymer solution will influence the purity as well as quality of a polymer solution.

In general, a binary polymer solution consisted of polymer and solvent. The volatile solvent was put into the mixing vessel first, followed with the polymer. The polymer in powder form should put in gradually to prevent agglomeration. The agglomeration would make the polymer becomes more difficult to dissolve. Mixing temperature should maintain lower than the boiling point of the volatile solvent because the solvent is tending to vaporize. However, low temperature will slow down the mixing process. The boiling point for dimethyformamide is 153 ^{o}C [F2]. Therefore, an optimum range of mixing temperature should be chosen. The mixing temperatures used in the study were 80-90^{o}C. The solution has to be stirred for about 7-9 hours to produce a completely homogeneous solution.

After the polymer was fully dissolved, the homogeneous solution was degassed to remove any micro-bubbles by using ultrasonic treatment (Branson Ultrasonics) for 48 hours. Finally, the homogeneous solution was store in a solution bottle and ready for the spinning process.

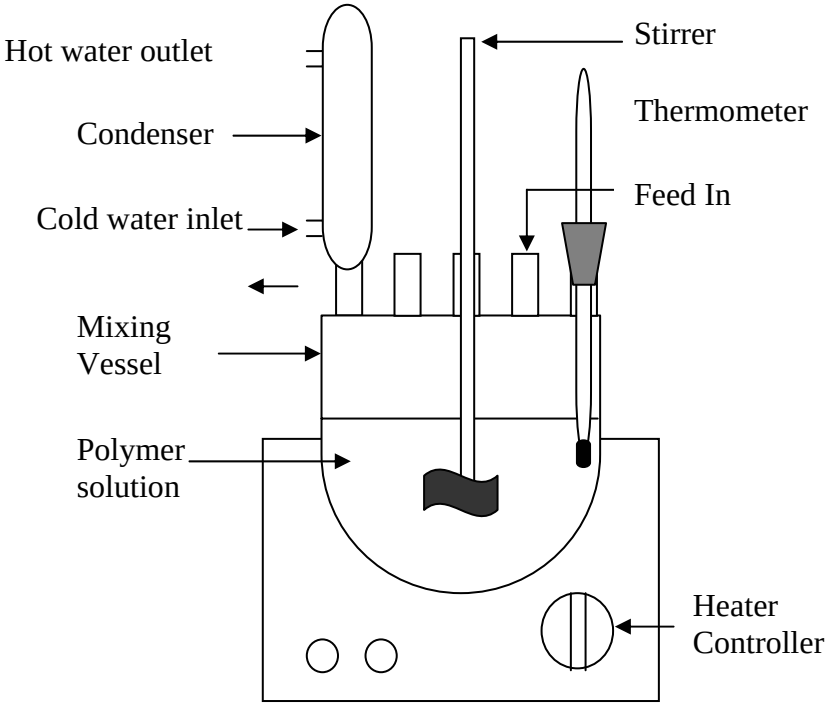

Figure 3.4: Solution preparation vessel

3.4 Dry/wet Spinning Process

In this research, dry/wet phase separation process [F1] was used to prepare asymmetric polyacrylonitrile (PAN) hollow fiber membranes according to the dry/wet spinning process. The dry/wet phase separation process has been known as a suitable process for preparing asymmetric membranes. The Figure 3.5 shows 8 basic steps involve in the dry/wet phase separation process.

Figure 3.6 presents a schematic diagram of a spinning system used in this research. In the spinning process, the dope was fed to the spinneret via a gear pump. The dope reservoir was kept under nitrogen pressure as a precaution against cavitation in the line to the pump. The gear pump smoothly delivered the polymer solution to the spinneret with 2.5 ml/min dope extrusion rate. An on-line filter prevented any extraneous material being passed to spinneret from the gear pump. Syringe pump provided an accurate and pulse-free supply of water to the capillary in the spinneret. A spinning solution and bore fluid were going extruded through a

spinnerette die to form a nascent hollow fiber at ambient temperature. The inside surface of hollow fiber was contacted with a bore fluid and experienced wet phase separation in order to form a circular hollow lumen [F1,F13]. Water was chose as bore fluid with flowrate 1ml/min. The bore flow rate 1ml/min typically applied in the previous studies [F1,F6].

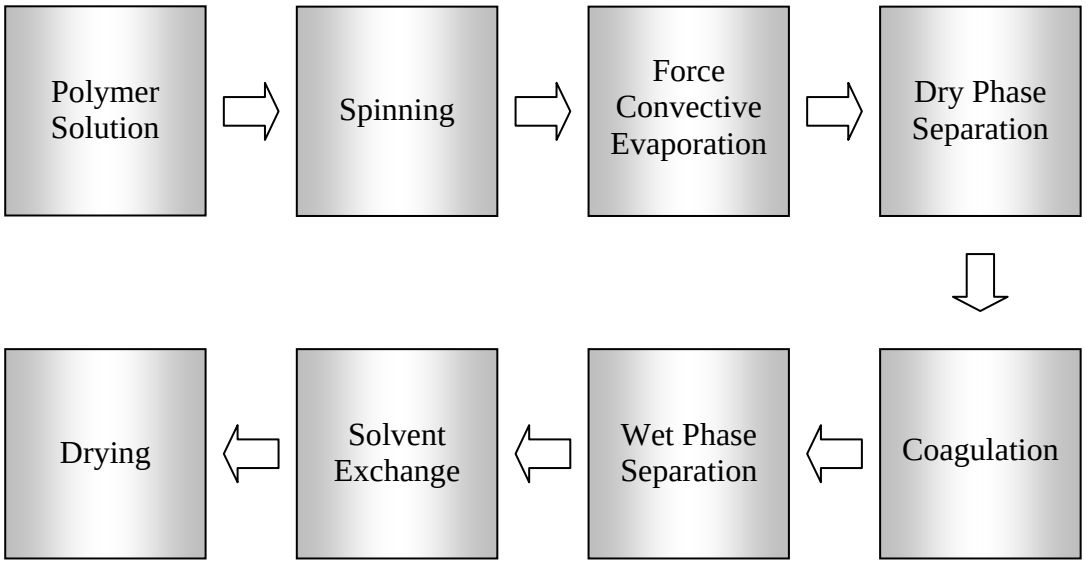

Figure 3.5: Preparation steps for asymmetric membranes according to the dry/wet phase separation process

In the spinning process, the shear field tends to orient the solidifying polymeric structure parallel to the direction of flow. PAN tends to precipitate into fibril form. This spinning process yield a precursor fiber in which the PAN molecules are organized into fibrils which, in turn, are generally oriented parallel to the fiber axis. This fibrillar network appears to be the precursor of the graphite network that develops during final heat treatment [C67]. Previous research showed that the shear affects the phase inversion dynamics of membrane precipitation as well as the orientation of the polymer molecules in the active layer [F3].

The fiber was then directed through a small blower which providing a controlled force convective environment for inducing dry phase separation. The inert gas used was nitrogen with flow rate 4 l/min[F1,F13]. The high inert gas flowrate is better for the fabrication thin skin layer of membranes [F8]. Sharpe et al. [F3] also reported that the residence time in the force convection chamber must be long

enough to allow skin formation but not too long as to allow excessive non-solvent encroachment from the lumen side. If membranes were spun at an optimized residence time, then surface imperfections would be minimized allowing thinner and more highly oriented defect-free active layers to be produced.

Clausi and Koros [F6] found that increasing air gap would lead to higher selectivity and lower permeability. It is due to larger air gap allows more time for mass transfer to occur and the resulting membrane has thicker skins with fewer defects. They concluded that the air gap played a significant role in the formation of the skin layer. However, humidity of air gap was not considered in this research because previous result showed that it has minor influence on the permeation properties of the resulting fibers [F6].

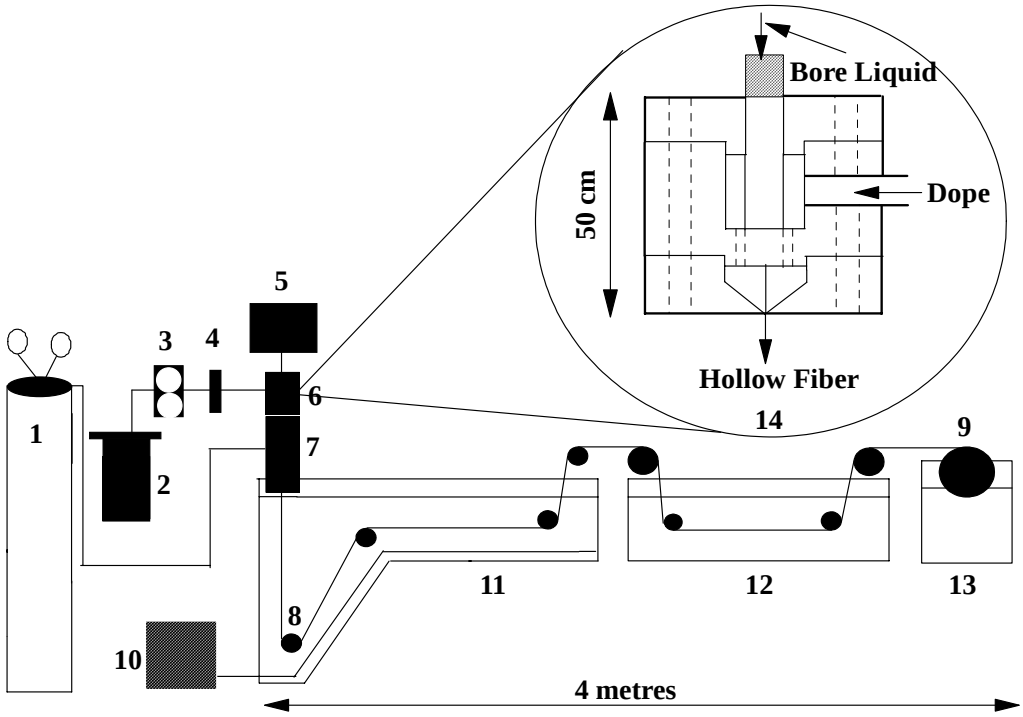

Figure 3.6: Schematic diagram of hollow fiber spinning system: (1) nitrogen cylinder; (2) dope reservoir; (3) gear pump; (4) on-line filter, 7 mm; (5) syringe pump; (6) spinneret; (7) forced convective tube; (8) roller; (9) wind-up drum; (10) refrigeration/heating unit; (11) coagulation bath; (12) washing/treatment bath; (13) wind-up bath; (14) schematic spinneret [Th1]

After the fibers passed through a 9 cm air gap, it was immersed into the nonsolvent (water) coagulation bath and the washing treatment bath. The temperature of water in the coagulation bath was controlled by a refrigeration/heating unit at 14^{o}C. The coagulation conditions ensures rapid solidification when the spinning dope comes in contact with coagulant. Wet phase separation process occurs in the coagulation bath [F1,F13]. If precipitation is rapid, the outer surface of hollow fibe forms a dense selectivie skin. Meanwhile, the underlying polymeric solution precipitates much more slowly, forming a porous matrix. As a result, the resulting membranes are markedly asymmetric. In contrast, the membrane with more symmetrical structure can obtained if the precipitation process is slow [C38].

Similar finding was observed by McKelvey et al. [F14]. They reported that exposing the nascent membrane to an environment drastically different than the quench bath prior to quenching can aid in the formation of highly asymmetric structures. The first enviroment initiates the formation of the permselective skin and the quench environment completes the formation of the porous structure.

After collecting the hollow fibers with wind up drum at 12.678 m/min take up rate, they were washed in water at 24^{o}C for 2 days. Then, put in methanol bath at 24^{o}C as a solvent exchange for 2 days and followed with hexane bath for another 2 days. It is necessary to replace the water contained within the pores of the membrane structure with a volatile organic liquid having a much lower surface tension. The purpose of the solvent exchange is to reduce the drying stress. The hollow fibers hung vertically and air-dried at room temperature for 7 days prior to testing [F1].

The resulting hollow fibers have outsie diameter 600 $\propto$m and inner diameter 290 $\propto$m. Typical average outside fiber diameter for gas separation application is in the range of 100 – 600 $\propto$m while average inside diameter is limited by gas pressure drop in the fiber bore. Pressure drop becomes severe at ID < 50 $\propto$m. In addition the rule of thumb regarding wall thickness is implying a value of 2 for the OD/ID. Smaller diameter fibers are favors because they possess high surface area in a given module volume, thereby promising to give high productivity [F14].

3.5 Solvent Exchange

Solvent exchange is one of the important steps, which cannot be neglect in the membrane fabrication process. Solvent exchange process was invented by Manos [F19] in 1978. Researchers found that direct drying water-wet membranes (porous substructures filled with water) can cause significant changes in the structure and properties of membrane. It is due to enormous capillary forces potentially present during pure water removal. High capillary forces exist especially in pores with relatively small radii and the pores are found just beneath the top layer of an asymmetric membrane. Thereby, the remaining solvent can result in plasticization of the polymer as well as densification of the structure in this part. The membrane skins are much thicker for the samples dried from higher surface tension fluids. Apparently, capillary forces collapse the underlying transition layer of the fibers, effectively changing it to less permeable skin [F19,F6,F15,F16,F18].

Solvent exchange processes typically involve removing the water in the membrane with a water-soluble/partially water miscible alcohol that is a nonsolvent for the membrane material. Subsequently, replacing the alcohol with a volatile and less polar organic compounds with low surface tension. The sequence often used during solvent exchange is water – alcohol – alkane – air [F6,F15,F17,F19]. Water-soluble alcohol and volatile organic solvent used in this research were pure methanol and pure hexane respectively. The aliphatic alcohols with 1 – 3 carbon atoms (methanol, ethanol and isopropanol) are particularly effective for replacing water from a membrane [F19].

Hexane was chosen to be the 2^{nd} solvent since it has minimal effect on the membranes during drying. Due to the slower evaporation rate of the 2^{nd} solvent, the solvent exchange process could prevent collapse of the pore structure and minimized the surface corrugations. Thereby, the surfaces were relatively smooth [F18]. Both 1^{st} and 2^{nd} solvents should be sufficiently inert to the membrane in order to prevent any significant depreciation of membrane properties [F19]. It was observed that polyacrylonitrile hollow fiber membranes have a serious shrinkage problem when dried without solvent exchange process. The hollow fibers shrunk and became curl form. Methanol is not effective enough for the solvent exchange purpose. The lack of

hexane for solvent exchange caused minor shrinkage problem. Besides that, the impurity of the solvent would also influence the resulting membranes.

3.6 Membranes Coating

Most of the gas flow through any surface pores or imperfections in polacrylonitrile membrane rather than diffusion through the solid PAN polymer itself because polyacrlonitrile polymer has low intrinsic permeabilities [F13]. Pores are defined to be passageways allowing communication between the upstream and downstream membrane face by a Knudsen or viscous flow process [F21]. Therefore, this membrane can be made into defect-free and thin skin structures by coating the membranes in a post-treatment with a dilute solution of silicone rubber. (The Monsanto Prism separator embodies this concept) [B18].

Coating is a standard procedure allows the hollow fiber to display permeation properties closer to the inherent characteristics of the membrane polymer itself [F13]. Coating will only prevent the hydraulic flux of gas through any defects in the membrane skin without altering the permeation characteristics of membrane material [F20]. The hollow fibers were coated with 3 % silicone (Sylgard 184, Dow Corning) in a hexane solution [F3,F12] for 15 minutes [F12,F13,Th1]. Previous research observed that the percentage of the silicone in the hexane solution was not much affected the permeation properties of membrane [F13]. After coating, the membranes were stored in a clean environment to allow curing. Figure 3.7 shows a bundle of PAN hollow fiber membranes.

Figure 3.7: Polyacrylonitrile hollow fiber membranes

3.7 Stabilization Process

Before carbonization process, the PAN hollow fibers were treated in an oxidizing atmosphere at temperature in the range of 200 – 300 °C [B21-1.2,B6-2.7]. The stabilization process is necessary to be carried out in order to cross-link PAN chains and prepare a structure that can withstand the rigors of high temperature processing. Stabilization process can insure that both the molecules and the fibrillar orientation will not be lost during final heat treatment. Therefore, either the inherent stiffness of the PAN molecules must be increased or the molecules must be “tied” together in order to eliminate or at least limit the relaxation and chain scission during the final carbonization step. The reaction is highly exothermic and if not controlled, can lead to run away autocatalytic processes resulting in “melting” down and coalescing of fibers [C65,C67]. The treatment converts PAN into a nonplastic cyclic or ladder compound capable of withstanding the high temperature present in the

subsequent process and increases the carbonization yield [B21-1.2]. This thermostabilization pretreatment brings the cross-linking of polymer which may reduce the fusion of nodules and ensures the asymmetric structure of the precursor hollow fiber can well held [C49].

Isothermal stabilization at high temperature will lead to oxidative degradation and may cause poor mechanical properties in carbonized hollow fiber membrane. Therefore, previous researchers suggested that it is more beneficial to stabilize the hollow fiber membrane using a constant heating rate to a high temperature. It is because by exposing the hollow fiber membrane to high temperature for a short period will prevent oxidative degradation and lead to the formation of well-stabilized hollow fiber membrane [C66].

In this research, the PAN hollow fiber membranes have gone through oxidative stabilization process until 250 ^{o}C with heating rate of 9 ^{o}C/min and held at 250 ^{o}C for 30 min. The thermostabilization temperatures should neither over nor close to the melting temperature of the polyacrylonitrile -- 317^{o}C. It is because of polyacrylonitrile tend to oxidize and melt rapidly at the melting temperature and the structure of the hollow fiber would collapse. The thermostabilization gases applied in this research were pure oxygen and compressed air. Without this treatment, the precursors soften during the pyrolysis and lead to the production of low performance carbon membranes [C2].

3.8 Pyrolysis Process

The heart of the carbon membrane fabrication process is the pyrolysis process or carbonization process. Porosity, which depends on the chemistry of pyrolysis, is of molecular dimensions and it is responsible for the molecular sieve property of carbons. (It is termed ultramicroporosity and is probably initiated by the small gaseous molecules channeling their way out of the solid matrix during pyrolysis) [C35]. Pyrolysis of certain types of substances (natural or polymeric) will lead to

carbon materials with a very narrow micropore distribution below 1 nm, which is able to separate gas pairs with very similar molecular dimension [C6].

A pyrolysis system was set up for the carbonization process. This system consisted of a wire wound tube furnace, flow meter, Pyrex tube or quartz tube, thermostabilization gases and inert gas. Figure 3.8 shows an inert gas pyrolysis system used in this research. In this study, tube furnace was chosen rather than box furnace because it allows the purging of the inert gas during heating process. Quartz tube was used in the pyrolysis system not only due to it can withstand high temperature; it would also not react with the membrane sample. Long quartz tube should be used to prevent the melting problem of the connecting tubing at the end of the quartz tube. However, Pyrex tubes that are more economic can be used for heating temperature not more than 600^{o}C.

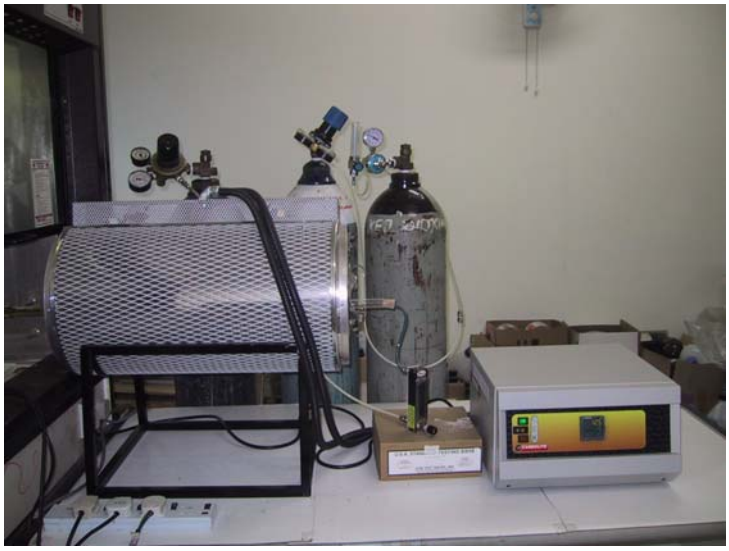

Figure 3.8: Inert gas pyrolysis system

Before the carbonization process started, the inert gas was purged into the pyrolysis system to remove unwanted air or oxygen. The purpose is to prevent the oxidation process happens during high temperature process. The heating rate for the entire pyrolysis process maintained at 9^{o}C/min and it was reduced when approaching final pyrolysis temperature in order to avoid an overshoot problem [C54]. Then, the precursor was heat to a required pyrolysis temperature and held for certain duration. After that, the resulting carbon membrane was cool down to ambient temperature in

the inert gas atmosphere. Finally, the precursor was completely carbonized to form carbon membrane. Figure 3.9 shows the resulting PAN carbon hollow fiber membranes.

Research was carried out to investigate a few very important parameters during carbonization process such as pyrolysis temperature, heating duration (soak time) as well as purge gas flow rate. This was in accord with the fact that carbon membrane performance is exclusively affected by the carbonization condition. Not much research had been conducted out to study the influence of soak time and purge gas flow rate on the carbon membrane performance.

Figure 3.9: Carbon hollow fiber membrane

3.8.1 Pyrolysis Atmosphere

Pyrolysis atmosphere can change the pore size and geometry or even nature of the surface by sintering (pore closure) or activation (pore opening by removal of surface groups or by burn-off) effects [C4]. In general, pyrolysis atmosphere can

divide into two categories. There are vacuum pyrolysis and purge gas pyrolysis. Vacuum pyrolysis technique is employed by Koros [C22,C44] and Suda et al. [C40,C41] while there are a lot of researchers using purge gas pyrolysis system. The inert gases typically applied in the purge gas pyrolysis system are nitrogen, helium and argon and carbon dioxide [C4,C44], hydrogen [C55].

Geiszler and Koros [C44] had made comparison between these two types of pyrolysis system. They found that the vacuum pyrolysis produced more selective but less productive membranes than the inert purge pyrolized membranes. When an inert gas was used, the degradation process was “enhanced”, presumably due to increased gas phase heat and mass transfer. The inert gas molecules can produce a more open porous matrix in the carbon molecular sieve membranes by accelerating the carbonization reaction. Thus, a higher permeability and less selective pore structure can be obtained.

Vacuum pyrolysis was not applied in this research due to the limitation of the high cost equipment such as vacuum tube furnace. Since the inert purge gas pyrolysis is more simple system which able to produce excellent carbon membrane, this method was used in this study. Type of purge gas used in a pyrolysis process will not much affect the membrane performance. Geiszler and Koros [C44] had reported that there was only minor difference seen among the membranes pyrolyzed in 3 different purge gases: argon, helium and carbon dioxide. Numerous researchers used nitrogen as the purge gas for pyrolysis process. Therefore, in this study, the nitrogen was chosen as purge gas owing to it is an economic, common and available gas in the laboratory.

3.8.2 Pyrolysis Temperature

The pyrolysis temperature applied in previous studies varied in accordance with the precursor. The common carbonization temperatures used by the previous researchers were in the range of 500^{o}C – 1000 ^{o}C [C4]. Hayashi et al. [C30] suggested that the optimum carbonization temperatures are in the range of

600 ^{o}C – 900 ^{o}C. It is desirable to keep the processing temperature low enough to prevent graphitization especially for coke-forming precursor materials [C44]. In this research, the pyrolysis temperatures in the range of 250^{o}C – 800 ^{o}C were applied.

3.8.3 Heating Duration (Soak Time)

The influence of soak time on the carbon membranes performance was studied. The range of the heating duration studied in this research was between 10 min to 3 hours. Heating duration more than 3 hours were rarely applied by the carbon membranes researchers.

3.8.4 Purge Gas Flow Rate

Purge gas flow rate ranged from 20 cm^3/min to 200 cm^3/min were applied in the pyrolysis process to study the influence of the different purge gas flow rate on the performance of carbon membranes. Gas flow meter was used to control the required purge gas flowrates.

3.8.5 Heating Rate

Various heating rates have been used in previous study. The range is between 1 – 13.3 ^{o}C /min [C4]. The heating rate applied in the thermastabilization and carbonization process is generally low (a few °C) in order to prevent destruction caused by the release of the volatiles byproducts [B21-1.2]. Suda and Haraya [C4] reported that as the heating rate decreased, the pyrolization proceeds very slowly and the pore becomes smaller. This caused the increasing of selectivity and the decreasing of the permeability. Although low heating rate requires long operation time and increases the operating cost, researchers [C4] found that the membrane

pyrolized at the slowest heating rate exhibited the highest selectivity. Moreover, Petersen et al. [C12] proposed that low heating rates should assist the increase of crystallinity of carbon.

This research did not emphasis much on the influence of heating rate to the carbon membrane performance. Therefore, in this research, relatively low heating rate 9°C/min was used in order to prevent rapid release of gases during pyrolysis, which can disrupt or destroy the membrane integrity and structure prior to the formation of complete carbon membrane [C70].

3.9 Fourier Transform Infrared Spectroscopy (FTIR)

Fourier Transform Infrared Spectroscopy (FTIR) is a very useful tool to detect the existence of the functional groups in a membrane. The FTIR results can display the change of the functional groups and elemental in the membranes when they were heated from room temperature to 800^{o}C.

3.10 Scanning Electron Microscopy (SEM)

Scanning Electron Microscopy (SEM) can be used to observe the macroscopic structure of the carbon membranes. Image of fiber surface, skin layer structure and cross sections of membrane prepared under different carbonization condition can be obtained. Before SEM scans, the membrane samples had cut into small piece in liquid nitrogen and gone through a gold coating. SEM Machine – Philip XL-40 was used for the scanning purpose.

3.11 Thermogravimetry Analysis

Thermogravimetry analysis was used to study the weight loss of the membrane samples during heat treatment. The change of the weight will indicate the structure change in the membrane.

3.12 Pure Gas Permeation Measurement

In this study, pure gases were used for the permeation testing instead of mixture gas. A lot of researchers have used pure gas to characterize the permeation properties of the membranes [C1,C2,C5,C9,C13,C18,C24,C28,C29,C30,C31,C38,C39,C45,F1,F2]. It is reported that the permeability of the N_2 was approximately same for both single and binary system [C28]. Anshu Singh-Ghosal and Koros also found that pure gas permeability and selectivity were within 3% of the mixed gas permeation properties [C54]. Petersen et al. [C12] also reported that each component of gas in a gas mixture showed nearly identical permeation behavior with that of the single gas. It is owing to gas molecules of light component can by-pass the sorbed molecules (heavy component) through the slit shape pores in carbon membrane. They concluded that the separation of mixed gases by the carbon membrane or its selectivities could roughly be estimated using data of single gas permeances. The schematic diagram of pure gas permeation testing system is displayed in Figure 3.10.

However, characterization of carbon membranes by single gas components underestimates the true separation factor of a gas mixture. This is a consequence of the restriction of diffusion of non-adsorbable gases (O_2, N_2 and CH_4) by adsorbable gas (CO_2) of the gas mixture [C38]. It means that the real selectivity of membrane is higher than the measurement result [C5]. Pure gases O_2 (3.46 ⊕) and N_2 (3.64 ⊕) were used to analysis the permeation characteristics of the membrane. Therefore, the problem mentioned above does not exist. The values in brackets correspond to the kinetic diameter of gas.

The permeation testing method applied in this research was variable volume-constant pressure method. Permeation of gas was measured at ambient temperature [C10,C22,C31,C34,C44]. It was reported that carbon membranes could obtain highest separation factor at 25^{o}C for O_2/N_2, CO_2/CH_4 and CO_2/N_2 system [C6]. Pressure gauge was used to measure the feed in pressure to the system. The feed in pressures are within 1 to 6 bars. The feed in pressure adjusted by the regulator on the gas cylinder and the needle valve. The permeate side of membrane was maintained at atmospheric pressure [C21]. Ball valve A allowed the permeate gas flowing to the burette while the retentate gas was purged through the ball valve B.

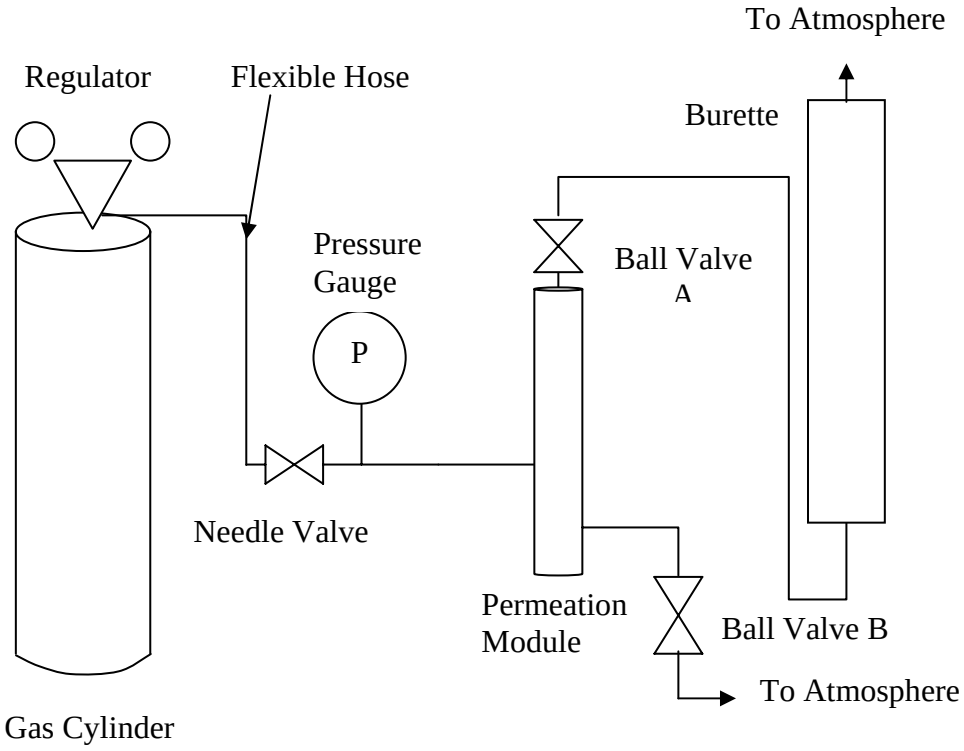

Figure 3.10: Schematic diagram of pure gas permeation testing system.

Hollow fiber membranes modules are one-end-opened types. One end of the fiber bundle was sealed in stainless steel tubing while the dead end part was potted in an aluminium cap both with the epoxy resin – Locite-L30 [C1,C24,C30]. The stainless steel tubing part was snapped off after the epoxy hardens [C10,C22].

There are two ways to feed in a gas into membrane module: bore side-feed and shell-side feed [F5]. The method used in this research was shell-side feed. It means that the feed gas was introduced to the outer surface of the hollow fiber and

the permeate gas would penetrate into the bore side. Previous researchers had used this method [C2,C8].

Simple soap film flow meter was used to obtain the permeation properties of the gas [C2,C8,C9,C30,C31,C37,C45,F1,F2] owing to it is suitable for the measurement of small and wide range flowrates. The performance of the carbon membrane can be characterized by two important parameters: permeability and selectivity [F1].

Permeability/Pressure-normalized fluxes, $\left(P/l\right)_i = \frac{Q_i}{\Delta p \cdot A}$

Q_i = Volumetric flow rate of gas i at standard temperature and pressure

Δp = Transmembrane pressure drop

A = membrane surface area

The permeability units usually applied in membrane research are GPU and Barrer.

GPU = $1\times10^{-6}\,\frac{cm^3(STP)}{cm^2 s \cdot cmHg}$

Barrer = $1\times10^{-10}\,\frac{cm^3(STP)\cdot cm}{cm^2 s \cdot cmHg}$

Ideal Separation factor/selectivity, $\alpha_{A/B} = \frac{P_A}{P_B} = \frac{(P/\ l)_A}{(P/\ l)_B}$

CHAPTER II

LITERATURE REVIEW

The development of porous inorganic membranes dates from before 1945, long before the development of today's synthetic organic membranes. Not much publicity was given to the early development of inorganic membranes because the first porous inorganic membranes were developed for separation of uranium isotopes ^{235}U and ^{238}U by the process generally known as gaseous diffusion. It is still the largest membrane separation process in terms of capital investment and energy requirements. Therefore, they were mainly used for military purposes or nuclear applications [C32,C42,C60].

Non-nuclear applications of inorganic membranes only started at the beginning of the 80's with Membralox produced by Ceraver (now SCT), Carbosep produced by SFEC (now TECHSEP) and Ceraflo produced by Norton (now by SCT) [C42]. The potential of inorganic membranes was not widely recognized until high quality porous ceramic membranes were produced for industrial usage on a large scale. These commercial ceramic membranes have consistent quality and narrow pore size distributions. Commercialization of ceramic membranes has been mostly the extension of technical development in gas diffusion membranes for the nuclear industry in the United State and France [C33]. Nowadays, inorganic membranes are used primarily for civilian energy-related applications. They have become important tools for beverage production, water purification and the separation of dairy products [C32]. Hence, they play a very important role in the separation processes of

industrial sector. Numerous European, American and Japanese companies are now competing to produce inorganic membranes [C42].

2.1 Inorganic Membranes

Hsieh has provided a technical overview of inorganic membranes in his paper [C33]. He divided the inorganic membranes into two major categories: porous inorganic membranes and dense (nonporous) inorganic membranes as shown in Figure 2.1. Besides that, porous inorganic membranes have two different structures: asymmetric and symmetric. Symmetric and asymmetric membranes are defined by the pore structure. Symmetric membranes exhibit homogeneous pore size or structure throughout the membranes while the asymmetric membranes have a gradual change of structure through the membranes [C42,C13]. Loeb and Sourirajan were the first to develop asymmetric membranes for desalination application due to the necessity of obtaining minimum effective thickness of membrane [T6].

Porous inorganic membranes with pores more than 0.3 nm usually work as sieves for large molecules and particles. Glass, metal, alumina, zirconia, zeolite and carbon membranes are commercially used as porous inorganic membranes. Other inorganic materials such as cordierite, silicon carbide, silicon nitride, titania, mullite, tin oxide and mica also have been used to produce porous inorganic membranes. These membranes vary greatly in pore size, support material and configuration [C33].

On the other hand, dense membranes made of palladium and its alloys, silver, nickel and stabilized zirconia have been applied or evaluated mostly for separating gaseous components. Application of dense membranes is primarily for highly selective separation of hydrogen and oxygen; transport occurs via charged particles. However, the dense membranes have limited industrial application due to their low permeability compared to porous inorganic membranes. Therefore, today’s commercial inorganic membranes market is dominated by porous membranes [C42,C33,C32].

Although inorganic membranes are more expensive than organic polymeric membranes, they possess advantages of: temperature and wear resistance, well-defined stable pore structure, and chemically inertness. These advantageous characteristics encouraged many researchers in the early 1980s to investigate the gas separation properties of these membranes, especially porous inorganic membranes. Furthermore, many studies regarding applications of inorganic membrane reactors have been carried out [C32].

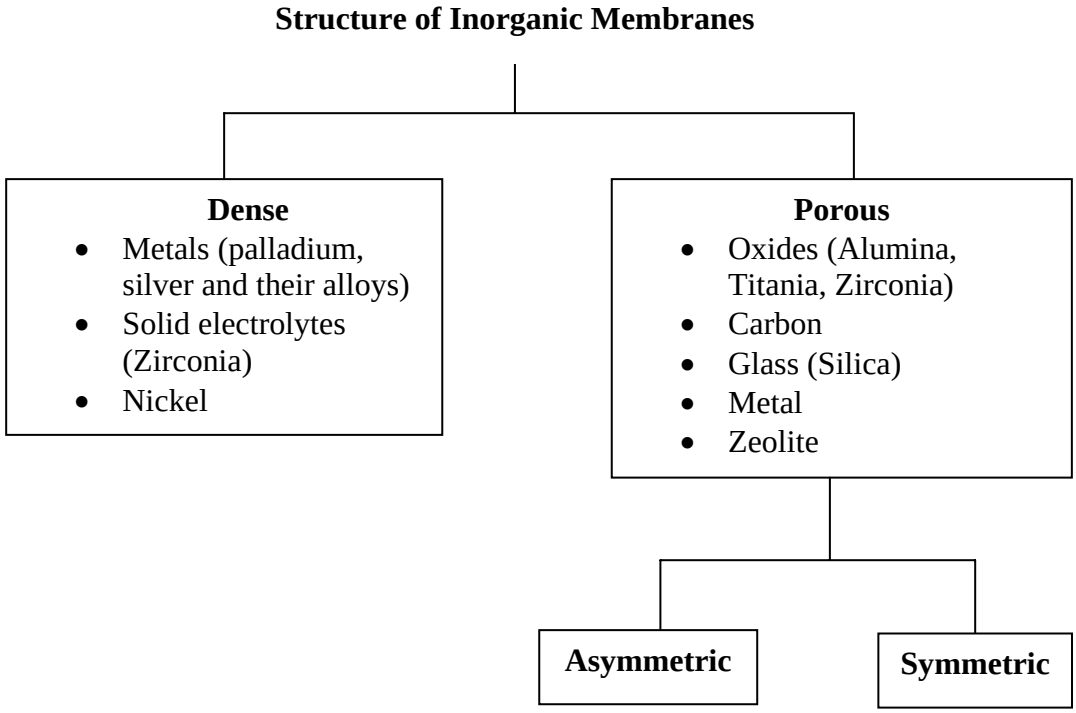

Figure 2.1: Structures of inorganic membranes

At present, interest in the development of porous inorganic membranes providing better selectivity, thermal stability and chemical stability than polymeric membranes has grown. The main interest and attention have been focused on materials that exhibit molecular sieving properties such as silica, zeolites and carbon [C6,C39], which appear to be promising in separation of gas as shown in Figure 2.2 [T9]. Figure 2.2 showed that the molecular sieving membranes providing higher permeability and selectivity than the upper limit performance of polymeric membranes. It means that the upper bound for polymeric materials does not constrain the nonpolymeric molecular sieve materials [G2].

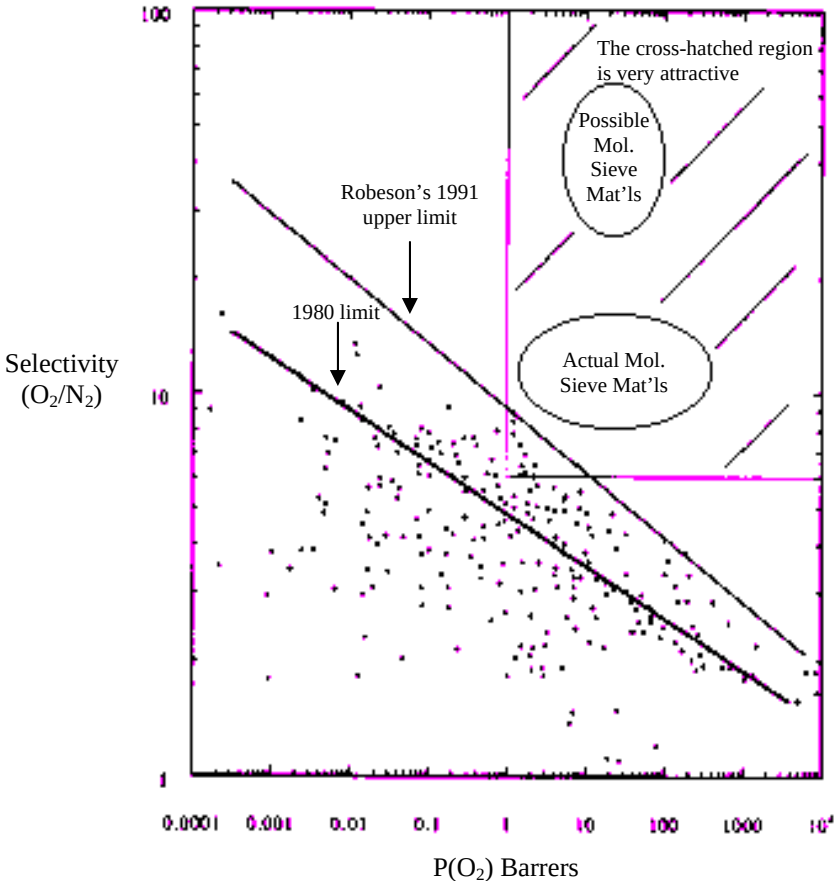

Figure 2.2: Upper limit performance of polymeric membranes [T9].

Silica-based inorganic membranes selectively separate hydrogen from other gases but permselectivity between similar-sized molecules such as oxygen and nitrogen is not sufficient [C30,C39]. This is due to the existence of defects/ "pin-hole" in the permselective layer [C39,C55]. In order to eliminate membrane defects, silica materials required synthesis in a clean room environment [C25]. In addition, there was no report on the application of silica membranes for the alkene/alkane separation, which contain the same number of carbon atom [C45].

Zeolites with a well-defined micropores constitute an excellent material to prepare gas separation membranes [C39]. Zeolites can separate isomers, such as i-butane and n-butane. Nevertheless, there were also no reports regarding the separation of alkene/alkane separations. Moreover, it is difficult to obtain a crack-free, large continuous thin film formed by zeolites crystals. The existence of intercrystallite voids dramatically reduces the permselectivity [C30,C15,C39,C45,C54].

Advantages of carbon molecular sieve compared with commercial molecular sieving zeolites including shape selectivity for planar molecules, higher hydrophobicity, higher resistance to both alkaline and acid media as well as better thermal stability under inert atmosphere at higher temperature [C78,C79]. Hence, it is more feasible to form carbon molecular sieve membranes because it has numerous advantages. Besides that, there were not many researches in this field.

2.2 Transport Mechanism of Inorganic Membranes

Mass transfer of gas through a porous plug can involve several different processes, depending on the nature of the pore structure and the solid [C26]. There are four different mechanisms for separation of a gas mixture through a porous membrane: Knudsen diffusion, partial condensation/capillary condensation, surface diffusion/selective adsorption and molecular sieving [C17,C33].

2.2.1 Knudsen Diffusion

Rao and Sircar [C46] had reported that dominant diffusion happens in a porous membrane is depending on the pore diameter of the membrane as shown in Table 2.1. Gas transport will occur predominantly by Poiseuille flow or viscous diffusion when the mean-free-path of the gas is much smaller than the pore diameter [C60] or gas molecules collide preferentially with each other instead of the pore wall [G2]. In other words, the membrane has large pores and no separation occur.

On the other hand, if the mean-free path of the gas is much larger than the pore diameter and the penetrant gas is very weakly adsorbed on the microporous medium, the gas transport mechanism dominant in the membrane is Knudsen diffusion [C60]. Separation of these membranes is based on the differences in the molecular weighs of the components of a gas mixture. The more rapidly moving low-molecular weight gas executes more frequent diffusional steps because it hits the

wall more frequently. The selectivity is equal to the square root of the molecular-weight ratio of the largest to smallest gas [G2]. It has very low selectivity and not practical to applied in the industry separation process [C17]. Knudsen diffusion is generally exists when the pore diameter measures around 50 – 100 ⊕ under pressure or 50 – 500 ⊕ in the absence of a pressure gradient [C33].

Table 2.1: Dominant diffusion occurs in different pore diameters

Dominant Diffusion	**Pore Diameters**
Viscous Diffusion	> 1000 ∑
Knudsen Diffusion	10 – 1000 ∑
Capillary Condensation	> 30 ∑
Activated Diffusion	< 10 ∑
- Surface Diffusion	➢ 5 – 7 ∑
- Molecular Sieving	➢ 3 – 5 ∑
Solution Diffusion	2 – 3 ∑

2.2.2 Surface Diffusion (Selective Adsorption)

Surface diffusion is important when one component is preferentially adsorbed or more strongly adsorbed than another component because the selectivity of separation for this transport mechanism is primarily governed by the adsorption selectivity between the components of a gas mixture. This transport mechanism happens when the adsorbed component diffuses faster than the other non-adsorbed components as the gas mixture accumulates on the pore surface. It means that certain components of the mixture are selectively adsorbed into the pores of the membranes and then they move across the membrane on the pore surface by surface diffusion. The separation mechanism in surface diffusion membrane is illustrated in Figure 2.3. Due to relatively lower activation energy required for this process, the surface diffusivity of the adsorbed gas can be very high. Besides that, the adsorbed molecules tend to create a hindrance for the transport of smaller non-adsorbed molecules through the void space in the pores. The adsorbed components then desorb at the low-pressure side to form permeate stream. Surface diffusion is important at a

pore diameter of 10 – 100 ⊕ or when specific surface area is large [C17,C33,C46,G1].

Nanoporous carbon membranes have this type of transport mechanism. Adsorption-selective carbon membranes separate non-adsorbable or weakly adsorbable gases (O_2, N_2, CH_4) from adsorbable gases, such as NH_3, SO_2, H_2S and CFC [C57]. Pore size and physiochemical nature of the pore surface play a significant roles in determining the separation efficiency of these membrane [C17].

2 main advantages of these membranes are: the diffusing gas can permeate across the membrane in order to obtain practical separation without requirement for a very large partial pressure gradient. Besides that, larger or more polar molecules of a gas mixture can be selectively separated from the smaller molecules [C17,C46]. In other words, the permeate stream contains larger sized penetrant while the smaller component was retained. This type of membranes is preferred to be used in the separation process, where the required product having larger molecular size. Additionally, that is no requirement for further product compression owing to the resulting product can be produced at the feed-gas pressure [C46].

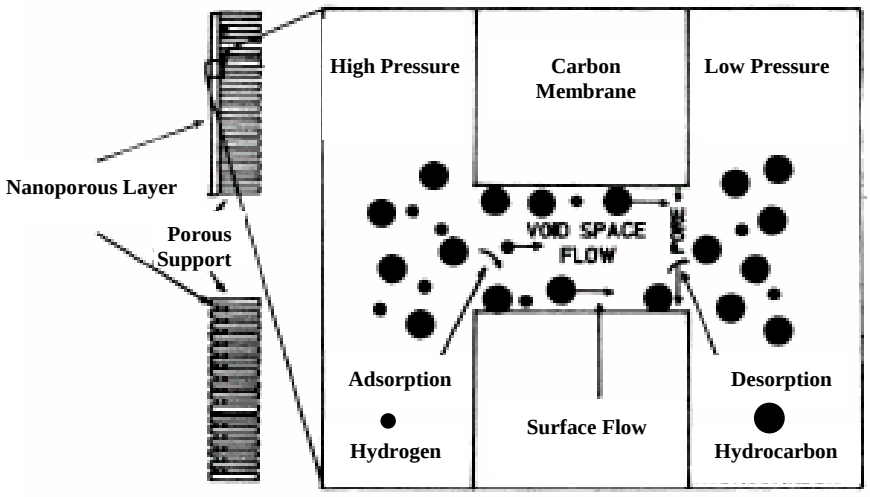

Figure 2.3: Separation mechanism in surface diffusion membrane [C17]

2.2.3 Capillary Condensation

At a relatively low temperature (for example near 0^oC), selective condensation of one or more components of the gas mixture and the condensed gases occupy the pores as a liquid followed by diffusion of condensed molecules through the liquid-filled pores. When other gases do not dissolve in the condensed component, separation occurs. This phenomenon happens in H_2S/H_2 and SO_2/H_2 system in which H_2S and SO_2, respectively condense in the pores and diffuse across the membrane; while H_2 in both cases is blocked from the pores as H_2 does not dissolve in either H_2S or SO_2 [C33,C46]. These membranes require the pore size in the range of pore diameter more than 30∑ and can achieve very high selectivity [C17].

2.2.4 Molecular Sieving

Carbon molecular sieve membranes have been identified as very promising candidates for gas separations, both in terms of separation properties and stability. The predominant transport mechanism of carbon membranes is molecular sieving as shown in Figure 2.4. Carbon molecular sieve materials are globally amorphous materials devoid of long-range order. Dislocation in the orientation of aromatic microdomains in the glasslike matrix gives rise to free volume and ultramicroporosity. The ultramicropores are usually considered to be nearly slit-shaped and the pore mouth dimensions are similar to the diameters of small molecules [C72].

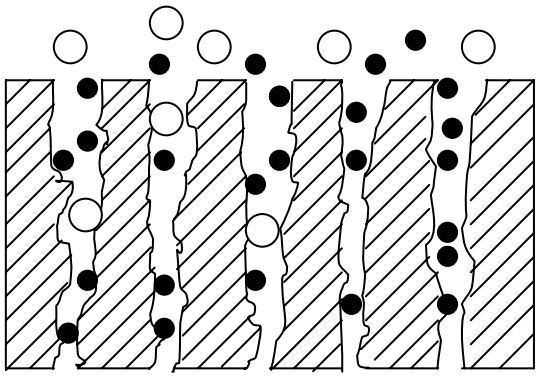

Figure 2.4: Typical molecular sieving transport mechanism

The carbon membranes contain constrictions in the carbon matrix that approach the molecular dimensions of the absorbing species [C10]. Molecules that are three-dimensionally smaller than the size of the slit width or planar shape with small cross-sections are selectively permeated through the molecular sieve carbon [C80]. Hence, carbon molecular sieve membranes are able to separate the gas molecules with similar size effectively. According to this mechanism, the separation is caused by passage of smaller molecules of a gas mixture through the pores while the larger molecules are obstructed. It exhibits high selectivity and permeability for the smaller component of a gas mixture [C17,C74].

The carbon matrix is assumed to be impervious, and permeation through carbon membranes is attributed entirely to the pore system [C35,C36]. The technique of activation or partial burnoff, which is used to enlarge the pore system in carbon, together with annealing at high temperatures in an inert atmosphere which brings about pore closure, has been employed recently to prove that the permeability of gases through the carbon membranes proceeds through a pore system of molecular dimensions. The pore system consists of relatively wide openings with narrow constrictions. The openings contribute the major part of the pore volume and responsible for the adsorption capacity, while the constrictions are responsible for the stereoselectivity of pore penetration by host molecules and for the kinetics of penetration [C36]. Hence, the diffusivity of gases in carbon molecular sieve change abruptly depending on size and shape of molecules because the carbon molecular sieve has ultramicropores with critical pore mouth dimensions and pores size similar to the dimension of gas molecules [C5,C72]. The pore size in the carbon molecular sieve depends upon a balance between removal of O_2 containing groups on the surface around the pore mouth (pore enlargement) and crystallite rearrangement enhancing sintering (pore shrinkage) [C80].

Kusakabe et al. [C28] have proposed that there are different types of pore shape in molecular sieving membranes. Three different permeation models for silica membrane, Y-type zeolite membrane and carbon molecular sieve membrane were reported in their paper. Figure 2.5 shows a schematic microstructure of a carbonized membrane while Figure 2.6 presents three permeation models for microporous membranes.

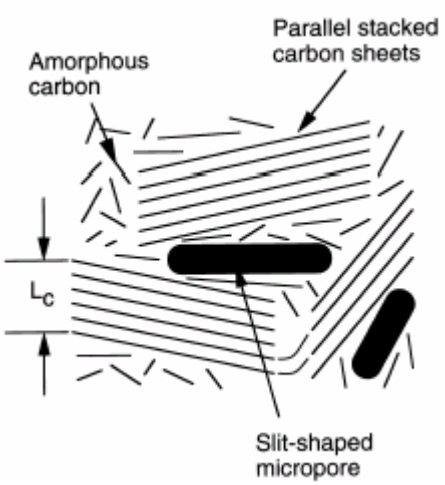

Figure 2.5: Schematic microstructure of a carbonized membrane

(a) Cylindrical pore, $d_p < d_{N2} + d_{CO2}$
(silica membrane)

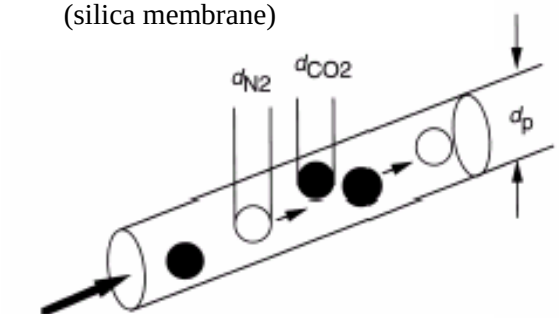

(b) Cylindrical pore, $d_p > d_{N2} + d_{CO2}$
(Y-type zeolite membrane)

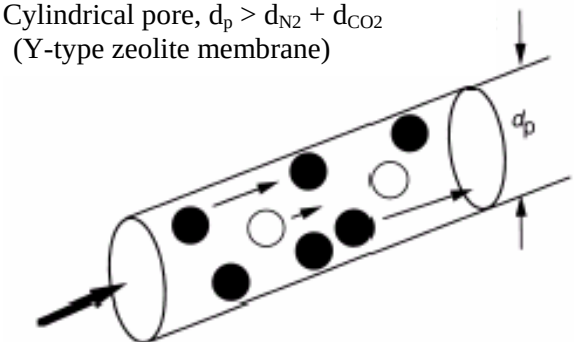

(c) Slit-shaped pore, $d_p < d_{N2} + d_{CO2}$ (CMS membrane)

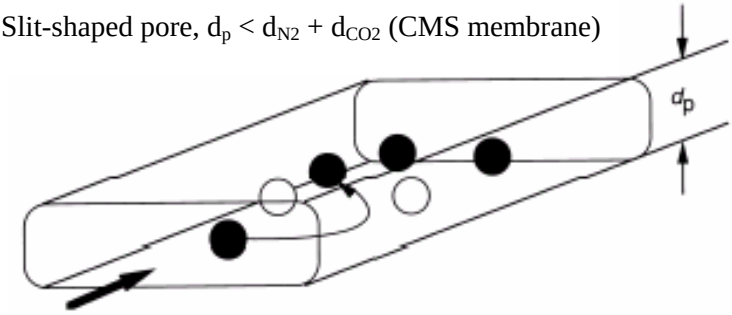

Figure 2.6: Permeation models for microporous membranes [C28]

As shown in the Figure 2.6, silica membranes have cylindrical pore having a size of $d_p < d_{N2} + d_{CO2.}$ Therefore, CO_2 permeation is limited by the permeation of N_2 because CO_2 and N_2 molecules, which are aligned in the pore unable to pass one another. The Y-type zeolite membranes have larger cylindrical micropores with $d_p > d_{N2} + d_{CO2}$. In this case, adsorptive molecules, CO_2 are concentrated on the pore wall and outrun non-adsorptive molecules, N_2 by a surface diffusion mechanism. On the other hand, carbon molecular sieve membranes have slit-shaped pores, which can distinguish sizes of alkane and alkene. In slit-shaped pores system, the gas molecules can move two-dimensionally and pass one another by moving to the wider side of the slit. The surface diffusion will not occur in this type of carbon membranes because the pore size is too narrow for adsorptive molecules to be concentrated on the pore wall. Due to the special shape of carbon molecular sieve membranes, the permeation results for CO_2 and N_2 obtained from single and binary system only displayed a minor difference [C28].

Carbon molecular sieves are porous solids that contain constricted apertures that approach the molecular dimensions of diffusing gas molecules. This similarity in pore mouth and gas molecules enhances the interaction between the pore wall and diffusing molecule. At these constrictions, the interaction energy between the molecule and the carbon is comprised of both dispersive and repulsive interactions. When the opening becomes sufficiently small relative to the size of the diffusing molecule, the repulsive forces dominate and the molecule requires activation energy to pass through the constrictions. In other words, smaller molecules experiences lower activation barrier to diffuse through the small micropore mouth since the repulsive forces is lower. In this region of activated diffusion, molecules with only slight differences in size can be effectively separated through molecular sieving [C22,C72]. The mechanism of gas permeation and uptake through porous solids is thus closely related to the internal surface area, dimensions of the pores and to the surface properties of the solid, rather than to the bulk properties of the solid as in the case with polymers [C36].

There are a lot of methods to prepare porous inorganic membranes. They consisted of phase separation and leaching, particle dispersion and slipcasting, anodic oxidation, thin-film deposition methods, track-etch method and pyrolysis

[C33], which will be discussed in next section. Carbons usually are produced by pyrolysis of a great variety of organic residues, synthetic polymers and natural coals in an inert atmosphere [C35]. However, molecular sieves carbon membranes suitable for gas separation are prepared by pyrolyzing thermosetting polymers. Carbon molecular sieve membranes with pore diameter 3-5 ⊕ have ideal separation factor for various combinations of gases ranges from 4 to more than 170. The ideal separation factor for N_2/SF_6 and He/CO_2 are 4. The values are in the range of 20 – 40 for He/O_2, He/N_2 and He/SF_6 separation. Meanwhile, ideal separation factor for O_2/N_2, H_2/N_2 and O_2/SF_6 are 8, 10 – 20 and more than 170 respectively [C33]. The permeation characteristics of the molecular sieve carbon membrane can be varied by changing the high temperature treatment parameters [C18].

The difference between structures of adsorption-selective carbon membranes (ASCM) with carbon molecular sieve membranes (CMSM) concerns the micropores. The definition of pore size according to the recommendation of IUPAC has been summarized in the Table 2.2. Adsorption-selective carbon membranes (ASCM) have a carbon film with micropores slightly wider than carbon molecular sieve membranes (CMSM), probably in the range of 5 – 7 ⊕ [C57].

Table 2.2: Definition of pore size [C63]

Type of Pore	Pore Size
Micropore	< 20 ⊕
-ultramicropores	< 7 ⊕
-supermicropores	7 ⊕ - 20 ⊕
Mesopore	20 ⊕ - 500 ⊕
Macropore	> 500 ⊕

It is known that the performance of an asymmetric membrane is dependent on the thin active layer [D1]. Meanwhile, the great difference between carbon asymmetric membranes and polymeric asymmetric membranes is the skin layer. Comparing with polymer membranes, carbon membranes may be considered as a refractory porous solid where, the permeates are non-soluble and merely penetrate through the pore system [C18]. The tiny (2 – 4⊕) short-lived intersegmental gaps that spontaneously appear in the selective layers to allow diffusion of gas through

conventional polymeric membranes are not considered as pores. Molecular sieving transport mechanism is greatly different with the transport mechanism of polymer membranes – solution-diffusion mechanism. The Figure 2.7 shows the solution-diffusion mechanism in the dense layer of a polymeric membrane. Size (diffusivity) and condensability (solubility) selectivity factors interact with polymer to determine which component passes though the membrane faster [G2].

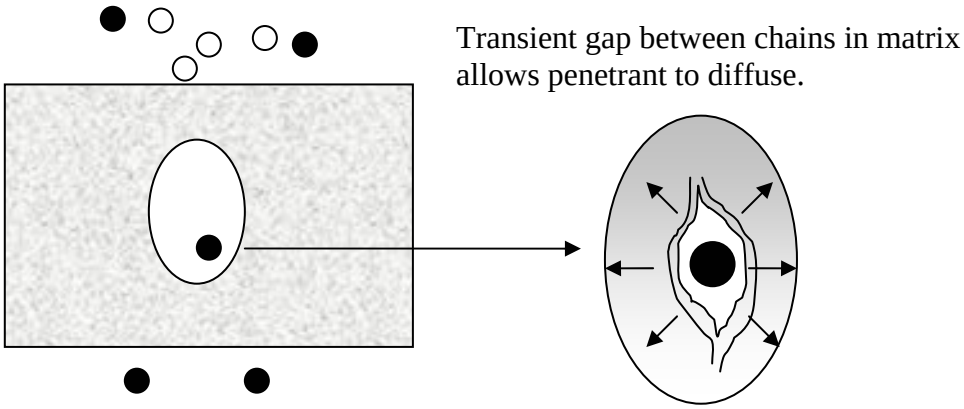

Figure 2.7: Solution-diffusion transport mechanism [G2]

In addition, diffusion on the asymmetric polymer hollow fiber membranes occurs in free space holes made by thermal motion of the polymer chains and those that existed originally because the polymer is the glassy polymer. On the other hand, the diffusion of the gases on the asymmetric carbon membrane occurs in holes that existed originally. It is proposed that the activation energy of the diffusion on the asymmetric carbon membranes are smaller than those on the asymmetric polymer hollow fiber membranes for gases especially having larger molecular size. As a result, the selectivities for the gas pairs such as H_2 hydrocarbons, CO_2 hydrocarbons, O_2/N_2 on the asymmetric polymer membrane decrease remarkably as the measurement temperature increases. However, the selectivities of the carbon membranes only decrease slightly [C2].

However, carbon membranes require very fine control of the pore sizes (diameter < 4⊕) and require operation at an elevated temperature in order to provide practically acceptable flux for the smaller molecules due to membrane thicknesses several microns [C17]. The influence of adsorption of permeates on the pore walls of

carbon have to be taken into consideration, especially in the case of penetrants with relatively high boiling point [C18].

2.3 Preparation Methods of Porous Inorganic Membranes

2.3.1 Phase Separation and Leaching (Glass membranes)

Glass membrane with a symmetric structure (isotropic sponge) of interconnected pores can be prepared by thermally demixing a homogeneous borosilicate glass (Na_2O-B_2O_3-SiO_2) phase into two phases by heating to 550°C – 800°C. The borate phase (Na_2O-B_2O_3-) is then removed by acid leaching creating a microporous silicon dioxide SiO_2-rich phase, which is insoluble boric phase rich in alkali. This technique can be used to produce either porous glass tubes or hollow glass fibers. The advantage of glass membranes is that capillaries (hollow fiber) can be easily formed and can be further modified to porous hollow fiber membranes. However, the instability of the surface is the main disadvantage of a porous glass membrane [C42,B6-2.2].

2.3.2 Anodic Oxidation (Anodic membranes)

This method is used to produce the commercial ANOPORE membranes. One side of a thin, high-purity aluminium foil is anodically oxidized in an acid electrolyte, which may contain sulfuric, phosphoric, chromic or oxalic acids. The unaffected part/unoxidized metal remaining on the other side is then removed by dissolution in a strong acid, leaving a regular pattern of pores. The membranes obtained are not stable under long exposure to water and having symmetric structure with a network of distinctive conical pores perpendicular to the surface of the membrane. Asymmetric structure with a thick layer of large pores and a thin layer of small pores connected to the large ones can be obtained by treated in hot water or in a base [C42,B6-2.2].

2.3.3 Particle Dispersion and Slip Casting (Ceramic membranes)

Composite ceramic membranes can be prepared by slip casting from particle dispersion. Slip is referred to colloidal suspension and polymeric solution. These particles and colloidal suspensions are obtained mainly by the so-called sol-gel process. Particles are deposited onto a porous support in one or more layers by dipping or casting. The dispersion medium is forced into the pores of the support by a pressure drop created by a capillary action of the microporous support. At the interface the solid particles are retained and concentrated at the entrance of pores to form a gel layer [C42,B6-2.2,B6-2.3].

2.3.4 Sol-gel Process

The sol-gel can be categorized into two main routes consisting colloidal suspension route and polymeric gel route. In both routes, a precursor is hydrolysed while a condensation or polymerization reaction occurs simultaneously. The precursor is either an inorganic salt or a metal inorganic compound [C42,B6-2.3].

2.3.5 Track-Etch

Track-etch method is applied for production of membranes with a very regular and linear shape pores. A thin layer of a material is bombarded with highly energetic particles from a radioactive source. The track left behind in the material is much more sensitive to an etchant in the direction of the track axis than perpendicular to it. This process has been applied on polymers (Nuclepore membranes) and on some inorganic systems like mica. The resulting membranes are attractive as model systems for fundamental studies [B6-2.2].

2.3.6 Pyrolysis

Polymers are coated onto porous supports and then degraded by controlled pyrolysis to produce an inorganic membrane. Silica membranes and carbon membranes can be produced by this method. Depending on the pyrolysis degree, the support can be weakly hydrophilic (low temperature) or more hydrophobic (high temperature). One or two layers of specific polymer are deposited onto the support surface. The carbon layer is formed by pyrolysis of the polymeric layer in a controlled environment (inert atmosphere) [C42,B6-2.2].

2.4 The Beginning of Carbon Molecular Sieve Membranes

The concept of carbon molecular sieve membrane or film for gas separation can be found in the early 1970. Barrer et al. compressed non-porous graphited carbon into a plug, called a carbon membrane [T1,C81]. The compression sintering of granular carbon is another synthetic method that has seldom been used besides pyrolysis of a polymeric precursor [C44]. Bird and Trimm used polyfurfuryl alcohol (PFA) to prepare unsupported and supported carbon molecular sieve membranes. During carbonization, they met shrinkage problem, which would lead to cracking and deformation of the membrane. Hence, they failed to obtain continuous membranes [C26].

Carbon molecular sieves produced from the pyrolysis of polymeric materials have proved to be very effective for gas separation in adsorption applications by Koresh and Soffer [C19,C19a,C19b,C19c] as well as Kapoor and Yang [C76]. Molecular sieve carbon can be obtained by carbonization of suitable carbon-containing materials. They are thermosetting polymers such as poly(vinylidene chloride) (PVDC), poly(furfuryl alcohol) (PFA), cellulose, cellulose triacetate, saran copolymer, polyacrylonitrile (PAN), phenol formaldehyde, polyimide, various coals such as coconut shell, graphite, pitch and plants under inert atmosphere or vacuum conditions [C19,C31]. They described that the pore dimensions of carbon depend on morphology of the organic precursor and the chemistry of pyrolysis [C35]. During

the research on molecular-sieve carbon adsorbents, they have shown that the molecular sieving effect of non-graphitizing carbons was extremely specific and adjustable by mild activation and sintering steps to the discrimination range 2.8 – 5.2Å [C18].

Pyrolysis of thermosetting polymers typically cellulosic, phenolic resin, oxidized polyacrylonitrile as well as pitch mesophase has been recognized to yield an exact mimic of the morphology of the parent material. They do not proceed through a melt or soften during any stage of the pyrolysis process. Hence, pyrolysis processes can produce carbon molecular sieve membranes from thermosetting polymer membranes [C35]. The interest in developing carbon membranes only grew after Koresh and Soffer [C35,C36,C18] had successfully prepared apparently crack-free molecular sieving hollow fiber membranes by carbonizing cellulose hollow fibers. They have shown the dependence of permeabilities and selectivities on temperature, pressure and extent of pore for both adsorbing and non-adsorbing permeates [C35,C18]. However, those membranes would be lack of mechanical strength for practical application.

2.5 Configurations of Carbon Membranes

Configurations of carbon membranes can be divided into two major categories: unsupported and supported carbon membranes [C6]. Unsupported membranes have three different configurations: flat (film), hollow fiber and capillary while supported membranes consisted of two configurations: flat and tube. Figure 2.8 shows various configurations of carbon membranes. The unsupported carbon membranes are more brittle than the supported carbon membranes. On the other hand, the supported carbon membranes require several times the cycle of polymer deposition-carbonization steps in order to obtain an almost crack-free membranes [C6].

The choice of a membrane configuration depends on many factors, consisting of nature of the polymer, the ease of formation of a given configuration and

structure, the reproducibility of a given structure, the membrane's performance characteristics and structural strength, the nature of the separation, the extent of use and the separation economics [F11].

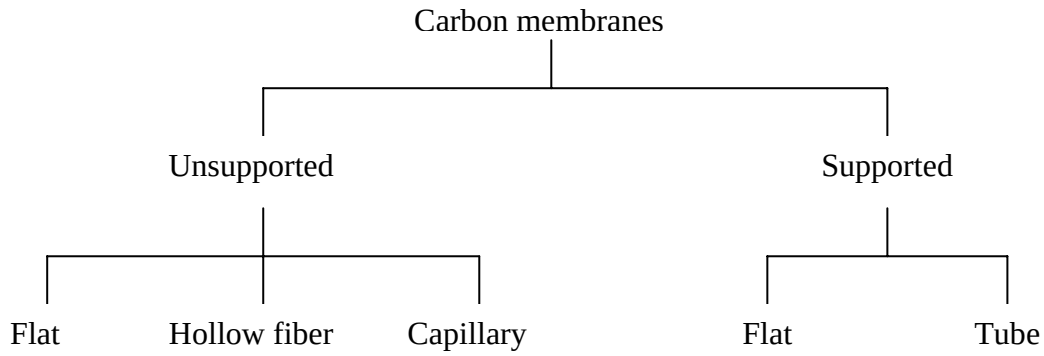

Figure 2.8: Configurations of carbon membranes

2.5.1 Supported and Unsupported Flat Carbon Membranes

A group of Japanese researchers, Hatori et al., have prepared porous carbon films from Kapton-type polyimide, including supported and unsupported carbon membranes [C20,C21,T3]. Hatori et al. reported that the carbon molecular sieve film used for gas separation is required to be as thin as possible in order to enhance the separation efficiency. However, the thin film should be supported with a porous plate for handling convenience. The flat homogeneous carbon films prepared by pyrolysis at 800 ^{o}C had O_2/N_2 selectivities of 4.2 [T3].

Rao and Sircar [C16,C17,C46] have introduced nanoporous supported carbon membranes, which were prepared by pyrolysis of polyvinylidene chloride layer coated on a macroporous graphite disk support. The diameter of the macropores of the dried polymer film was reduced to the order of nanometer as a result of a heat treatment at 1000^{o}C for 3 hours. These membranes with mesopores can be used to separate hydrogen-hydrocarbon mixtures by the surface diffusion mechanism, which selectively adsorbs gas molecules on pore wall. This transport mechanism differs from the molecular sieving mechanism. Therefore, these membranes were named as selective surface flow (SSF^{TM}) membranes. They possess a thin (2 – 5μm) layer of

nanoporous carbon (effective pore diameter in the range of 5 – 6Å) supported on a mesoporous inert support such as graphite or alumina (effective pore diameter in the range of 0.3 – 1.0μm). The procedures for making the selective surface flow membranes were described in those two authors' papers [C17,C46]. The requirement to produce a surface diffusion membrane has been described clearly in the author's paper [C46].

A solution to overcome reproducibility problems of nanoporous carbon (NPC) membranes has been introduced by Acharya and Foley [C25]. They have used spray-coating system for the production of thin layers of nanoporous carbon on the surface of a porous stainless steel support. A solution of poly(furfuryl)alcohol (PFA) in acetone was sprayed onto the support in the form of a fine mist using an external mix airbrush with nitrogen gas. This was the first reported technique for supported carbon membrane synthesis. The advantages of this preparation method are reproducibility, simplicity and good performance for oxygen-nitrogen separation. The resulting membranes were found to have oxygen over nitrogen selectivities up to 4 and oxygen fluxes on the order of 10^{-9} mol/m^2 s Pa.

Chen and Yang [C15] have prepared large, crack-free carbon molecular sieve membrane supported on a macroporous substrate by coating a layer of polyfurfuryl alcohol followed by controlled pyrolysis. Diffusion of binary mixtures was measured and the results were compared with the kinetic theory for predicting binary diffusivities from pure-component diffusivities. Good agreement was obtained between theoretical predictions and experimental data for binary diffusion.

Suda and Haraya [C40] have prepared flat, asymmetric carbon molecular sieve membranes, which exhibited the highest gas permselectivities among those in the past research by pyrolysis of a Kapton type polyimide derived from pyromellitic dianhydride (PMDA) and ODA. They used the permeation measurements and X-ray powder diffraction to relate the relationship between the gas permselectivity and microstucture of the carbon molecular sieve membrane. They proposed that that the decrease of the interplanar spacing, amorphous portion and pores upon heating might be the origin of the "molecular sieving effect".

Suda and Haraya [C4] also made a clarification of the factors that determine the microstructure and the permeation properties of carbon molecular sieve dense membranes derived from Kapton polyimide film. They have gained insight into the permeation mechanism through the study of permeability versus kinetic diameter in connection with diffusivity and sorptivity. They suggested that the factors determining the microstucture and gas permeation properties of carbon molecular sieve membranes are not completely open to controlled pyrolysis of a precursor, because these properties are significantly affected by several factors: the choice of polymer precursor, the membrane formation method and the pyrolysis conditions.

Shusen et al. [C13] reported that the asymmetric carbon membranes produced by Le Carbon-Lorraine using a two-step procedure (carbon support preparation in the first step and top layer deposition in the second step) seems to be complicated. By using this method, the porous carbon support is made by pyrolysis of a tube with 1mm wall thickness. On top of the support, thin polymeric films are deposited; followed by controlled pyrolysis to the desired pore shape. Hence, Shusen et al. used simpler and more flexible one-step preparation method (one heat treatment step for support and functional top layer) to fabricate asymmetric supported carbon membranes, consisting formation of phenol formaldehyde film followed by pyrolysis and unequal oxidation.

In this process, micropores were achieved as a result of small gaseous molecules channeling their way out of the solid matrix of the polymer during pyrolysis. The micropore structure was further widened by oxidation, which removed carbon chains in the pores. The pore structure was made narrower by high temperature sintering which shrinks the pore size. All of the preparation conditions which shrink the pore size of the carbon membrane would be beneficial for improvement of selectivities while the conditions for widening pore size should be favorable for increasing permeabilities [C37]. They have proposed that the key point to create a carbon membrane with asymmetric structure was to keep a different oxidation atmosphere on two sides of the membranes in the activation process, for example, a relatively strong activation condition on one side and a relatively weak activation conditions on the opposite side [C13,C37].

Kita et al. [C47] synthesized an unsupported polypyrrolone film by means of a casting method. The authors found that the membranes, which have been carbonized at 700^{o}C for 1 hour, gave the highest performance in their research. The membranes exhibited excellent stability up to 500^{o}C under nitrogen atmosphere, without weight loss.

Liang et al. [C31] have produced carbon membranes for gas separation from coal tar pitch. The result showed that the 'separation power', which is refer to production of permeability by selectivity of carbon membranes of carbon membranes prepared from coal tar pitch was generally higher by at least 3 orders of magnitude compared with polymeric membranes for H_2/O_2 and H_2/N_2 separation.

Spain researchers, Fuertes and Centeno have investigated the method to prepare flat, supported carbon molecular sieve membranes by using different polymeric or precursors. They used BPDA-pPDA [C3,C6], phenolic resin [C5] as precursor to make flat carbon molecular sieve membranes supported on a macroporous carbon substrate.

In another study, they chose polyetherimide as a precursor to prepare flat, supported carbon molecular sieve membranes. Method for the preparation of carbon molecular sieve membranes from a polyetherimide and their structures as well as gas permeation properties have been described in their paper [C7]. Polyetherimide was chosen because it can be used economically. On the other hand, these polyetherimide carbon membranes showed similar performance with the carbon molecular sieve membranes prepared by Hayashi et al. [C9], which were obtained from a laboratory-synthesized polyimide (BPDA-ODA).

Furthermore, they also used two other commercially available polyimide-type polymers, Matrimid and Kapton to prepare supported carbon composite membranes in a single casting step [C38]. They reported that the different structures of carbon membranes could be obtained depending on the polymeric precursors, the casting solution and the preparation condition. However, preparation conditions have a great effect on the structure and separation properties of the Matrimid-based carbon membranes.

Recently, they have investigated the preparation of supported carbon molecular sieve membrane formed by a microporous carbon layer, obtained by carbonization of a poly(vinylidene chloride-co-vinyl chloride) (PVDC-PVC) film [C39]. They discovered that the oxidation of PVDC-PVC samples did not significantly affect the micropore volume of the carbonized materials. However, the pretreatment in air at 200^{o}C for 6h leaded to a less permeable carbon membrane than the untreated membrane but much more selective. The selectivity of CO_2/N_2 was increased from 7.7 to 13.8 after the pretreatment.

Some researchers have studied the entropic contributions to diffusivity selectivity as the polymer matrix evolved to a rigid carbon matrix [C54]. Polymer precursor, membranes pyrolyzed at intermediate steps in the pyrolysis process and finally pyrolyzed membranes were tested for the purpose to study the development of gas separation properties as the material progresses from a polymer to a completely carbonized membrane.

2.5.2 Carbon Membranes Supported on Tube

Hayashi et al. [C9] have produced carbon molecular sieve membranes by dip-coating of BPDA-4,4'-oxydianiline (ODA) solution on an α-Al_2O_3 porous support tube follow by pyrolysis at 500-900^{O}C in an inert atmosphere. In their study, the sorptivity and diffusivity of penetrants in the carbonized membrane were greatly improved because of the increased micropore volume (free space) and segmental stiffness. The selectivity of CO_2/CH_4 larger than 100 was achieved although BPDA-ODA membrane usually can only reached 65 at 35^{o}C. This indicated that the carbonization procedure was optimized and excellent permselectivities of penetrants were obtained.

They modified the resulting carbon molecular sieve membranes by chemical vapor deposition (CVD) using propylene as carbon source at 650^{o}C [C30]. At pyrolysis temperature 700^{o}C, the CVD modification was effective to increase the

CO_2/N_2 selectivity from 47 to 73 while O_2/N_2 selectivity increased from 9.7 to 14 because the pore structure was further controlled and the micropores were narrowed.

Hayashi et al. [C45, T5] also found that a carbonized membrane prepared with a BPDA-pp'ODA polyimide gave higher C_3H_6/C_3H_8 and C_2H_4/C_2H_6 permselectivities than those of polymeric membranes. This was in accord with the fact that carbonized membrane possess a micropore structure, which was capable of recognizing size differences of alkane and alkene molecules. In addition, Hayashi et al. [T5] evaluated the stability of a membrane based on BPDA-ODA polyimide and carbonized at 700^oC by exposing it to air at 100 ^oC for one month. It was suggested that the carbon molecular sieve membranes were usable for a prolonged period under an atmosphere that contains low levels of oxidants, which is refer to the level of oxidants in atmosphere air.

Their study also showed that the permeation properties of carbon membrane could be improved by treating carbon membrane under an oxidizing atmosphere. Hayashi et al. [T5] have oxidized BPDA-ODA carbon membrane with mixture of O_2-N_2 at 300 ^oC or with CO_2 at 800 – 900 ^oC. Nevertheless, excessive oxidation fractured carbon membrane. They concluded that carbonization under optimum condition shifted the trade-off relationship of the BPDA-pp'ODA polyimide membrane toward the direction of higher selectivity and permeability. The resulting membranes exhibited permeances approximately $1x10^{-8}$ $mol.m^{-2}s^{-1}Pa^{-1}$ for C_2H_4, $2x10^{-9}$ $mol.m^{-2}s^{-1}Pa^{-1}$ for C_2H_6, $4x10^{-9}$ $mol.m^{-2}s^{-1}Pa^{-1}$ for C_3H_6 and $1x10^{-10}$ $mol.m^{-2}s^{-1}Pa^{-1}$ for C_3H_8. The selectivities were 4-5 for C_2H_4/C_2H_6 separation and 25-29 for C_3H_6/C_3H_8 separation [C45].

Tennisson and co-workers [C23] have prepared microporous carbon membranes by carbonization and activation of an asymmetric phenolic resin structure comprising a dense resol layer, supported on a highly permeable macroporous novolak resin tube.

A BPDA-ODA/DAT copolyimide, which contains methyl groups; was used as a precursor for carbon molecular sieve membrane by Yamamoto et al. [C29]. Methyl groups would be expected to be decomposed during the post-treatment under

an oxidative atmosphere and to result in expanded micropores. They reported that the permeation properties of the resulting membranes were dependent on the composition of the precursor films, carbonization temperature and oxidation conditions. In spite of the permeance increasing with increasing permeation temperature, the separation coefficients were not greatly influenced by the oxidation and carbonization treatments.

They suggested that the oxidation in air by increasing temperature up to 400^{o}C with a one-hour hold and carbonization up to 700^{o}C was most suitable for increasing permeance with no damage in separation coefficient. The carbon membranes gave $3x10^{-8}$ $molm^{-2}s^{-1}Pa^{-1}$ for CO_2 permeance and the separation coefficient of CO_2/CH_4 reached 60 at permeation temperature of 35^{o}C. In addition, the trade-off line for the BPDA-ODA carbon membrane for O_2/N_2 system was 3-fold higher in the direction of separation coefficient than that for polyimide membrane reported by Stern. They have concluded that optimization of the treatment procedure was more important than changes in diamine portion of the copolyimide [C29].

A study on the structure of the phenol-formaldehyde carbon membrane has been conducted by Steriotis et al. [C77]. They studied bulk and skin structure of the membrane by using various characterization methods including nitrogen adsorption, small-angle neutron scattering and scanning electron microscopy (SEM).

Kusakabe et al. [C28] made a further study regarding carbon molecular sieve membranes, which were formed by carbonizing BPDA-pp'ODA polyimide membranes at 700^{o}C and then oxidized with either an O_2-N_2 mixture or pure O_2 at 100^{o}C – 300^{o}C under controlled conditions. The study showed that the oxidation increased permeance without greatly damaging the permselectivities. This was due to the oxidation at 300^{o}C for 3h significantly increased the micropore volume but the pore size distribution was not broadened. The result was similar with the author previous research [T5] regarding the effect of oxidation on gas permeation of carbon molecular sieving membranes based on BPDA-pp'ODA polyimide.

They also formed the condensed polynuclear aromatic (COPNA) resin film on a porous α-alumina support tube. Then, a pinhole-free carbon molecular sieve

membrane was produced by carbonization at 400 – 1000^{o}C [C8]. The mesopores of the COPNA-based carbon membranes did not penetrate through the total thickness of each membrane and served as channels, which increased permeances by linking the micropores. Molecular sieving carbon membranes produced using COPNA and BPDA-pp'ODA polyimides showed similar permeation properties although they had different pore structures. At permeation temperature 100^{o}C, the selectivities of CO_2/N_2 were 17 for pyrolysis temperature at 700^{o}C and 19 for pyrolysis temperature at 800^{o}C respectively. This suggests that the micropores are responsible for the permselectivities of the carbonized membrane.

Research team leaded by Sircar has produced tubular support selective surface flow carbon membranes for gas separation application [C69]. They coated the bore side of the tube using polyvinylidene chloride-acrylate terpolymer latex. The resulting membranes exhibited very good separation properties at low to moderate feed gas pressure. Details of the practical applications and advantages of the selective surface flow membranes had reported in their paper [C69]. The membrane has been successfully tested for H_2 enrichment applications from fluid catalytic cracker and H_2-PSA off-gases at low pressures. The use of SSF membrane-PSA hybrid system is very attractive for the production of high purity H_2 from a waste gas [C71]. In addition, they found that the SSF membrane could be efficiently applied for the separation of H_2S-CH_4 gas mixtures without high feed gas pressures. Experiments also carried out to evaluate the effect of feed gas pressure, feed gas composition and permeate gas pressure on the separation of binary H_2S-CH_4 gas mixtures [C79].

On the other hand, Wang et al. [C56] used a gas phase coating technique, vapor deposition polymerization (VDP) to prepare supported carbon membranes from furfuryl alcohol. They reported that the membranes prepared by VDP have comparable CO_2/CH_4 selectivities but lower CO_2 permeabilities than certain PFA-based membranes prepared by dip-coating techniques. The selectivity for CO_2/CH_4 separation was 80 – 90 with CO_2 permeances in the range of $27x10^{-10}$ – 58 $x10^{-10}$ $molm^{-2}Pa^{-1}s^{-1}$.

There are other different coating methods on porous stainless steel support media in the production of carbon membranes supported on tube: brush coating,

spray-coating and ultrasonic deposition of the polymer resin. Shiflett and Foley have reported various approaches to preparing carbon molecular sieve layers on the stainless steel support by ultrasonic deposition [C55]. They reported that the reproducible production of nanoporous carbon membranes could be achieved through automated ultrasonic spray system [C70]. Figure 2.9 shows the nanoporous carbon membrane produced. The permeances results for H_2, He and O_2 were reproducible within ±20% while separation factors reproducible within ±30%.

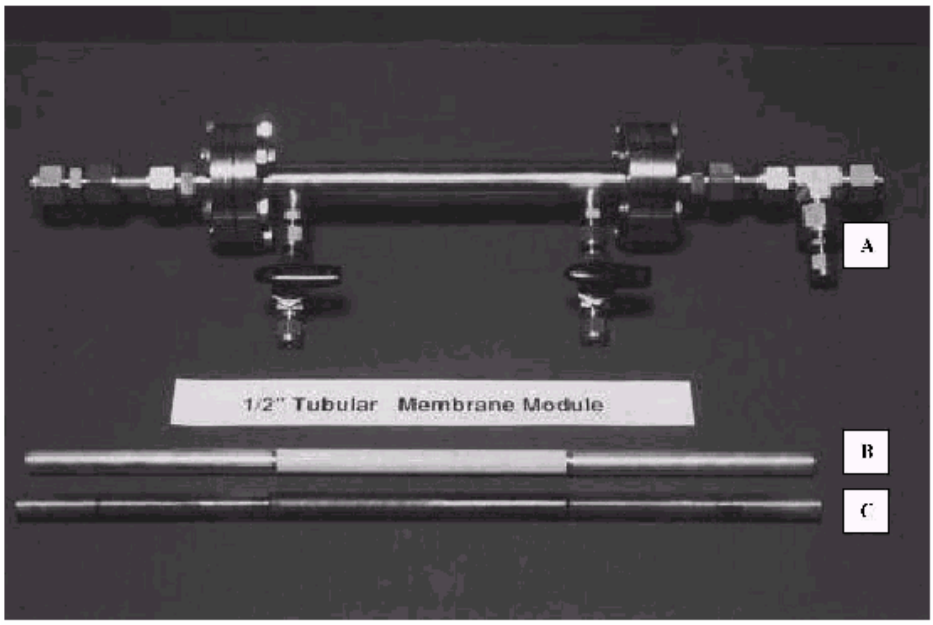

Figure 2.9: Membrane test module and supported nanoporous carbon membrane. (A) Membrane module, (B) sintered metal tube, (C) continuous carbon film supported on sintered metal tube [C70]

Besides that, Fuertes [C57] used phenolic resin to prepare adsorption-selective carbon membrane supported on ceramic tubular membranes. The dip coating technique was used in the research. Study also conducted to analysis the effect of the oxidation post treatment process on the separation properties of carbon membranes [C68]. It is reported that a carbon molecular sieve membrane can be transformed into an adsorption-selective carbon membrane by using air oxidation post treatment process. The post treatment would slightly widen the carbon micropores. Besides that, the study showed that the oxidation temperature more than

450°C and long oxidation time (6 hrs) would cause the loss of membrane separation properties.

2.5.3 Carbon Capillary Membranes

Damle et al. [C75] have put effort to modify the commercial liquid microfiltration carbon membrane to gas separation carbon membrane, which based on Knudsen diffusion mechanism. The techniques applied include dip coating of polymer precursors, in-situ polymerization and gas phase pyrolysis.

Haraya et al. [C41] have reported a novel preparation of asymmetric capillary carbon molecular sieve membranes from Kapton polyimide membrane and their gas permeation properties. Capillary carbon molecular sieve membrane must have controlled asymmetric structure, consisting of a dense surface layer with molecular sieving properties and a porous supporting layer in order to attain both high permselectivity and permeance. However, it is not easy to control the structure of the capillary carbon molecular sieve membrane. They described that the structure of membrane was formed in the gelation step of polyamic acid and was also maintained in the imidization and shrank about 30% at pyrolysation steps. They observed that the surface layer became thinner and the pore dimension became larger, with acceleration in the exchange rate of solvent with coagulant. Slow gelation process would result in a thicker dense surface layer.

Petersen et al. prepared carbon molecular sieve membrane (capillary tubes) by using precursor derived from Kapton [C12]. They worked at improving the fabrication method of capillary carbon membrane for high-temperature gas separations.

2.5.4 Carbon Hollow Fiber Membranes

Besides the configurations mentioned in the preceding section, there are also a lot of studies regarding carbon hollow fiber membranes. The main variation in the structure of the carbon hollow fiber membrane with the polymeric hollow fiber membrane has been shown in Figure 2.10.

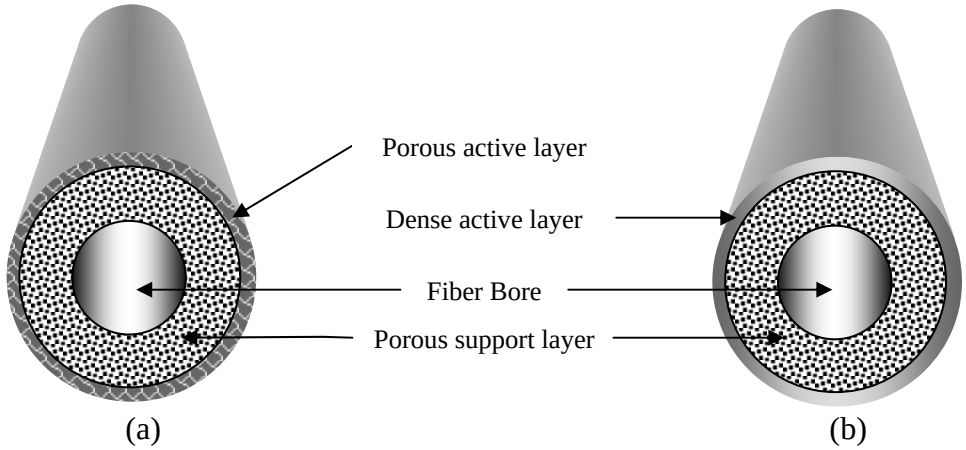

Figure 2.10: Comparison of carbon molecular sieve hollow fiber membrane (a) with the polymeric hollow fiber membrane (b)

Linkov et al. [C14] summarized a number of special techniques, which have been developed to obtain narrow pore-size distribution in carbon membranes. They consisted of introduction of monomers with low carbon content into polyacrylonitrile macromolecules, irradiation of polymer films with high-energy ions, in-situ polymerization on the surface of dip-coated polymeric precursors, treatment with concentrated hydrazine solution and the dispersion of a finely divided inorganic material in the casting solution of polyacrylonitrile (PAN).

They reported that the carbonization of highly asymmetrical PAN precursors, produced by the use of various combinations of solvent and non-solvents in precipitation media, resulted in the formation of a range of flexible hollow fiber carbon membranes with high porosity and good mechanical properties. Morphology of this type carbon membrane as well as the possibility of altering of the pore structure was studied. It was suggested that precursor preparation (solution formulation and fabrication procedure) and stabilization as well as carbonization conditions have possibility to alter the pore sizes of carbon membranes [C14].

Linkov et al. [C27] also used vapor-deposition polymerization method to coat hollow fiber carbon membranes. Then, the coated membranes were heated in a nitrogen atmosphere to produce composite carbon-polyimide membranes. The composite membranes had low wall and active skin thickness with good mechanical properties. They have resistance against high pressures and high flexibility.

Polyimide derived from a reaction of 2,4,6-trimethyl-1,3-phenylene diamine,5,5-[2,2,2-trifluoro-1-(trifluoromethyl)ethylidenel]-1,3-isobenzofurandione and 3,3',4,4'-biphenyl tetra carboxylic acid dianhydride was used by Jones and Koros to prepare carbon molecular sieve asymmetric hollow fiber membranes [C22]. Those membranes were developed and optimized for air separation applications. However, they were also effective for the separation of other gas mixtures such as CO_2/N_2, CO_2/CH_4 and H_2/CH_4 with the selectivities 55-56, 140-190 and 400-520 respectively. On the other hand, the selectivities for conventional polymeric membranes only reached 15-25 for CO_2/N_2 separation, 15-40 for CO_2/CH_4 and less than 200 for H_2/CH_4. It is noteworthy that the selectivities obtained were much higher than those seen with conventional polymeric materials without sacrificing productivity.

Jones and Koros have found a few problems or weakness of carbon membranes in their studies [C10,C34]. Carbons generally have nonpolar surfaces. As a result they are organophilic. Therefore, ultramicroporous carbon membranes would be very vulnerable to adverse effects from exposure to organic contaminants due to its adsorption characteristics of organics. Membrane performance will deteriorate severely if feed streams having as low as 0.1 ppm organics. As organic sorption proceeds, capacity for other compounds is diminished and membrane performance losses occur rapidly. Once a monolayer has been established, a prohibitive resistance to other permeating species exists.

However, a unique regeneration technique developed by Jones and Koros [C34] seem to be very promising for removing a number of organic contaminants. Pure propylene at unit or near-unit activity has found to be suitable for the regeneration process. The propylene most likely acted as a solvent, removing other sorbed compounds from the carbon surface. Propylene exposure resulted in a small

“opening up” of the pore structure and membrane recovery was significantly boosted.

Jones and Koros [C10] also found that the micropores of carbon membranes would gradually plugged with water at room temperature and resulting in the decrease of the non-polar gases permeabilities and its selectivities. The reason is the surface of membrane carbonized at relatively low temperature is affected by oxygen remaining in the inert purge gas during pyrolysis [C44]. The surface is partially covered with oxygen-containing functional groups, thus giving the membrane a hydrophilic character [C28]. The resulting oxygen-containing surface complexes will act as primary sites for water sorption. Sorbed water molecules then attract additional water molecules through hydrogen bonding, leading to the formation of clusters. The cluster grows and coalesces, leading to bulk pore filling. As the amount of sorbed water in microporous carbon adsorbents increases, it will greatly diminishing the diffusion rate of other permeating species [C10].

The problem can be overcome by coating the membrane with a highly hydrophobic film, which does not prohibitively reduce the flux of other permeating species. Therefore, the resulting carbon composite membranes demonstrated a greater resistance to the adverse effects from water vapor while retaining very good separation properties [C11]. Thus, Kusakabe et al. [C28] reported that the modification of the surface properties of carbon molecular sieve membrane is a key technology for the selective gas separation.

Geiszler and Koros [C44] have studied the effect of polyimide pyrolysis conditions on carbon molecular sieve membranes properties. They compared the carbon membrane performances prepared by vacuum pyrolysis and inert purge pyrolysis. In addition, they also studied other pyrolysis variables such as the processing temperatures, purge gas flow rate and residual oxygen concentration in the purge gas. They observed that pyrolysis atmospheres and flow rates of purge gas strongly influenced H_2/N_2 and O_2/N_2 selectivities of carbon molecular sieve membranes. In argon purge pyrolysis, the O_2/N_2 selectivity was 2.8 – 6.1 while the H_2/N_2 selectivity was 6.8 – 31.2. The selectivities were increased to 7.4 – 9.0 for O_2/N_2 and 64 – 110 for H_2/N_2 when the membrane carbonized in vacuum condition.

The purge gas flow rate changed from 20 cm^3/min to 200 cm^3/min had resulted in the increasing of permeability of O_2 from 0.05 – 0.54 GPU to 71 – 284 GPU. It is noteworthy that pyrolysis condition has significant influence to the carbon membranes performance.

Kusuki et al. [C2] have made the asymmetric carbon membranes by carbonization of asymmetric polyimide hollow fiber membranes. The effects of different experimental conditions on the membrane performance have been investigated. They reported that those carbon membranes showed high permselectivities compared with polyimide hollow fiber membranes. They achieved the selectivity of H_2/CH_4 ranging from 100 – 630 with permeation rate of H_2 ranging from 10^{-4} to 10^{-3} cm^3(STP)/(cm^2 s cmHg).

.

Tanihara et al. [C1] have made the asymmetric carbon membranes by carbonization of asymmetric polyimide hollow fiber membranes. In their study, they found that the permeation properties of carbon membrane were hardly affected by feed pressure and exposure of toluene vapor. Furthermore, there was only little change in the permeation properties of the carbon membrane with the passage of time.

Ogawa and Nakano [C24] have investigated the effect of gelation conditions on the properties of the carbonized membrane in their previous study. The carbonized hollow fiber membrane was formed by gelation of polyamic acid solution in a coagulant by phase inversion method, imidization and carbonization. The microstructure of the carbonized membrane was evaluated by the micropore volumes, which depended on gelation temperature and pH of coagulant. Hence, the gelation process was important to control microstructure, permeance and permselectivity of the carbonized membrane.

They observed that the gelation time was not a predominant factor to control the micropore volume, the permeances and CO_2/CH_4 permselectivity. However, they found that the gelation temperature would influence the permeation properties of the carbon membranes. They also reported that the permeance reduced with the increase of pH value of the coagulant. The micropore volume also decreased remarkably in

the alkali region, resulting in reduction of micropore size. However, the permselectivity increased with the increase of pH [C24].

They proposed that the most important factor to achieve both high permeance and high permselectivity in the carbonized membrane was pH control of the coagulant (water). They realized that the high permeance of CO_2 and the high CO_2/CH_4 permselectivity were obtained under the specific conditions of gelation: time 6h, temperature 275K and pH 9.4. They concluded that the transport of CO_2 was mainly governed by the adsorption effect and transport of CH_4 was restricted by the molecular sieving effect, yielding high CO_2/CH_4 permselectivity [C24].

They also investigate the difference in permeation behaviors of CO_2 and CH_4 between single component and multicomponent of CO_2/CH_4 system from the viewpoint of the microporous structure, which was created through the formation process of the carbonized membrane [C53].

Table 2.3 summarized the various configurations of carbon membranes produced by previous researchers. From the literature review, it is observed that most of the carbon membranes produced during 1980 until early 1990 were flat disk or flat sheet membranes. During the middle of 1990, carbon membranes supported on tube have been made followed with carbon capillary membranes and carbon hollow fiber membranes. Flat sheet or flat disk carbon membranes are more suitable for laboratory or research applications while carbon membranes supported on tube, carbon capillary membranes and carbon hollow fiber membranes are more practical and suitable to apply in industry.

The carbon membrane is preferable to be fabricated in asymmetric structure and capillary or hollow fiber configurations for commercial applications of membrane in order to increase its permeation products [C12].

Table 2.3: Configuration of carbon membranes produced by previous researchers

Researcher(s)	**Configuration**	**Period/Year**	**Reference(s)**
Ash et al.		1967-1968	C22
Barrer et al.		1973-1976	T1,C81
Bird & Trimm	Flat	1983	C26
Koresh & Soffer	Hollow fiber	1980-1987	C18,C19,C35,C36
Kapoor & Yang		1989	C76
Damle et al.	Capillary	1991	C75
Bauer et al.	Tube	1991	C43
Hatori et al.	Flat	1991-1992	C20,C21,T3
Rao & Sircar	Flat	1993	C16,C17,C46
Chen & Yang	Flat	1994	C15
Linkov et al.	Hollow fiber	1994	C14,C27
Jones & Koros	Hollow fiber	1994-1996	C10,C22,C34,C11
Hayashi et al.	Tube	1995-1997	C9,C30,C45,T5
Suda & Haraya	Flat, Capillary	1995-1997	C4,C40,C41,C48
Shusen et al.	Flat	1996	C13,C37
Kita et al.	Flat	1997	C47
Petersen et al.	Capillary	1997	C12
Kusuki et al.	Hollow fiber	1997	C2
Tennisson et al.	Tube	1997	C23
Yamamoto et al.	Tube	1997	C29
Steriotis et al.	Tube	1997	C77
Kusakabe et al.	Tube	1998	C28,C8
Sircar et al.	Tube	1997-1999	C71,C69,C79
Geiszler & Koros	Hollow fiber	1999	C44
Tanihara et al.	Hollow fiber	1999	C1
Okamoto et al.	Hollow fiber	1999	C49
Ogawa &Nakano	Hollow fiber	1999-2000	C24,C53
Liang et al.	Flat	1999	C31
Acharya & Foley	Flat	1999	C25
Fuertes & Centeno	Flat	1998-2000	C3,C5,C6,C7,C9,C38,C39
Singh-Ghosal & Koros	Flat	2000	C54
Shiflett & Foley	Tube	2000-2001	C55,C70
Wang et al.	Tube	2000	C56
Fuertes	Tube	2000-2001	C57,C68

2.6 Formation of Hollow Fiber Membrane

Hollow fiber membranes were first reported in a series of patents by Mahon in 1966 assigned to the Dow Chemical Company [F14]. Nowadays, hollow fiber has been used in numerous commercial applications including medical field, water reclamation (purification and desalination), pervaporation and gas separation owing to its excellent mass transfer properties. In fact, the development of hollow fiber membrane technology has been greatly inspired by intensive research and development of reverse-osmosis membrane during 1960s. Hollow fibers allow selective exchange of materials across their walls. Additionally, they can be used as containers to affect the controlled release of a specific material or as reactors to chemically modify a permeate as it diffuses through a chemically activated hollow fiber wall [B18].

In general, the tubular membranes consisted of hollow fiber membrane, capillary membrane and tubular membrane. The variation is only in terms of fiber inner diameter [B3-3].

- Hollow fiber membranes (inner diameter: < 0.5 mm)
- Capillary membranes (inner diameter: 0.5 – 5 mm)
- Tubular membranes (inner diameter: > 5 mm)

Hollow fiber membranes can be divided into 2 categories: open hollow fiber and loaded hollow fiber. In open hollow fiber, the flow of lumen medium gas/liquid is not restricted. On the other hand, lumen of the loaded fiber is filled with an immobilized solid, liquid or gas [B18].

There are numerous methods to prepare synthetic membranes. The most important methods are sintering, stretching, track-etching, phase inversion and coating. Among those methods, phase inversion method is typically applied in production of commercial available membranes [B3-3]. Koros and Fleming [F21] have divided the phase inversion process into four broad categories:

(a) Wet cast/Wet phase inversion
(b) Dry cast/Wet phase inversion
(c) Dry cast/Dry phase inversion
(d) Dry cast/Dry-wet phase inversion

The distinction between dry cast and west cast is refers to whether the outlet of the spinneret or casting knife that transfers the dope from a closed reservoir is exposed to air or is submerged directly in a liquid coagulation medium which is a non-solvent for the polymer [F2].

A number of different techniques can be used in a phase inversion process including solvent evaporation, precipitation by controlled evaporation, thermal precipitation, precipitation from the vapor phase and immersion precipitation. Most of the phase inversion membranes fabricated using immersion precipitation technique. Precipitation process involves casting or spinning of polymer solution and followed by immersion in a nonsolvent coagulation bath. Solvent and non-solvent exchange causes precipitation of polymer. The membrane is produced by combination of mass transfer and phase separation [B3-3]. In this research, dry cast/dry-wet phase inversion spinning process was used in the fabrication of PAN hollow fiber membranes. In the following section, a numbers of different spinning process are discussed.

2.6.1 Spinning Process

Previous researchers [F4] proposed that a satisfactory spinning process must provide fibers having the requisite permeability, surface pore size and stability under long-term compression. The principal variables during spinning process are solution composition, solution viscosities spinning temperature, solution pumping rates, coagulation agents (inside & outside), coagulation temperature and nascent fiber drawing rate. Different spinning techniques are illustrated in Appendix A.

There are 4 conventional synthetic fiber spinning methods that can be implemented for the production of hollow fiber membranes:

(a) Melt Spinning : A polymer melt is extruded through a spinneret into a cooler atmosphere, which induces phase transition and solidifies into fiber form. The resulting hollow fiber is isotropic/homogeneous dense membrane [B18, F11,C67]. These membranes are normally used for the characterization of the intrinsic properties of the membrane materials [Th3].

(b) Wet Spinning: The spinning dope, consisting of polymer volatile solvent, is spun through a spinneret into a liquid coagulating bath (solvent more soluble in the coagulation fluid than in the precursor). The precursor solution precipitates into fiber form after emerges from spinneret capillaries [B18,C67]. This process can produce anisotropic and asymmetric membrane [F11].

(c) Dry spinning : As the solution extruded into a drying chamber, evaporation of the solvent will cause the precursor precipitates into fiber form [C67]. The evaporation from a nascent membrane dope containing nonsolvents with lower volatility than those of the solvents produces a critical concentration leading to transformation from a single phase to two-phase structure [F21].

(d) Dry/wet spinning : This method is a combination of the 2nd and 3rd methods. In this process, all three mechanisms of formation (temperature gradient, solvent evaporation and solvent-nonsolvent exchange) can be combined. Spinning rate is relatively low (up to 100 m/min but usually 15-50 m/min) [B18].

2.6.1.1 Wet Phase Separation Process

Wet phase separation process is characterized by the demixing of a stable, homogeneous polymer solution in a nonsolvent precipitation bath. During wet phase separation process, the cast membrane is immersed prior to reaching phase

instability. Therefore, the entire phase separation occurs by the diffusional exchange of solvents and non-solvents in the coagulation bath. Loeb and Sourirajan successfully implemented wet phase separation process in the 1960's for the desalination of brackish seawater. If sufficient time is allowed for a fraction of the cast structure to phase separate before the structure is immersed in a nonsolvent to complete the phase separation throughout, this process is called as a dry-wet phase separation process, which will discuss in next section [F2,F21].

Wet phase inversion membranes have either too many defects to allow their use in gas separation without further treatment or a rather thick selective skin (>2000 ⊕). The thin selective layer of such defective membranes can be caulked with a high flux, low selectivity material like silicone rubber to eliminate viscous or Knudsen flow without causing serious productivity loss. However, properties of the composite membrane are complex averages of those of the membrane polymer and the caulking agent. The caulking agent may add significant resistance to the overall transport process and limit ones ability to benefit from the productivity and selectivity of high performances in thin skinned forms [F2].

2.6.1.2 Dry/wet Phase Separation Process

Dry/wet phase separation process is the most common industrial approach to fabricate gas separation membranes [F21]. Dry/wet phase inversion process first demonstrated by Pinnau and Koros in producing a flat-sheet membrane without requirement for post-treatement [F10]. Pinnau and Koros have shown that it is possible to produce simultaneously ultrathin and defect-free asymmetric polysulfone membranes by the dry/wet inversion technique using forced-convective evaporation [F7].

Dry/wet phase separation describes evaporation-induced phase separation in the outermost regions of nascent flat sheet and hollow fiber membranes prior to coagulation. The selective loss of the volatile solvent causes destabilization in the outermost region of nascent membrane. Interfacial "dry" phase separation can be

observed by the almost instantaneous onset of turbidity in this outermost region. After that, the casting solution is immersed in a non-solvent coagulant, thus undergoing a “wet” phase separation, where the formation of membrane bulk structure as well as extraction of the remaining solvents and non-solvent occurred [F1]. Rapid phase separation and vitrification processes are required during wet phase inversion step in order to generate the highest performance gas separation membranes [F7].

A process for producing ultrathin and defect-free selecting layers on asymmetric membranes using dry/wet phase separation has been reported earlier for organic coagulation media. Peinemann and Pinnau prepared ultrathin polyethersulfone membranes from a casting solution by using methanol as coagulant. However, the resulting membranes were defective [F10].

Hence, Pinnau and Koros have successful eliminate the defects and achieved thinner selecitve skins by changing the casting solution composition and the addition of a convective evaporation step in the spinning process. However, the flammability, toxicity, difficulties in reclamation of the organic quench media makes it not attractive for commercial use. Hence, it is desirable to have option to use more conventional aqueous quench media in large-scale production operations. Pesek and Koros developed an aqueous quenched, dry/wet system to produce flat sheet polysulfone membrane [F2]. The dry/wet phase separation process with aqueous coagulants used in this research is based on earlier work where organic coagulants were used.

Despite the coagulant can have a tremendous effect on morphology, it is believed that the membrane skin and much of the transition region is formed during the dry phase separation step. Under optimum formation conditions, the membrane skin has been found to be much thinner than those formed in traditional wet phase separation processes as well as defect-free [F2].

It is clear from the above discussion, the important properties for the formation of optimized asymmetric membranes made by the dry/wet phase inversion process are shown below [F8].

(a) The composition of the casting solution should be as close as possible to the thermodynamic instability limit: binodal composition.

(b) The force convective evaporation should be carried out by using inert gas to induce phase separation in the outermost region of the cast film (dry phase inversion).

(c) A thermodynamically strong non-solvent should be chosen as coagulant in the quench step (wet phase inversion). Besides that, the quench medium must be miscible with the solvents of the casting solution.

2.6.1.3 Advantages of Dry/wet Spinning Process

The dry/wet phase separation process is a suitable method for the preparation of ultrathin and defect-free integrally skinned asymmetric membranes. It does not have severe limitation and successfully employed for many polymers, solvents, non-solvents, solution viscosities and coagulation media. [F2]. It can obtain almost every known membrane morphology [B18].

2.6.1.4 Different Types of Spinneret

Spinneret is the most important part in a spinning process. In general, there are 3 types of spinnerets used for the hollow fiber spinning process [B18]:

(a) The segmented-arc design

This spinneret has a C-shaped orifice and it is suitable for melt spinning. In this system, extradite rapidly coalesces to complete the annular configuration. This

system does not require gas injection to prevent collapse of hollow fiber because the gas is drawn through the unwelded gaps.

(b) Plug-in-orifice design

This design simply provides the extrudate with the annular shape. A gas supply is usually required to prevent collapse.

(c) Tube-in-orifice jet design

This is the most versatile combination since it can be applied to all spinning techniques mentioned in the preceding section. Gas, liquid or suspended solids can be delivered through the inner tube to maintain the annular structure and to control coagulation of the fiber bore as well as to encapsulate gases, liquid or solids to form the so-called loaded fibers.

(d) Multiannular design

This design is employed in spinning of multilayer fiber walls or for entrapping (encapsulating) activated species in a composite hollow fiber wall. The gas used (in all cases) is usually inert (N_2) so no chemical interactions occur between gas and organic polymers.

2.6.2 Advantages of Hollow Fiber

Hollow fiber membrane has been applied in this research due to its abundant advantages and it is well known as a suitable configuration for gas separation process as shown in Table 2.4. The advantages of hollow fiber have listed as below.

(a) Hollow fibers exhibit higher productivity per unit volume. They have high packing density and large surface area. In order word, high surface area to volume ratio. 0.04 m^3 membrane device can easily accommodate 575 m^2 of effective membrane area in hollow fiber form (90 μm in diameter) while the same device only can put in 30 m^2 of spiral wound flat-sheet membrane or 5m^2 of membrane in a tubular configuration [B18,F15]. Table 2.5 displays that

hollow fiber membrane has highest surface area to volume ratio among different membrane module.

(b) They are self-supporting and can operate under high pressures condition. Thereby, simplify the hardware for fabrication of a membrane permeator [B18].

(c) High recovery in individual units [B18].

(d) Low cost [C56].

Table 2.4: Different modules for different process [G5]

Process	**Plate-and-frame**	**Spiral-wound**	**Disc-tube**	**Tubular**	**Capillary**	**Hollow fiber**	**TFM**
Microfiltration	+			++	+		++
Ultrafiltration	+	+	+	++	++		++
Nanofiltration	+	++	+	++	++	+	+
Reverse Osmosis	+	++	+	+		++	
Gas Separation		++	+		+	++	+
Pervaporation	++	+	+		+		
Electrodialysis	++						
Dialysis	+			+	++	++	

++ : Best suited for a given process.

+ : Suited under certain circumstances

Table 2.5: Characteristics of different membrane modules [G5]

Module Type	**Characteristics**	**Surface to volume ratio (m^2/m^3)**
Plate-&-frame	Flat sheet membranes	100 – 200
Spiral-wound	Flat sheet	700 – 1,000
Disc-tube	High pressures possible	100 – 200
Tubular	ID > 5 mm	100 – 500
Capillary	0.5 < ID < 5 mm	500 – 4,000
Hollow fiber	ID < 0.5 mm	4,000 – 30,000
Transverse flow	Fibers perpendicular to feed	500 – 20,000

2.6.3 Disadvantages of Hollow Fiber

The main disadvantage of hollow fiber membranes is its sensitivity to fouling and plugging by particulate matter due to a relatively low free space between fibers [B18]. However, feed stream in gas separation are relatively clean. Beside that, the pressure drop is significant with gas flow through the membrane bore. Therefore, the fiber length is an important criterion in the design of a separation unit [F11]. Moreover, other drawbacks are fragility and difficulty of packaging into modules [C56].

2.6.4 Hollow Fiber Flow Configurations

There are a few hollow fiber flow configurations applied for different industry applications [B18]:

(a) Countercurrent flow with the feed enters outside the fiber and permeate is inside the fibers bore. This flow configuration usually used for reverse osmosis and ultrafiltration application

(b) Countercurrent flow with the feed flows in the fiber bore and permeate is outside the fiber. Large diameter fibers are used in this flow configuration and it is appropriate for the application, where the feed has a high loading of particulates.

(c) Cross flow with shell side feed. Microfiltration generally applied this type of flow configuration.

Both three flow patterns can be utilized in the gas separation application.

2.7 Influence of Carbonization Process on the Carbon Membrane Structure

Carbonization process is utilized for the fabrication of carbon hollow fiber membranes from the PAN polymeric membranes. Carbon membrane usually consisting of 3 structural zones: an inner layer of coarse pores, finger-like channels and a dense skin. Linkov et al. [C14] have concluded that carbon membranes with internal coarse pore structures and thin separation layers can be produced by the carbonization of PAN precursors. A few important parameters that will control the pore sizes of the outer skin are intrinsic viscosity of the PAN polymer, the precursor preparation, stabilization atmosphere and the carbonization temperature. Carbonization process has significant influence on the carbon membrane structure.

2.7.1 Physical Structure Evolution

The carbonization of polymeric materials in membrane form leads to structures approaching the hexagonal structure of graphite, characterized by a 3.354∑ interlayer spacing. The final product of the pyrolysis process may approach the graphitic structure to various degrees with regard to crystallinity, interlayer spacing and domain size depending on the polymeric precursor (carbon, cross-link content and other structural details) and the carbonization conditions (temperatures,

heating duration, heating rate, atmosphere and purge gas flowrate). Furthermore, the final product may have a nearly compact form or develop considerable porosity at one or more level (microporosity, mesoporosity and macroporosity) [C77].

The volume of the carbon hollow fiber membrane reduced with increasing of the carbonization temperatures due to the shrinkage of fiber inner diameter and outside diameter as well as length [C1,C61]. The diameter of fiber can decreased from 35 μm to 7 μm [C67]. Besides that, carbonization process increased the micropore volume without widening the size distribution [C9].

Steriotis et al. [C77] described that some interparticle macropore (10 – 20 ∝m) are preserved in the bulk structure of the carbon membrane and some additional macropore (0.1 ∝m) are generated during carbonization process. However, carbonization does not result in any significant effect on the skin macroporosity. There are typically no openings analogous to the interparticle voids of the bulk on the skin layer of membrane.

The absence of macroporosity in the skin may be attributed mainly to the special characteristics of the skin carbonization, which located at the exterior of the membrane and made from a solution precursor. Therefore, the skin undergoes the carbonization reactions first with the presence of a free surface. Consequently, the skin material has the freedom to pack more efficiently while the interior (bulk) undergoes structural changes under dimensional constraints because hollow fiber diameter becomes fix as the skin hardens. Eventually, the bulk material (especially the less dense or less-rigid interparticle materials) preserves or develops macroporosity while the skin becomes compact of the micron scale [C77].

The carbonization process produces a cross-linking between adjacent chains. This crosslinking obtained by carbonizing the stabilized hollow fiber resulted in the increasing of carbon fiber strength. In addition, density increased rapidly below carbonization temperature of 1000°C. This observation showed that the aromatization and cross-linking of the heterocyclic rings and the lengthening and

broadening of carbon basal planes rendered the repacking of the structure in carbon hollow fiber membrane [C62].

At about 600°C, the fusion to larger structures of the ladder polymer chains formed at lower temperature in the precursor. This 600°C fusion does not result in a sharp narrowing of the spacing between lamellar plate-like structures formed along the fiber axis during the stabilization, which can only occur at higher temperature. The spacing formed at 600°C or below can range from 10 nm to several tens of nanometers and is in the form of open pores [C14].

The stabilized hollow fiber membrane was composed of lamellar-platelike structure (LPLS) along the fiber axis. The large spacing between 2 LPLS is one kind of open pore. During the carbonization stage, the lamellar plates could be packed together, thus narrowing the pores. The dimensions of the large open pores decreased when the carbonization temperature was raised. It was found that the preferred orientation of the carbon hollow fiber membrane increased with temperature throughout the range of 320 – 800°C. In addition, the broadening of the carbon basal planes could lead to rearrangement and misorientation of structures along the fiber axis. It was reported that the main reason for the conversion of open to closed pores could be the broadening of the basal planes during carbonization. This could lead to the closing of the surface entrances from open structure [C62].

2.7.2 Chemical Structure Evolution

The chemical structures of PAN membranes undergo oxidation, cyclization, dehydrogenation and denitrogenation during pyrolysis process as displayed in Figure 2.11 to Figure 2.13. At low pyrolysis temperatures (28°C – 250°C), the heat causes the cyano repeat units to form cylces and favors of the formation of a ladder polymer in which oxygen is present as carbonyl groups (–C=O) as seen in Figure 2.11.

The Figure 2.11 displays that the subsequent heat treatment at 250°C – 400°C removes hydrogen and oxygen and leads the rings become aromatic. This polymer is

a series of fused pyridine rings. As the cyclization or aromatization (the production of aromatic carbon) and condensation reactions take place, consuming the oxygen and hydrogen atoms will lead to the development of the pore structure in carbon molecular sieve membranes [B21-1.2,B6-2.7,C72,Th2]. The processes happen owing to the combination of carbon atoms to form a sp2 bonding structure that is similar to that of graphite while losing non-carbon atoms [Th2]. There is a considerable evolution of H_2O in the early stages of carbonization (300°C – 500°C). The evolution of H_2O results from the cross-linking condensation reactions between two monomer units of the adjacent ladder polymeric molecular chains [B21-1.2,B6-2.7,C62].

At 400°C – 600°C, these cyclized structures undergo dehydorgenation and begin to link up in the lateral direction, producing a graphitelike or ribbon-like fused ring polymer structure consisting of a numbers of hexagons in the lateral direction and bounded by nitrogen atom as displayed in Figure 2.12. It was suggested that the lateral molecular growth occurs by condensation reactions in which the carbon atoms in one cyclized sequence fit into spaces left by the nitrogen atoms in adjacent cyclized sequence. In addition to ring-system carbon, significant amounts of carbon must be available for the interchange mechanism to be operative [B21-1.2,B6-2.7].

Figure 2.13 shows the denitrogenation process happens at 600°C – 800°C and the newly formed ribbons will join together to form even wider ribbons with nitrogen atoms along its edges until most of the nitrogen is removed and remaining almost pure carbon in the graphite form [B21-1.2,B6-2.7]. Eventually, carbon hollow fiber membranes are produced.

Final processing step varies depending on the structure of the precursor. Those structures with some interdomain organization (as a result of the preservation, induction or enhancement of order during low temperature carbonization) require relatively mild final processing conditions for the formation of large ordered domains. In contrast, materials with strongly disordered structures (such as those with heavily cross-linked precursors or poorly preserved original order) require quite intense final processing for the formation of larger ordered domains. They may

instead develop strongly interwoven graphitic sheaths (glassy carbon), especially when the processed object has a pronounced three-dimensional form [C77].

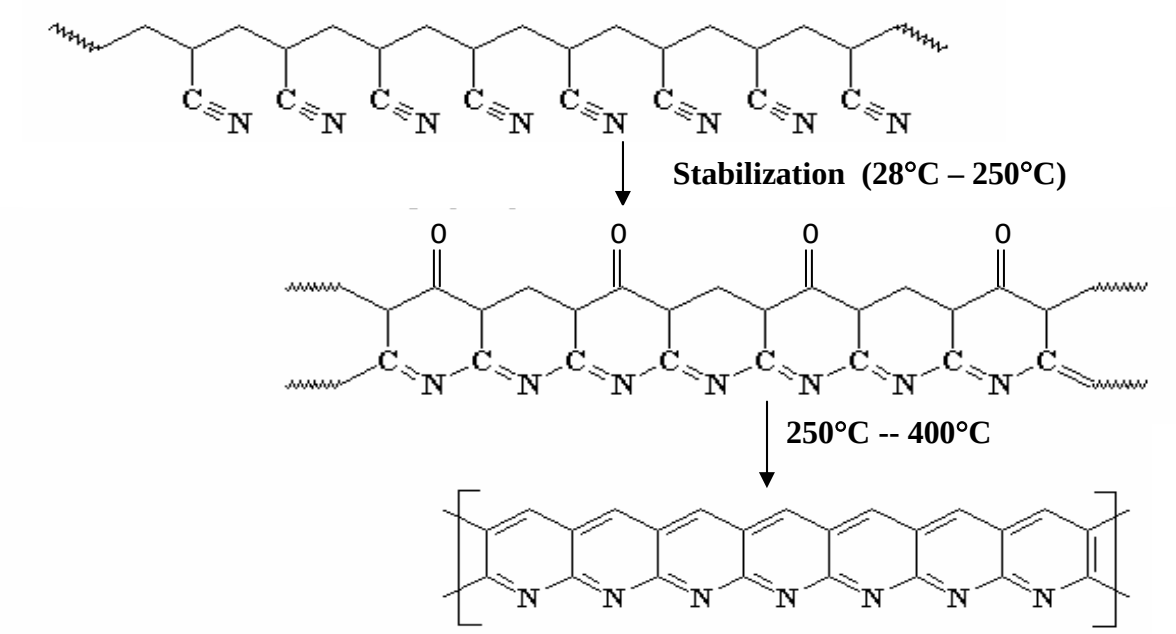

Figure 2.11: Oxidative stabilization process

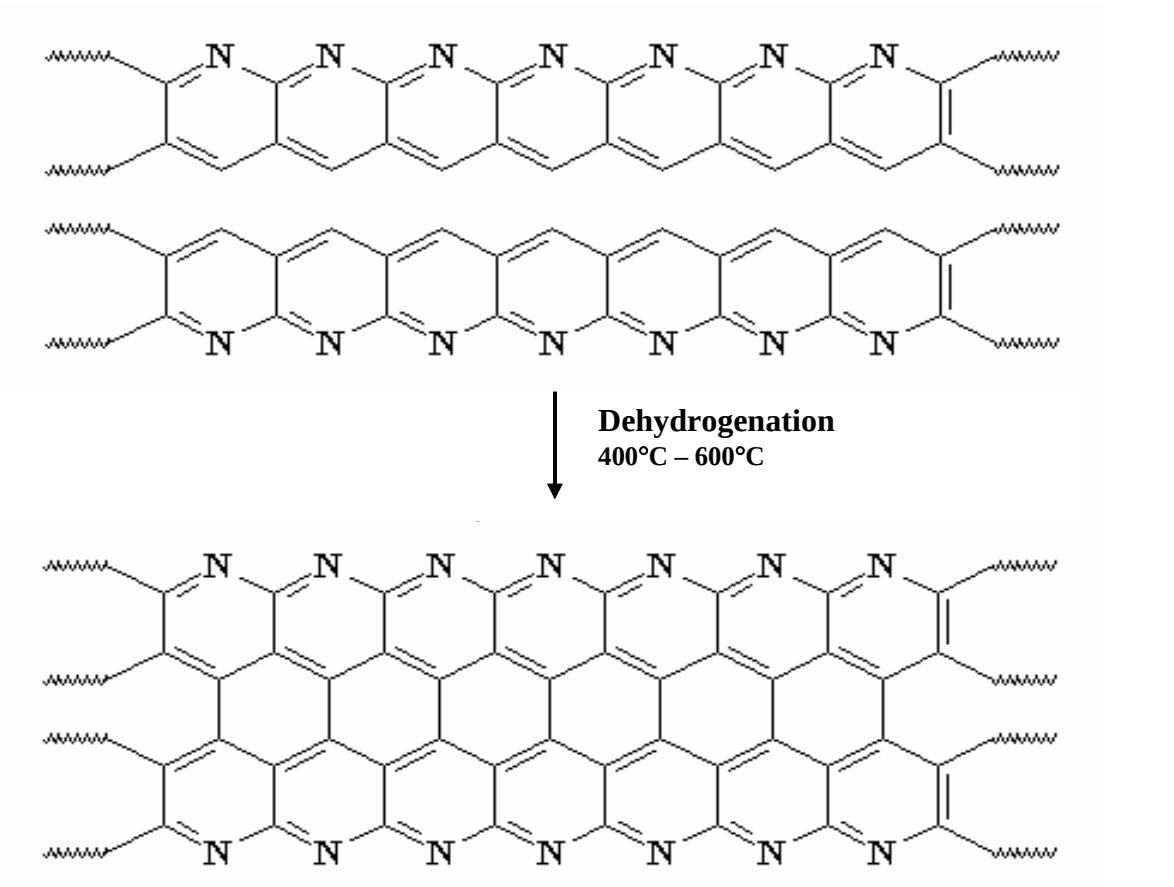

Figure 2.12: Dehydrogenation process at 400 – 600°C

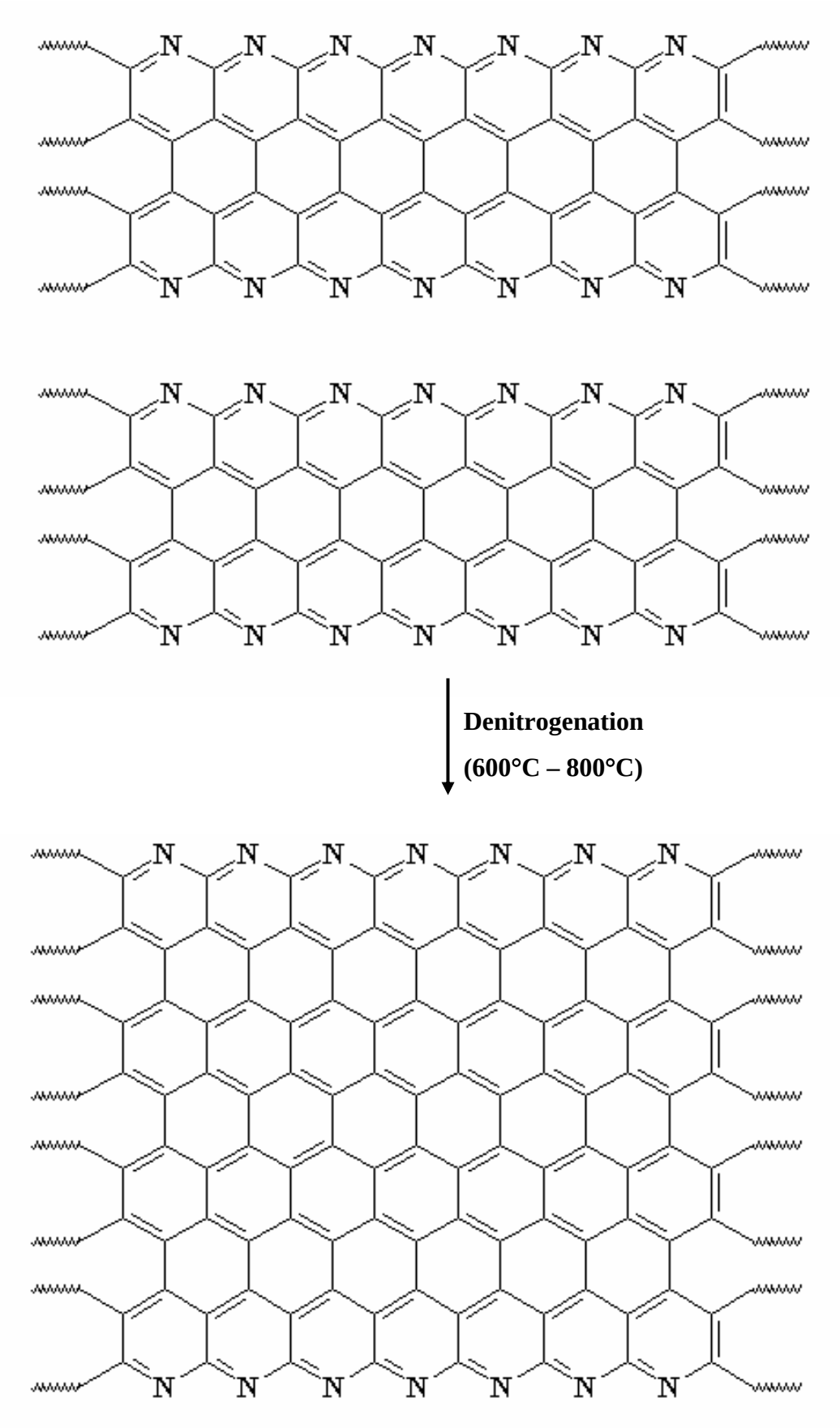

Figure 2.13: Denitrogenation at 600°C – 800°C

2.8 Structure of PAN-based Carbon Hollow Fiber Membrane

The structure of PAN-based carbon hollow fiber membrane is fibrillar in nature, mimicking the fundamental structure of the polymeric precursor fiber. PAN-based carbon hollow fiber membranes contain extensively folded and interlinked turbostratic layers of carbon with interlayer spacings considerably larger than those of graphite as shown in Figure 2.14. The turbostratic layers within PAN-based carbon hollow fiber membranes appear to follow the original fibril structure of the PAN precursor fiber. Although the turbostratic layers within these fibrils tend to be oriented parallel to the fiber axis, they are not highly aligned. This fibrillar structure that makes PAN-based carbon hollow fiber membrane less prone to flaw-induced failure [C67].

It was observed that the crystallites within the PAN-based carbon hollow fiber membranes are not perfectly aligned and misoriented crystallites are relatively common. The superior compressive strength of carbon hollow fiber membrane is mainly attributed to the inter-crystalline and intra-crystalline disorder, which mostly caused by its fibrillar structure as displayed in Figure 2.15. Edie inferred that the fundamental fibrillar structure of PAN-based carbon fibers is ultimately created during initial fiber formation [C67].

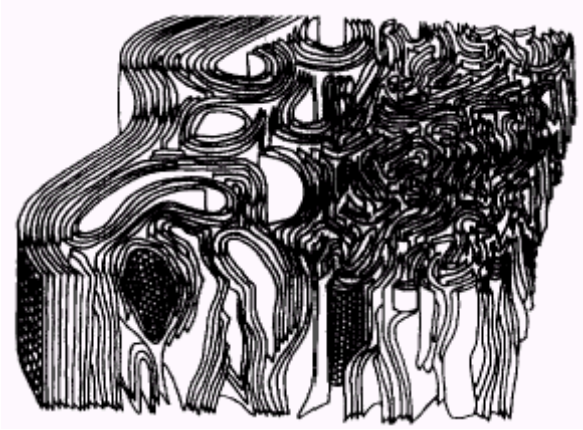

Figure 2.14: Microstructure of PAN-based carbon fiber proposed by Johnson [C67]

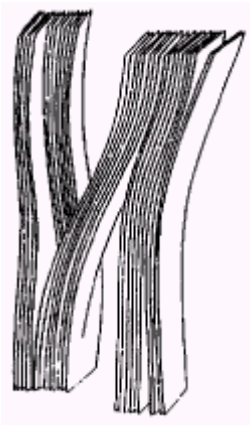

Figure 2.15: Misoriented crystallite linking two crystallites parallel to fiber axis [C67]

2.9 Permeation Measurements of Carbon Membrane

The performance of carbon membrane can be characterized by its selectivity and permeability. These two parameters can be measured by a few permeation measurement methods.

2.9.1 Constant Pressure-Variable Volume Method

For this method, high gas pressure applied on the feed in side while the permeate side with low pressure (usually at atmosphere pressure). The change in the volume of permeates measured as function of time by using the displacement of a short column of liquid/soap film bubble in a capillary. The series of pure gases are always tested in the order of increasing permeability with the purpose to reduce the permeability of the faster gases by any remaining slow gas. This will reduce the calculated selectivity and obtain a worst selectivity [F20,F9]. This method successfully used by Brubaker and Kammermeyer [F9].

2.9.2 Constant Volume-Variable Pressure Method

In this method, the both sides of the membrane are initially evacuated. Constant gas pressure applied on one side of the membrane. Increasing of the permeating gas pressure is measured on the opposite of the membrane by pressure measurement equipment such as pressure transducer while the downstream pressure of 10 mmHg or less was always negligible relative to the upstream pressure [F9,F20].

2.9.3 Variable Concentration Method

2 different gases are allowed to contact the opposite sides of the membrane. Gas composition is monitored as a function of time on either side of the membrane. The measurements are conducted under zero total pressure differentials. This method developed by Landrock and Proctor [F9].

The first 2 methods have proved to be more popular because they do not require high cost and analytical apparatus. The variable pressure method in particular is widely used at the present time and has been adopted as a standard by the American Society for Testing Material. However, the variable volume method offers the advantages of accurate and rapid permeability measurements. Beside that, it is suitable for the application with wide range of temperature and pressure. In addition, relatively unskilled person can conduct the measurements, since they do not require the use of vacuum techniques. Besides that, leaks in the apparatus and pinholes in the membrane being tested are easy to detect and identify.

The permeability data obtained by the variable volume method with thin membranes, of the order of 0.002 in, were found to agree within experimental error with comparable values determined by the variable pressure method. On the other hand, permeabilities determined by the former method were 15-30 % higher for thicker membranes with about 0.01 in thickness [F9].

CHAPTER IV

RESULTS & DISCUSSIONS

4.1 Permeation Properties of Carbon Membrane

Generally membrane is characterized foremost by its permeation properties, which consists of two importance parameters: permeability and selectivity. These two parameters describe the performance of carbon membrane. Permeability of a membrane will determine the productivity of a membrane process while selectivity of a membrane will determine the purity of the product.

The permeation rate in carbon membrane is mainly depending on the kinetic diameter of the gas molecules instead of their molecular weights or solubility and diffusivity coefficient [C6,C7,C38]. The selectivities achieved for different gas pairs were much higher than those expected from Knudsen diffusion. Knudsen separation factor for O_2/N_2, CO_2/CH_4 and CO_2/N_2 are 0.94, 0.60 and 0.80 respectively [C6].

High selectivity indicates that carbon membranes have micropores with similar size to the dimensions of gas molecules. It is evident that transport mechanism owned by carbon membrane is molecular sieving mechanism [C6,C38]. If the Knudsen diffusion mechanism occurred, the lighter molecules N_2 (in O_2/N_2 mixture) and CH_4 (in CO_2/CH_4 mixture) would permeate faster [C8].

This chapter reports the results and effect of a few important parameters in pyrolysis process including pyrolysis temperatures, heating duration/soak time, purge

gas flowrate and thermastabilization condition. These parameters have significant influence on the permeation properties of the carbon membranes.

4.2 Influence of Pyrolysis Process on Carbon Membrane Performance

4.2.1 Effect of Pyrolysis Temperature

Pyrolysis temperature is important in the carbon membrane production, as it will alter its properties and transport mechanism. As the pyrolysis temperature increases, the gas permeation mechanism changes from solution diffusion for the polymeric and thermostabilized membranes to molecular sieving or adsorption-activated diffusion for the pyrolyzed membranes.

If the membranes are not pyrolyzed at high temperature, they are not considered as a real “carbon” membrane because they usually contain subdomains where the structure of the polymer/precursor can be recognized in part [C49,C72]. The revolution in the structure of membrane will also affect the permeation properties of the membranes. From previous study [C44,C4], the increasing of the final pyrolysis temperature will result in the decreasing of the permeability and the increasing selectivity.

The structural revolution of the membrane can be seen from its skin layer and substructure through SEM results as shown in Figure 4.1 and Figure 4.2. As seen in those figures, the membrane polymer changed from amorphous polymer to rigid and crystalline polymer. Carbon membranes carbonized at 250°C have partial structure of the original PAN membrane as displayed in Figure 4.1a – 4.1b and Figure 4.2a – 4.2b. The carbon membranes carbonized at 400°C – 800°C have similar bulk structure (in terms of cross section and skin layer). This indicates that the PAN membranes must be carbonized at minimum temperature of 400°C.

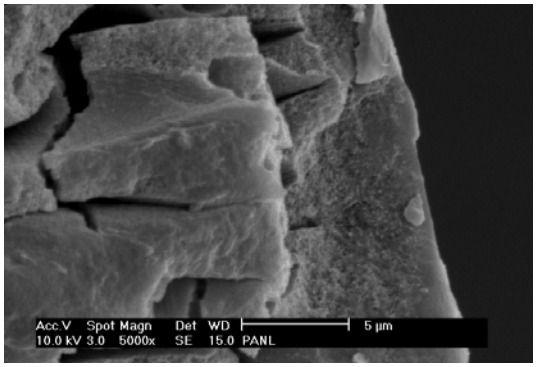

(a) PAN membrane

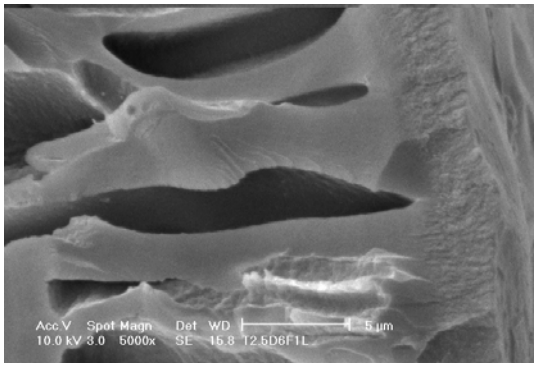

(b) $T_{pyrolysis}$ = 250°C

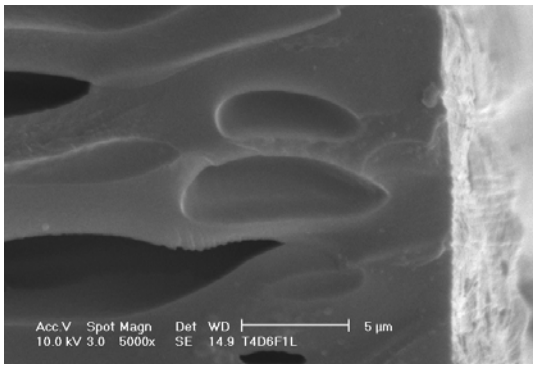

(c) $T_{pyrolysis}$ = 400°C

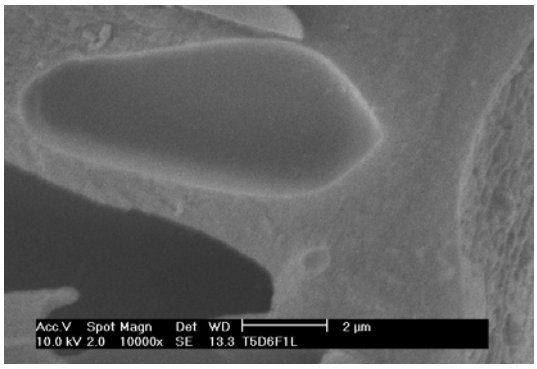

(d) $T_{pyrolysis}$ = 500°C

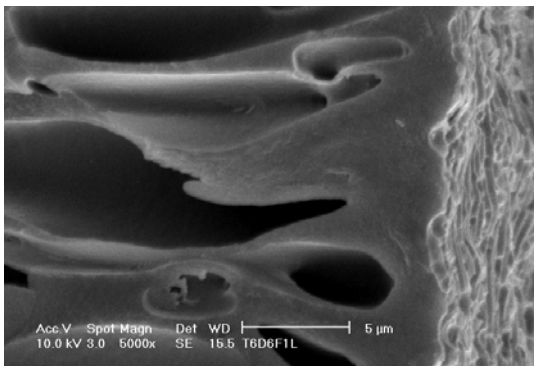

(e) $T_{pyrolysis}$ = 600°C

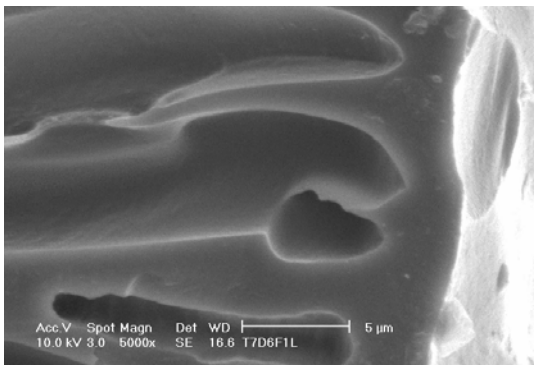

(f) $T_{pyrolysis}$ = 700°C

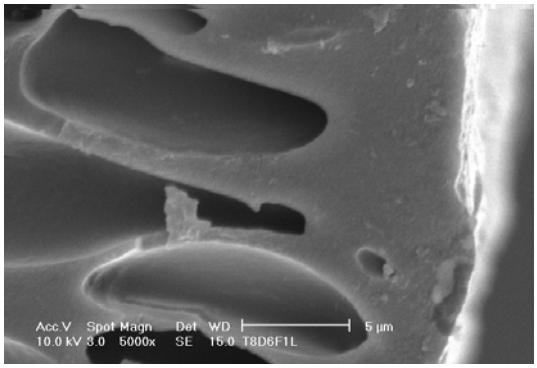

(g) $T_{pyrolysis}$ = 800°C

Figure 4.1: Structural change of the membrane skin layer at different pyrolysis temperatures

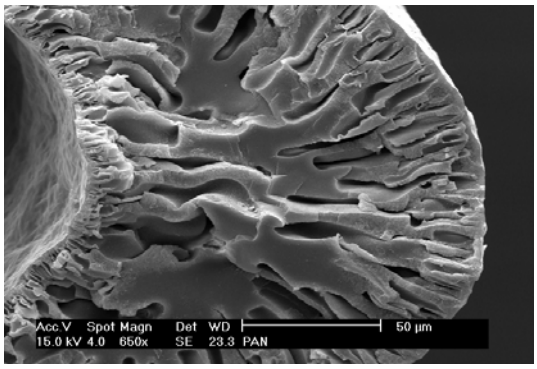

(a) PAN membrane

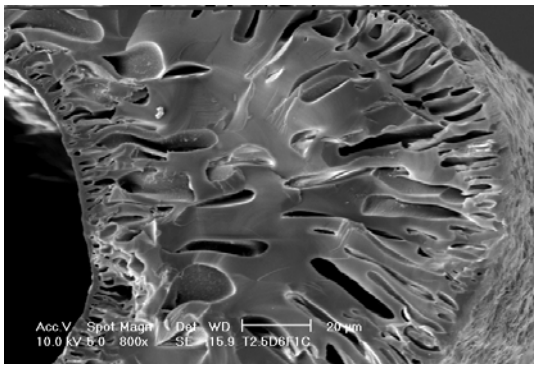

(b) $T_{pyrolysis}$ = 250°C

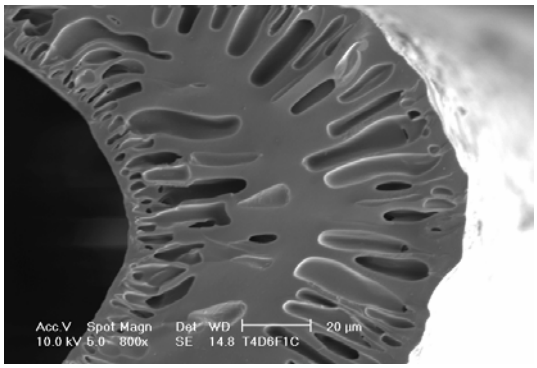

(c) $T_{pyrolysis}$ = 400°C

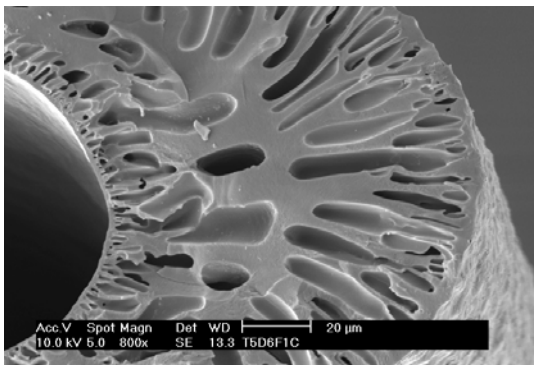

(d) $T_{pyrolysis}$ = 500°C

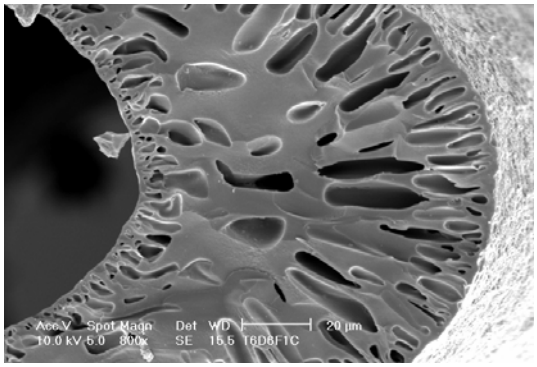

(e) $T_{pyrolysis}$ = 600°C

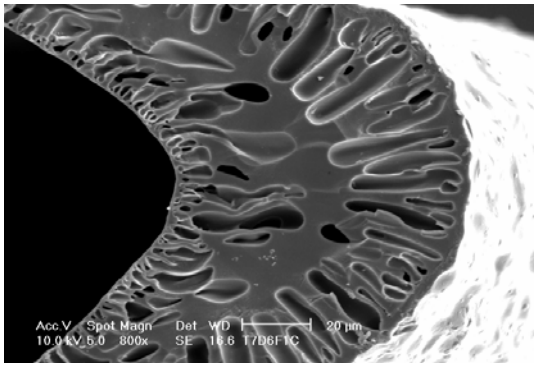

(f) $T_{pyrolysis}$ = 700°C

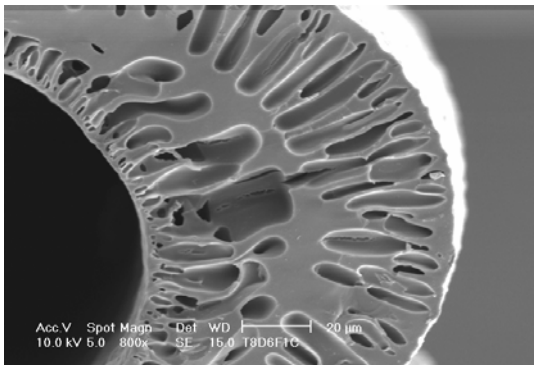

(g) $T_{pyrolysis}$ = 800°C

Figure 4.2: Structural change of the membrane substructure at different pyrolysis temperatures

However, the permeation results of PAN membrane carbonized at 400°C were unable to obtain in this research because it was extremely brittle and fragile membrane. It was reported that the main reactions occurred below 500°C were the evolution of H_2O, CH_4 and CO_2. These reactions promoted a cross-linking of heterocyclic rings, which formed sufficient carbon basal planes to cause a dramatic increase in the modulus and tensile strength. It was found that the modulus increased slowly below 500°C. In contrast, increasing temperature over 500°C promoted the formation of longer and broader basal planes, which led to a rapid increase in modulus and tensile strength [C62].

4.2.1.1 Effect of Pyrolysis Temperatures on the Membrane Selectivities

At early stage of pyrolysis process, the selectivity of the membranes decreased due to pore formation on the surface of the membranes as seen in Figure 4.3. At 250°C, the carbon membranes were partially formed. There were only a few small pores that existed at this period as shown in SEM image of Figure 4.4b. The membranes still have the characteristic of the nonporous polymeric membranes.

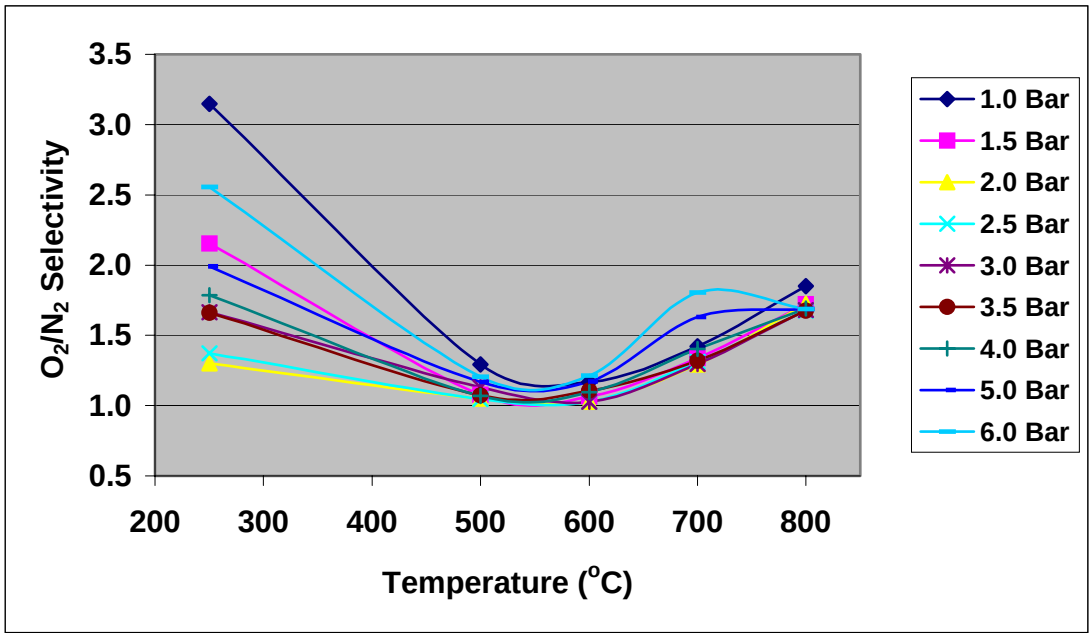

Figure 4.3: Influence of pyrolysis temperatures on the carbon membrane selectivity at different feed pressure

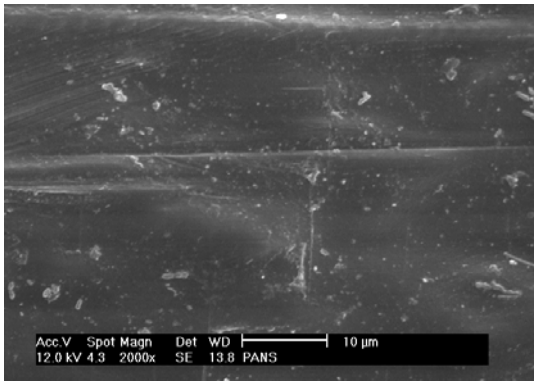

(a) PAN membrane

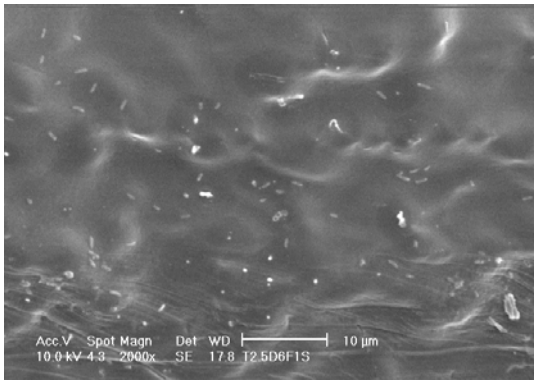

(b) $T_{pyrolysis}$ = 250°C

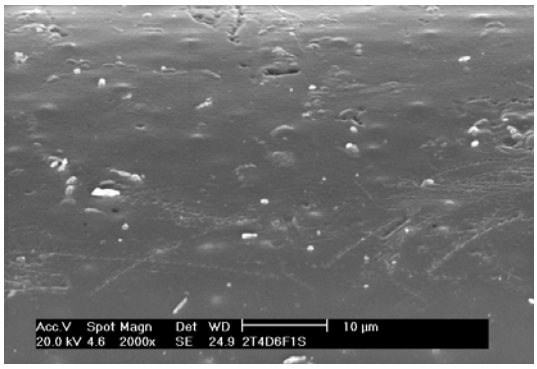

(c) $T_{pyrolysis}$ = 400°C

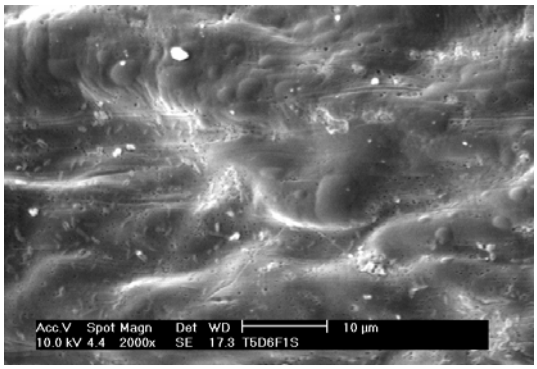

(d) $T_{pyrolysis}$ = 500°C

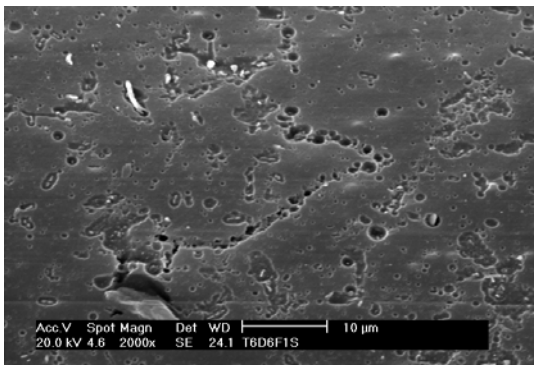

(e) $T_{pyrolysis}$ = 600°C

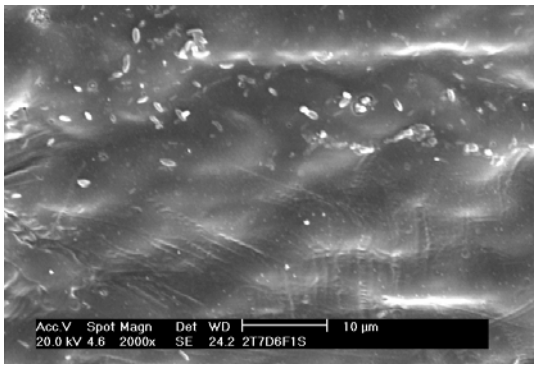

(f) $T_{pyrolysis}$ = 700°C

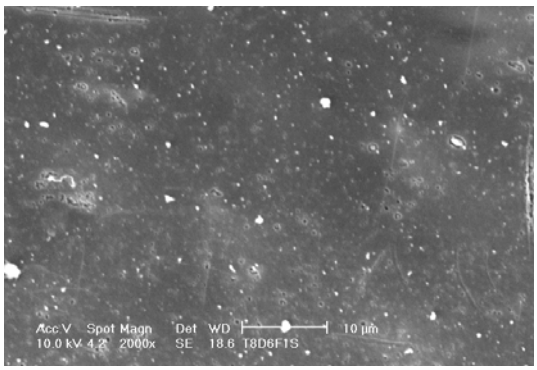

(g) $T_{pyrolysis}$ = 800°C

Figure 4.4: Surface of membranes pyrolyzed at different carbonization temperatures

The increasing amount of the pores at 500°C and 600°C as displayed in Figure 4.4d and Figure 4.4e. had reduced the selectivity of the membranes Nevertheless, the relatively high pyrolysis temperature is favorable for increasing carbon membrane selectivity as displayed in Figure 4.3. The selectivity of the membranes increased as the pyrolysis temperatures were being increased to 700°C and 800°C, which is in agreement with previous studies [C2,C54]. Therefore, the selectivities obtained were higher than original PAN membrane as shown in Figure 4.5. This is because of the material progress from a low selectivity flexible polymer to a rigid high selectivity carbon [C54]. In addition, carbon membranes carbonized at 700 – 800°C seem not much influenced by the feed in pressure. The pyrolysis temperatures can change several parameters of the membrane, which directly or indirectly influence the selectivity of the membrane.

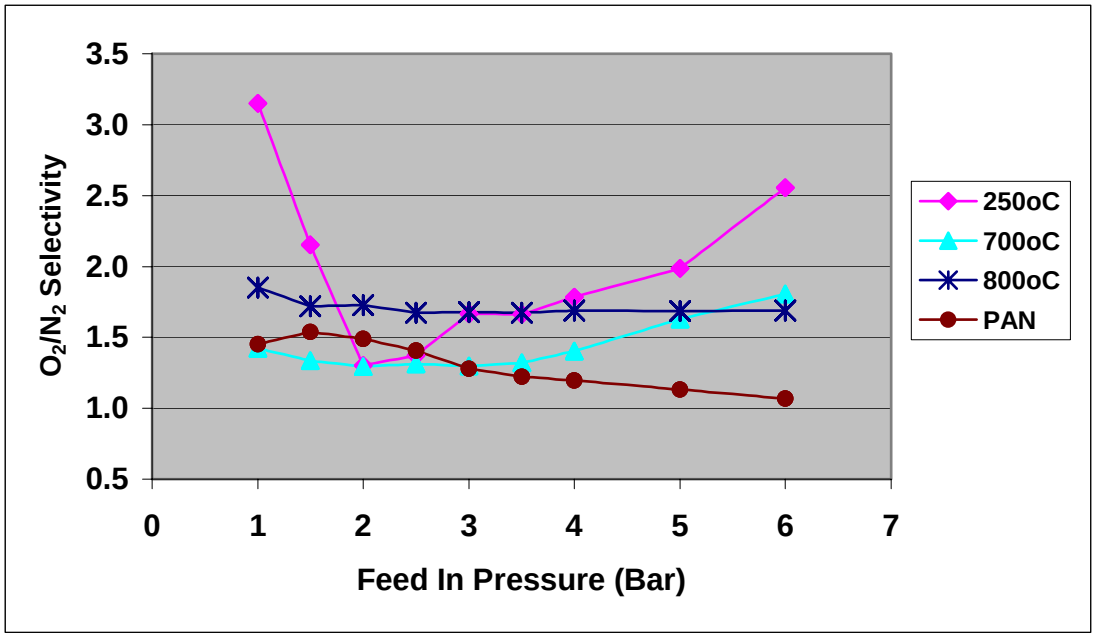

Figure 4.5: Comparison between PAN membrane and carbon membrane at 250°C, 700°C and 800°C

(a) The pyrolysis kinetics of the precursor

The TGA results in Table 4.1 shows that the weight loss was most significant at 800°C compared with other carbonization temperatures. Higher weight loss indicates higher carbon ratio to other elements such as oxygen, nitrogen and hydrogen can be obtained. This means that less void were exist in the membrane.

Previous studies found that the variety in weight loss as a function of pyrolysis temperatures was more pronounced in the inert purge pyrolysis system compared with vacuum pyrolysis system [C44].

Table 4.1: Weight loss of the membranes at different pyrolysis temperatures

Pyrolysis Temperature	Weight Loss	Remaining Weight Percentage
Original PAN Fibers	0.0 %	100.0%
250°C	1.9 %	98.1%
400 °C	12.0 %	86.1%
500 °C	12.3 %	73.8%
600 °C	4.4 %	69.4%
700 °C	4.4 %	65.0%
800 °C	19.2 %	45.8%

The FTIR results showed that the functional groups of the membranes decreased with the increasing of carbonization temperatures. PAN membranes possess functional groups such as methyl (CH_3) and nitrile (C≡N) as shown in Figure 4.6. Other FTIR results were presented in Appendix D-1 to D-6. As seen in Appendix D-1, membranes carbonized at 250°C have methyl group (C-H), nitril group (C≡N), amines group (C-N) and alkene group (C=C). C=C group existed due to the aromatization process occurred during thermastabilization process. At 400°C, the methyl group was removed while C≡N, C-N and C=C were eliminated at 500°C.

At high heating temperatures such as 600°C – 800°C, all functional groups were not found because the heat treatment has successfully removed H and N element from the membrane. Kusuki et al [C2] described that the asymmetric structure of the membrane become dense due to the physical shrinking of the membrane with a decomposition and chemical condensation of the precursor and the evolution of the compounds.

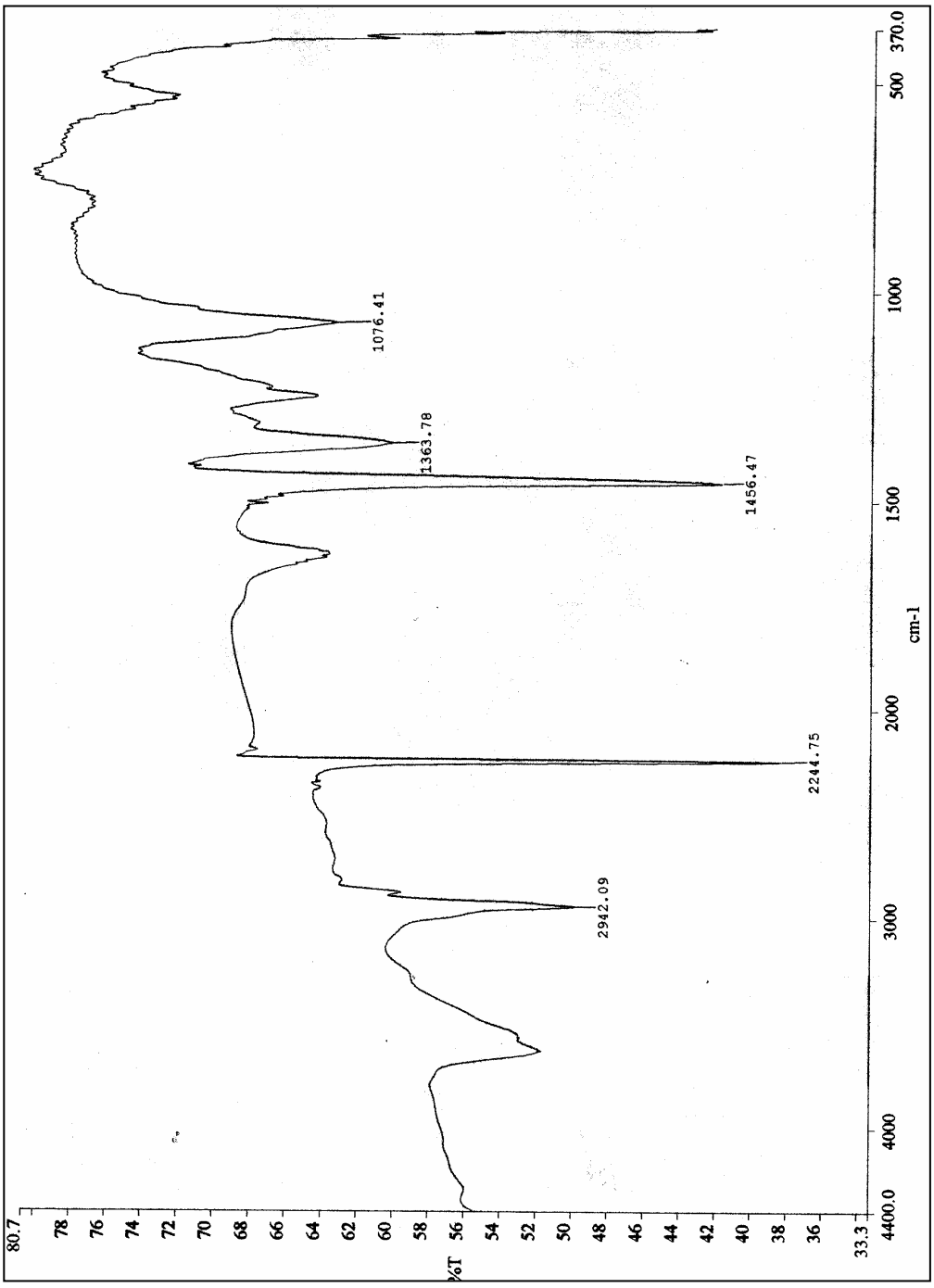

Figure 4.6: FTIR results for PAN membrane

(b) The pyrolysis kinetics of the polymer degradation byproducts.

At low pyrolysis temperature, the pyrolysis byproducts would degrade prior to complete removal and were plugging the membrane “pores” when low purge gas flowrate was applied. However, at high pyrolysis temperature, it was proposed that a thin layer of carbon could have been deposited inside the “pores” without sealing them. In other word, average pore size was being modified or reduced without complete pore blocking [C44,Th2].

(c) The compactness of the turbostratic carbon structure (interplanar spacing, amorphous portion and pores)

Densification of the porous carbon matrix occurs at high pyrolysis temperature. At high temperature, variety of weight losses is lesser but larger diameter and linear shrinkage was evident which resulted in higher bulk density. It was observed that the outer diameter of the hollow fiber membranes can reduced from 0.6 mm to 0.25 mm, which is more than 50% of shrinkage. This definitely produces tighter porous carbon morphology. Thereby, the selectivity increases while the permeability decreases [C44,Th2]. Besides that, Tanihara and his co-workers [C1] have suggested that carbon membrane is composed of network of the aromatic fragments having less molecular mobility. The aromatic fragments grow and crosslink between the fragments progresses, then the asymmetric structures of the membranes become dense with the increasing of pyrolysis temperatures.

Moreover, gases are likely to permeate through the cross-linked voids of the amorphous region and the interlayer spacing of the graphite-like microcrystallines [C4]. Higher pyrolization temperature will increase the formation of a turbostratic structure, which means the occurrence of graphite domains in amorphous carbon [C12]. Suda and Haraya [C40] observed that high temperature pyrolysis would cause a higher crystallinity, density and a narrower interplanar spacing of graphite layers of the carbon, which produces a carbon membrane with high gas selectivities. In addition, Steriotis et al. [C77] explained that the maximum temperature of pyrolysis process is a major factor affecting the size and interplanar spacing of the evolving carbon domains.

The increasing of pyrolysis temperature contributes to the decreasing of amorphous portion leading to high gas selectivity. The carbon prepared by the pyrolysis of organic materials has a turbostratic structure, in which layer-planes of graphite-like structure are dispersed in non-crystalline carbon. Several types of pores with diameter of a few ten of angstrom may also exist at the surface and in the structure into which molecules can penetrate. Most of the molecules may penetrate and diffuse into the membrane via these voids. As crystallization proceeds at elevated temperatures, the larger molecules are restricted from permeate through the smaller and narrower cross-linked voids. [C40].

In addition, permeation properties of carbon membranes are dependent on pore volume and pore size distribution, which are decided by carbonization conditions [C28]. Kusakabe et al. [C8] suggested that the micropores are responsible for the selectivities of the carbon membranes. Numerous researchers [C37,C31,C72,C80] proposed that high pyrolysis temperatures are responsible for pore shrinkage. The pores mouth dimension becomes narrow owing to the graphitization. In other words, the graphitization by heat treatment would improve the sieving performance of the carbon membrane [C80]. Mochida et al. [C80] proposed that the carbon tends to give slit-type pores consistent with its graphitic layer. High heat treatment induces the shrinkage of graphitic layers and may produce new slits and reduce the slits distance of the micropores in the carbon molecular sieve membrane [C80].

(d) Entropic selectivity

Anshu Singh-Ghosal and Koros [C58] suggested that the selectivity of membrane is depending on sorption selectivity and diffusivity selectivity. Diffusivity selectivity can be divided into entropic selectivity and enthalpic selectivity. Enthalpic selectivity/energetic selectivity is an energetically biased selection process. A penetrant sorbed in a nonporous polymer matrix diffuses by executing a size-dependent jump. These jumps are moderated by the activation energy needed to create transient gaps of sufficient size to enable the jump to occur. Smaller penetrants require the localization of less activation energy, thereby easier penetrate through the membrane.

However, carbon membranes with higher selectivity than polymeric membranes are not only attributed to this energetic factor but also entropic factors. The entropic factor for polymeric membrane is negligible regarding its contribution to diffusivity selectivity owing to the polymer chains [C58]. Entropic selectivities arise from the ability of molecular sieving media to selectively reduce the rotational degrees of freedom of N_2 versus O_2 in the diffusion transition state. Thus, the entropic selectivity arises from O_2 retained more degrees of freedom in the transition state than nitrogen. The polymer chains, which are in constant thermal motion are incapable of selectively restricting the motion of N_2 in the transition state leading to a complete loss of entropic selectivity. These significant segmental motions present in polymers prevent exercising this fine level of control, thereby limiting the performance of polymeric materials compared to molecular sieves [C54,C58].

On the other hand, the sorption selectivity for O_2/N_2 is lies in the range of 1–2 in almost all glassy polymers and in the range of 0.7 to 2 for molecular sieving materials like zeolite 4A and carbon molecular sieve. According to Anshu Singh-Ghosal and Koros, the diffusivity selectivity/mobility selectivity is responsible for the remarkable differences in the separation properties of membrane. They reported that the mobility of the polymer chains might have become severely hindered as the pyrolysis temperatures increased. Therefore, restricting the motion of the larger gas molecule. By tightening of periodic pore mouths exist between the free volume sorption sites, hence accounts for greater size and shape selectivity. Therefore, the increasing of selectivity is due to the increasing of mobility selectivity because the thermodynamic sorption selectivity of materials does not change measurably [C54,C58].

4.2.1.2 Effect of Pyrolysis Temperatures on the Membrane Permeability

The changes in gas permeance with pyrolysis temperature are related to the modification of the textural characteristics (micropore volume and the mean micropore size) of the selective film [C5]. Figure 4.7 and Figure 4.8 display that at initial stage (250°C), both oxygen and nitrogen permeability increased with

increasing of carbonization temperature until a maximum stage at 600°C. It was followed with the decreasing of permeability at 700°C and 800°C. The similar trend was also observed by previous researchers [C5,C9,C18,C39,C54,C72].

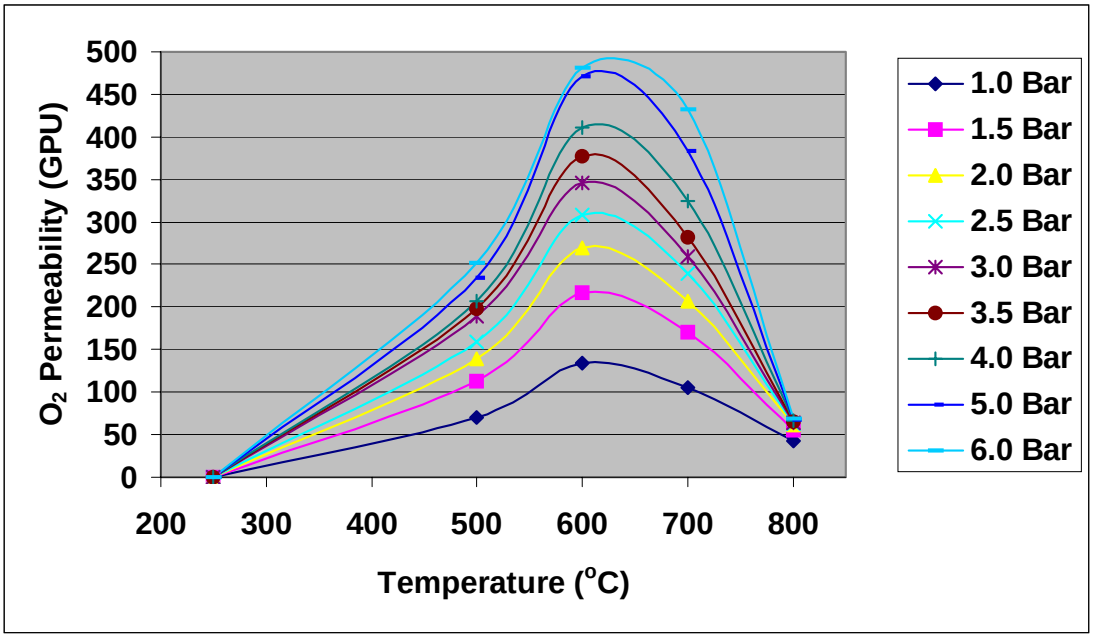

Figure 4.7: Influence of pyrolysis temperatures on the oxygen permeability of the membranes at different feed pressure

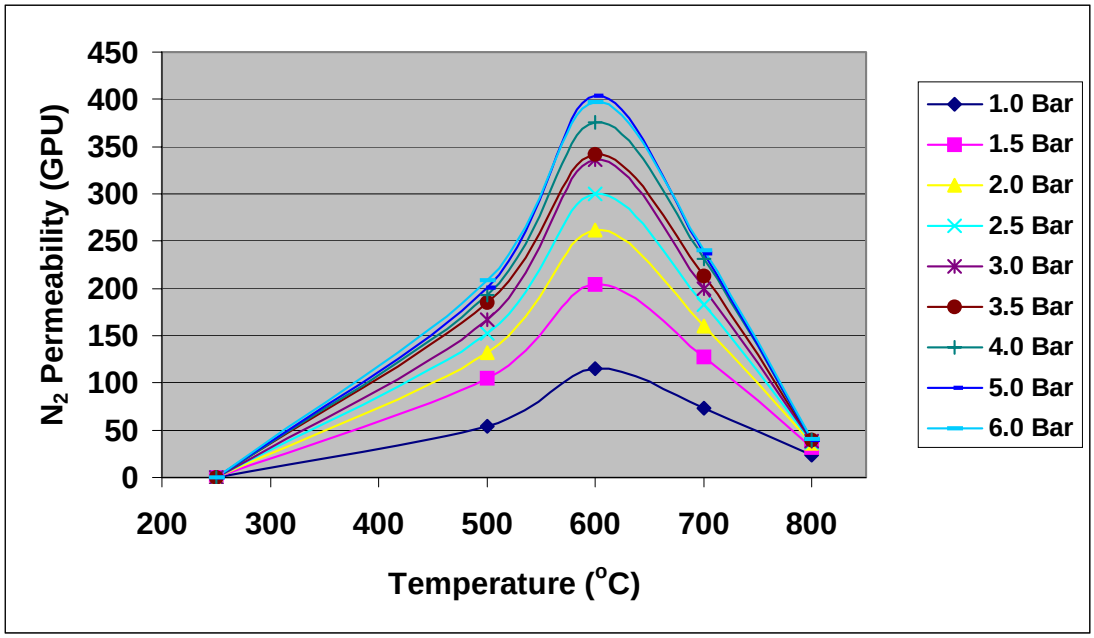

Figure 4.8: Influence of pyrolysis temperatures on the nitrogen permeability of the membranes at different feed pressure

As shown in Figure 4.9, the permeability of oxygen and nitrogen for membranes heated at 250°C were much lower than PAN membranes at pressure 1 – 6 bar. Oxygen and nitrogen permeability of membrane carbonized at 250°C were in the range of 0.02 – 0.036 GPU and 0.01 – 0.018 GPU respectively. Meanwhile, the oxygen and nitrogen permeability for PAN membranes obtained were 12 – 50 GPU and 8 – 46 GPU respectively. This probably means that the partial carbon membranes have lower diffusivity and solubility than original PAN membranes.

At initial stage of pyrolysis, the pores will gradually appear and subsequently follow by the pore enlargement due to abstraction of surface carbon atom as carbon monoxides. This means that the micropore volume increases initially until it reaches a maximum stage. The increase in the total micropore volume proves that carbonization process is effective in enlarging the total volume of the micropores. At higher pyrolysis temperature, the limiting pore volume and pore size start to decrease and the pore size distribution becomes sharper. Additionally, it also reduces the portion of larger pores. At last, the pores will shrink and finally collapse and disappear/pore closure owing to progressive annealing [C4,C5,C9,C18,C28,C36,C39].

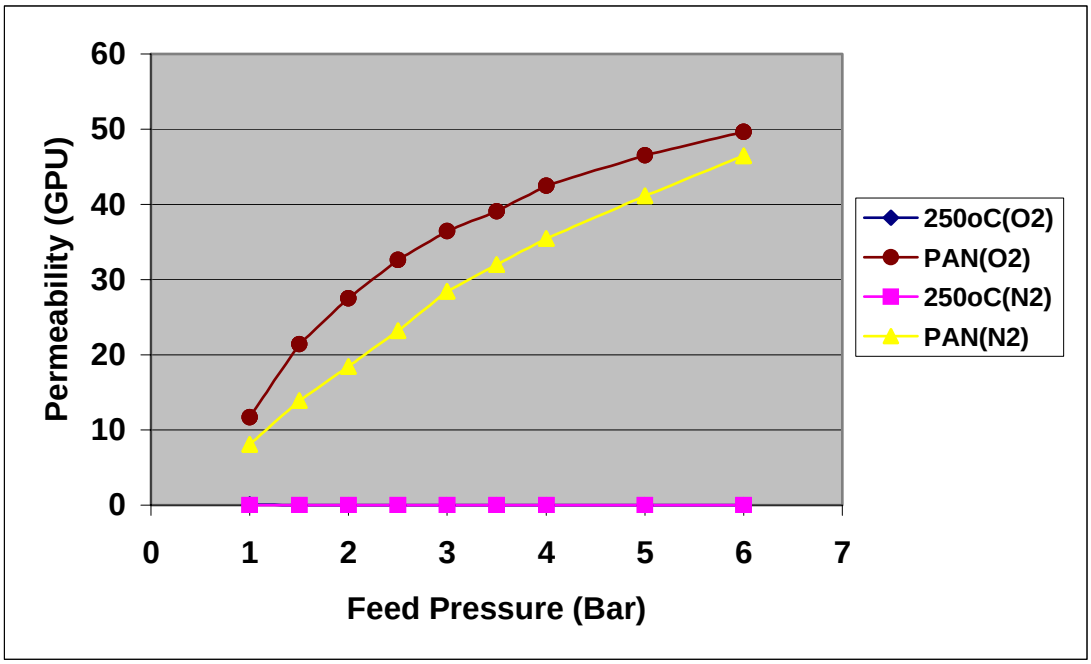

Figure 4.9: Comparison between PAN membranes with membrane heated at 250°C

The SEM results in Figure 4.4 support the preceding observation. Formation of pores started at 400°C while large amount of pores with maximum pore size obtained at 600°C. The subsequent heat treatment at 700°C and 800°C reduced the pore size and amount of pores. Some researchers [C9] proposed that the permeability of permeating gas is controlled by the size distribution of the micropores rather than the total micropores volume.

Anshu Singh-Ghosal and Koros [C54] observed that activation energies for gas diffusion increased as the pyrolysis temperature increased. Activation energies of diffusion and effective heats of sorption for a penetrant in a material contribute to the total of activation energies for permeation. Higher activation energy of diffusion means higher resistance to diffusion in the molecular matrix and reduced the permeation of gas. This finding is in agreement with Lafyatis et al. [C73] observation, which indicated that the higher temperatures treatments induce greater diffusional barriers to gaseous sorption in the carbon molecular sieve structure.

In order to achieve carbon membranes with excellent performance, controlling the pyrolysis temperature is obviously a way to tailor the microstructure as well as permeation properties of carbon membrane [C4]

4.2.2 Effect of Heating Duration (Soak Time)

The literature review showed that the heating duration usually applied during pyrolysis processes were between 30 min to 3 hours. However, a few researchers used soak time which less than 5 minutes [C1,C2] or 5 hours and even 10 hours [C47]. Although there are a few researchers involved in the investigation of heating duration during pyrolysis process, both researchers are using polyimide based polymer such as PMDA-ODA [C4,C12] and AP [C54] as the carbon membranes precursor. It is noted that very few studies were on the influence of heating duration in the carbon membranes production process especially research regarding non-polyimide based polymer.

Figure 4.10 and Figure 4.11 displayed that the increasing of heating duration has caused the increasing of the oxygen and nitrogen permeability. At low heating duration, the resulting membrane might not a pure/real “carbon” membrane because the samples did not have sufficient time to break the molecular chain of the PAN membrane and convert it into the carbon membrane structure. Thereby, the resulting membranes still have the characteristic of the polymeric membranes with nonporous skin layer as supported by the Mariwala and Foley [C72]. They proposed that some structural vestiges of the original precursor are still preserved at short soak time (heating duration).

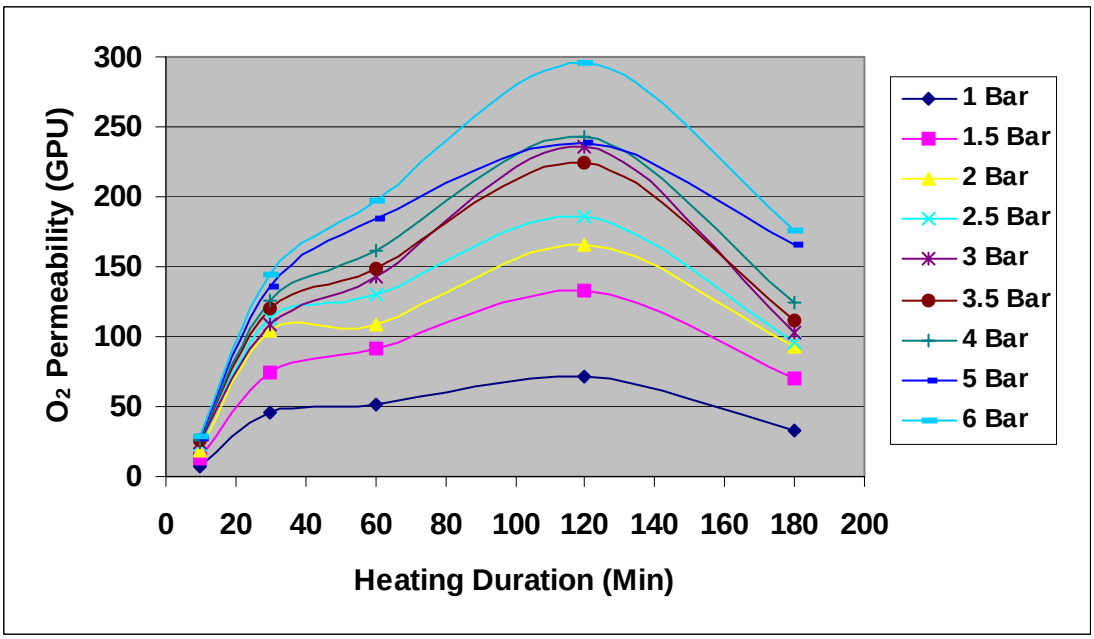

Figure 4.10: Influence of heating duration on the oxygen permeability at different feed pressure

Therefore, the membrane carbonized at 10 min had lower permeability than the PAN membranes owing to the partial carbon membranes possess impermeable bulk structure and incomplete pore system. Gases were difficult to permeate through the membrane by either solution diffusion or molecular sieving transport mechanism. The comparison between the permeability of membrane carbonized at 10 min with original PAN membrane is illustrated in Figure 4.12. 30 min heating duration only resulted in the formation of small amount of pores. Therefore, the permeabilities still relatively low. Longer heating duration provides sufficient time for the formation of complete pore system. Therefore, maximum permeability achieved as the heating

duration reached 120 min. Nevertheless, excessive long heating duration (180 min) leading to the reduction of the pore sizes and resulted in the decreasing of permeability for both oxygen and nitrogen gases.

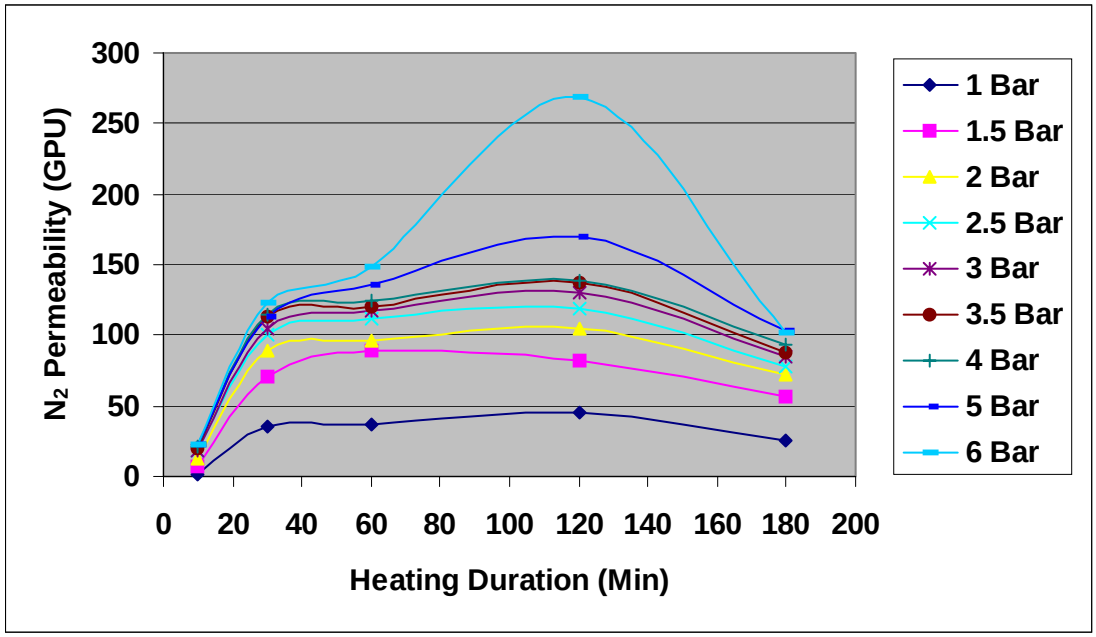

Figure 4.11: Influence of heating duration on the nitrogen permeability at different feed pressure

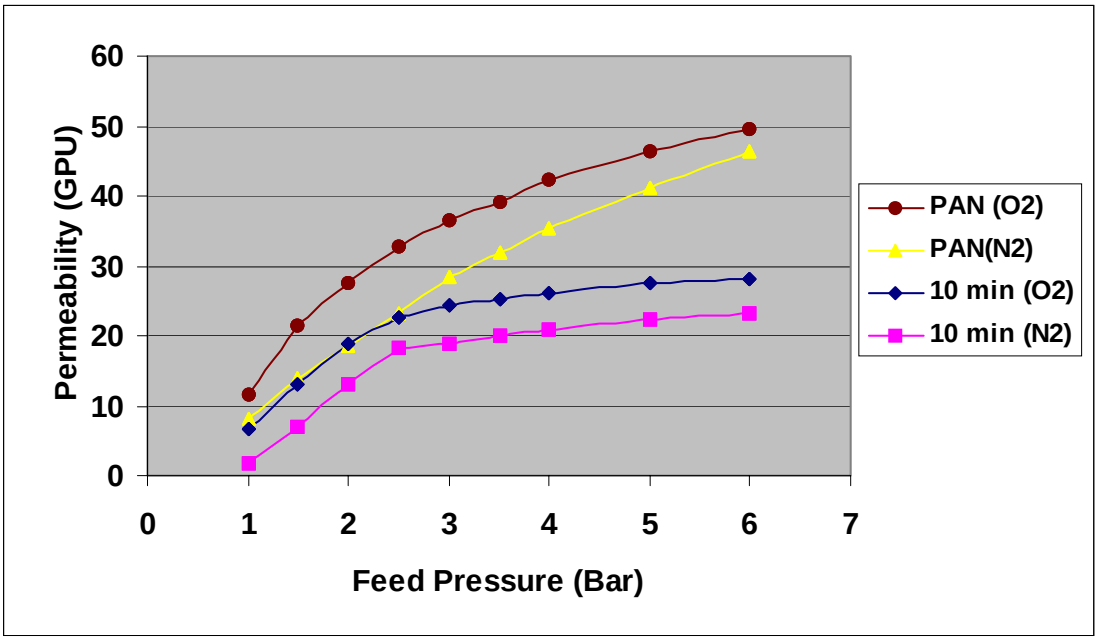

Figure 4.12: Permeability comparison between membrane carbonized at 10 min with PAN membrane

However, the selectivity of the membranes was improved by increasing the heating duration as shown in Figure 4.13. The results are in agreement with the result of previous researchers [C4,C12,C54] which found that the selectivities of the membrane were increased with the increasing of the heating duration [C54]. Peterson et al. suggested a long duration of pyrolysis and reported that high selectivities membranes were obtained at that condition [C12].

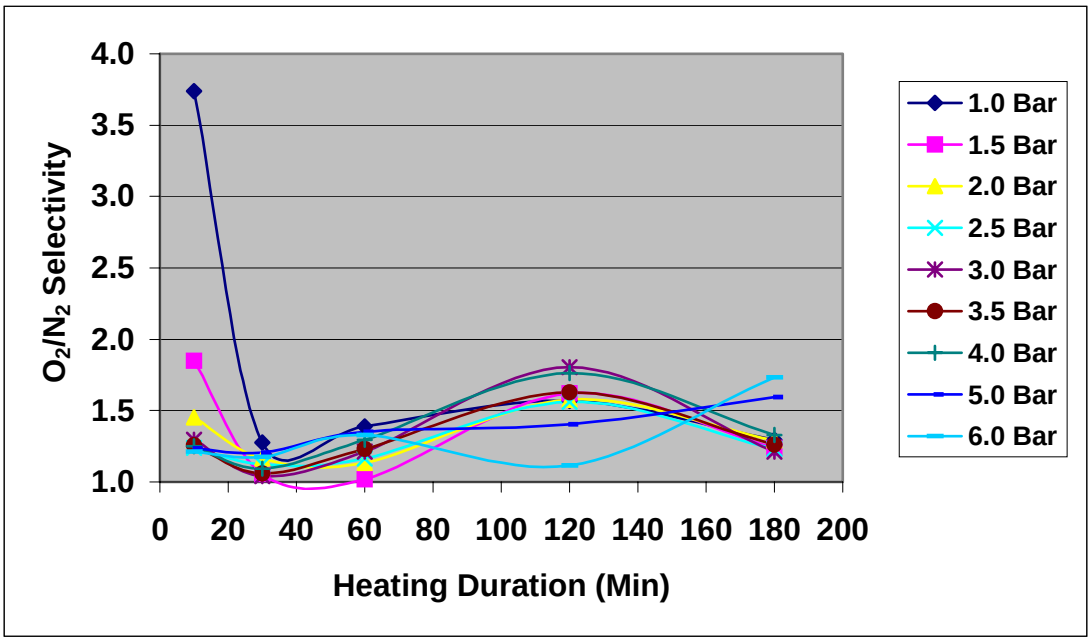

Figure 4.13: Influence of heating duration on the membrane selectivity at different feed pressure

Suda and Haraya observed that the longer pyrolysis duration contributes to the pore size reduction due to a sintering effect [C4]. Futhermore, Mariwala and Foley [C72] found that the soak time narrows the pore mouth dimension in carbon molecular sieve as the structure evolves toward a metastable equilibrium state at any pyrolysis temperatures. Foley et al. [C73] also observed that the increasing of soak time would result in decreasing of the micropore size in the carbon molecular sieve materials. The porous structure would move closer to the nonporous and graphite structure. Obviously, the difference in porosity at different heat treatment duration is due to the kinetic conversion of amorphous porous carbon to more crystalline graphitic carbon.

SEM results (Figure 4.14) supports the permeation results obtained, as there were no pores exist on the surface of 10 min carbonized membrane. But the surface had been changed from smooth nonporous PAN membrane to rough surface with the spots. The surface might in the progress of pore formation. A few tiny pores were found on the surface of 30 min carbonized membrane while the numbers of pores gradually increased with increasing of the heating duration until soak time 120 min. The amount of pore and pore size were reduced as the membrane carbonized at 180 min. Nevertheless, increasing heating duration did not give any significant alteration on the substructure and skin layer of the membranes as shown in Figure 4.15 and Figure 4.16.

In addition, the FTIR results exhibited that the amount of the functional groups in membranes decreased with increasing of the heating duration indicating that the duration of heat treatment should be sufficient to break the polymer chain in the membranes and remain carbon elements. Figure 4.17 displayed that the membrane carbonized at 10 min still had functional groups consisting of C-N, C≡N and C=C. However, the functional group remained in the membranes carbonized at 30 min – 180 min were C-N only as shown in Appendix D-7 to Appendix D-10.

TGA results in Figure 4.18 illustrated that the weight losses continue occurred for 180 min heat treatment. Therefore, the formation of real carbon membranes ultimately required long heating duration in order to remove completely the noncarbon elements.

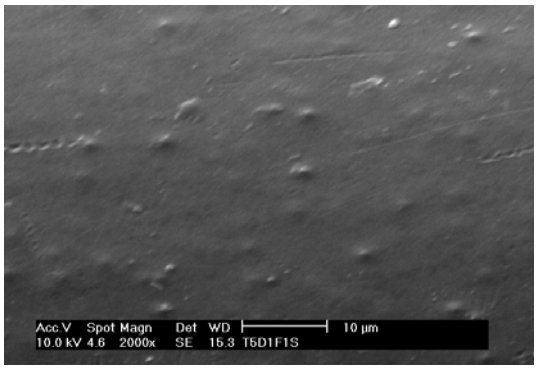

(a) 10 min

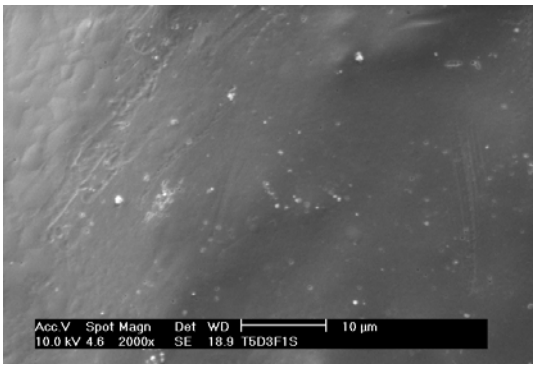

(b) 30 min

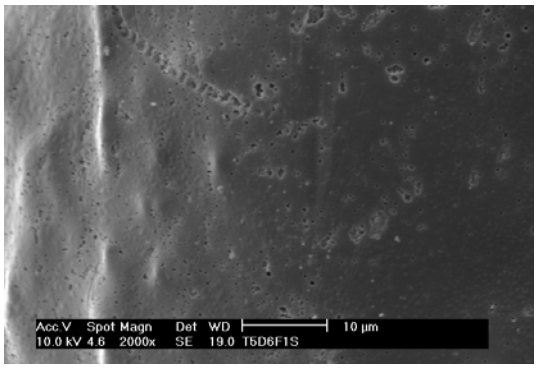

(c) 60 min

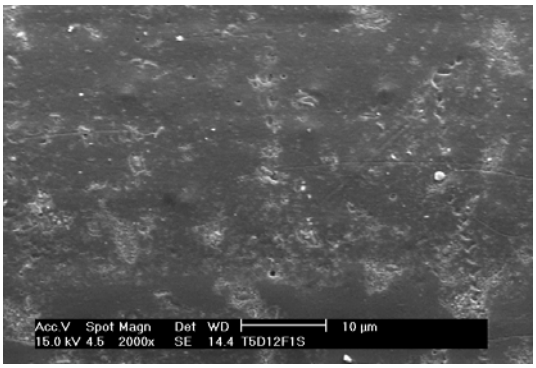

(d) 120 min

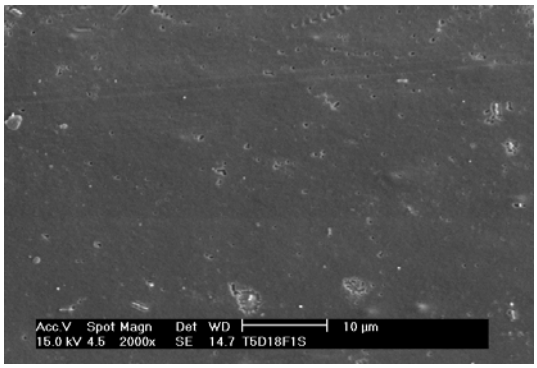

(e) 180 min

Figure 4.14: Surface of PAN membranes carbonized at different heating duration

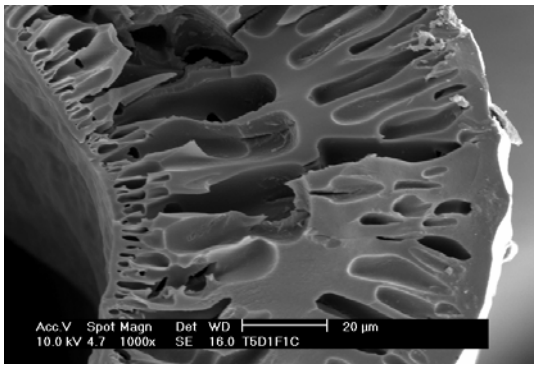

(a) 10 min

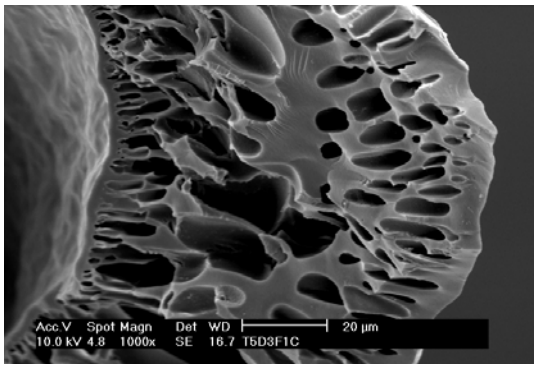

(b) 30 min

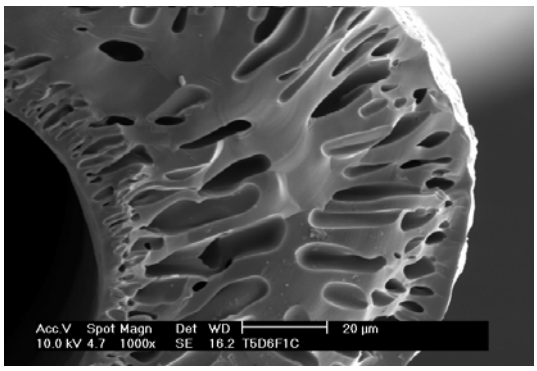

(c) 60 min

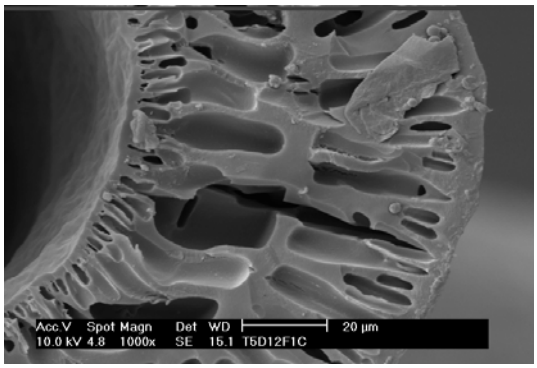

(d) 120 min

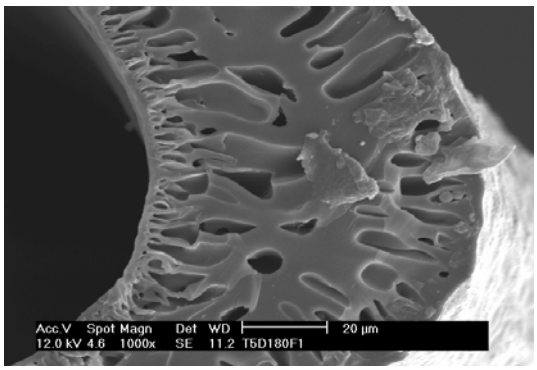

(e) 180 min

Figure 4.15: Cross section of membranes carbonized at different heating duration

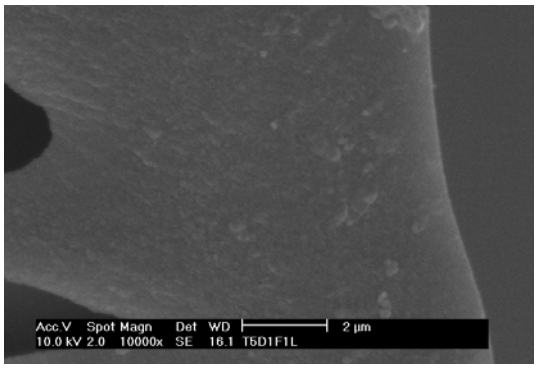

(a) 10 min

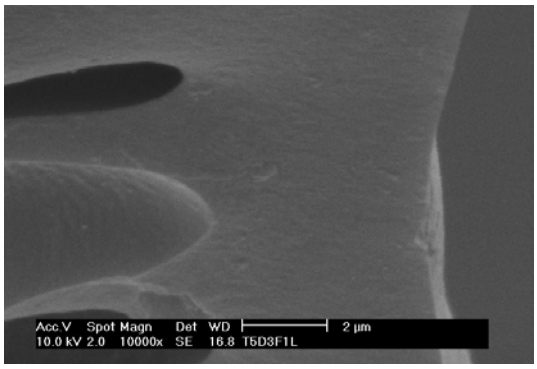

(b) 30 min

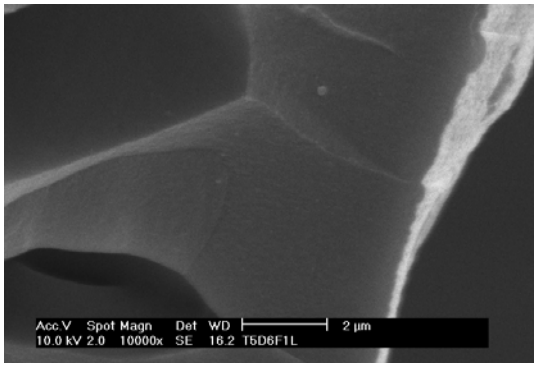

(c) 60 min

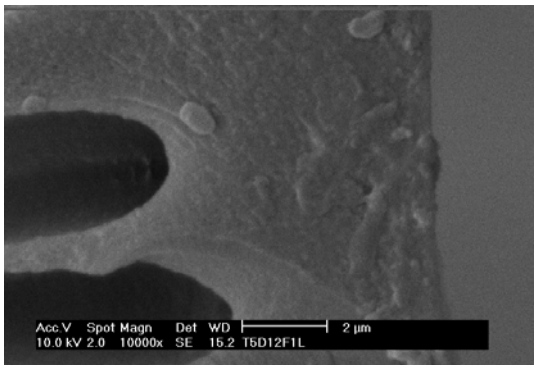

(d) 120 min

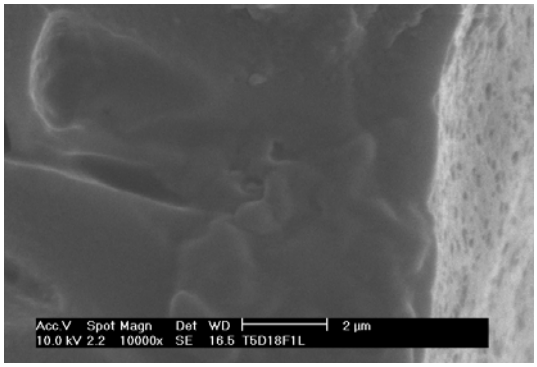

(e) 180 min

Figure 4.16: Skin layer of membranes carbonized at different heating duration

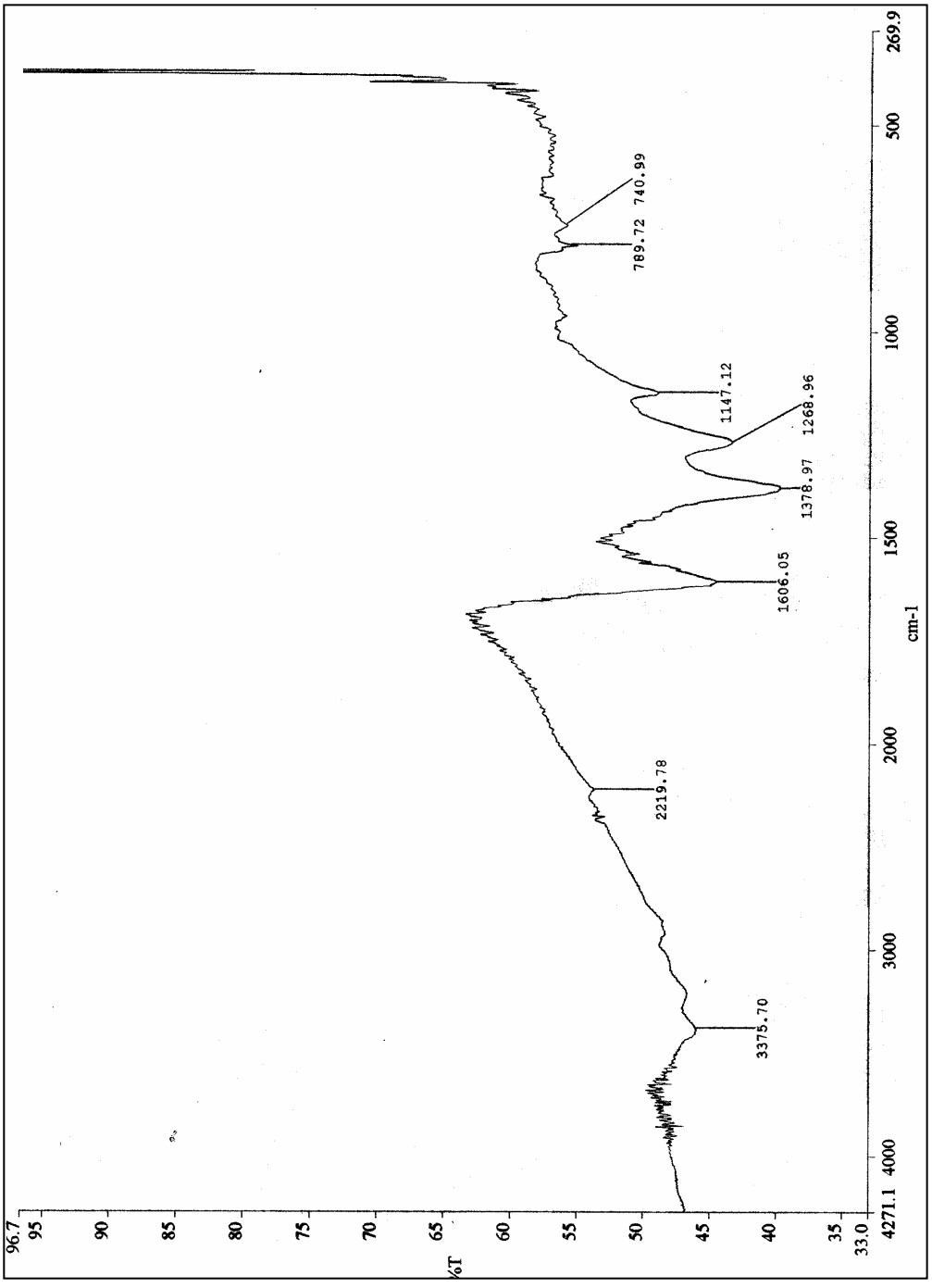

Figure 4.17 : FTIR result for carbon membrane carbonized with 10 min

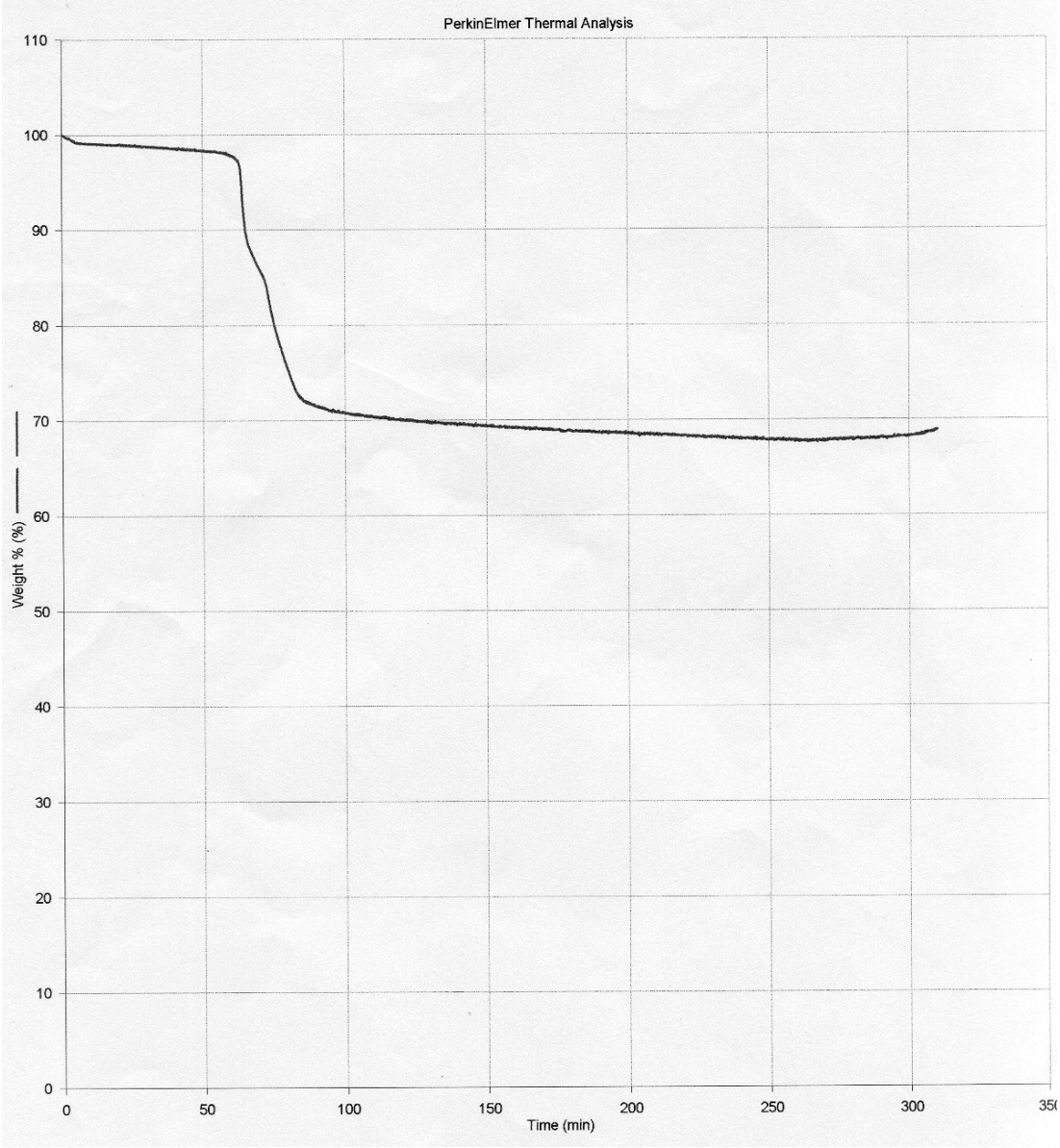

Figure 4.18: TGA result of a membrane heated at 500°C for 180 min

An explanation regarding the decreasing of permeability and increasing of selectivity at high heating duration and pyrolysis temperatures was mentioned by Mariwala and Foley [C72]. The conceptual model for the structure evolution in PFA-derived carbon molecular sieve is displayed in Figure 4.19. At low pyrolysis temperatures (200°C – 500°C), a highly chaotic structure consisting of amorphous carbon and very small aromatic microdomains are formed. At longer soak time, sp^3 carbons collapse and only sp^2 carbon is observed. These sp^2 carbons form the basis for the aromatic microdomains. This structure has a critical average pore dimension of $r_{pore\ 1}$, which is relatively large. This low temperature structure may have some

reiminiscene of the original precursor, thereby increasing the overall disorder of the material and its porosity.

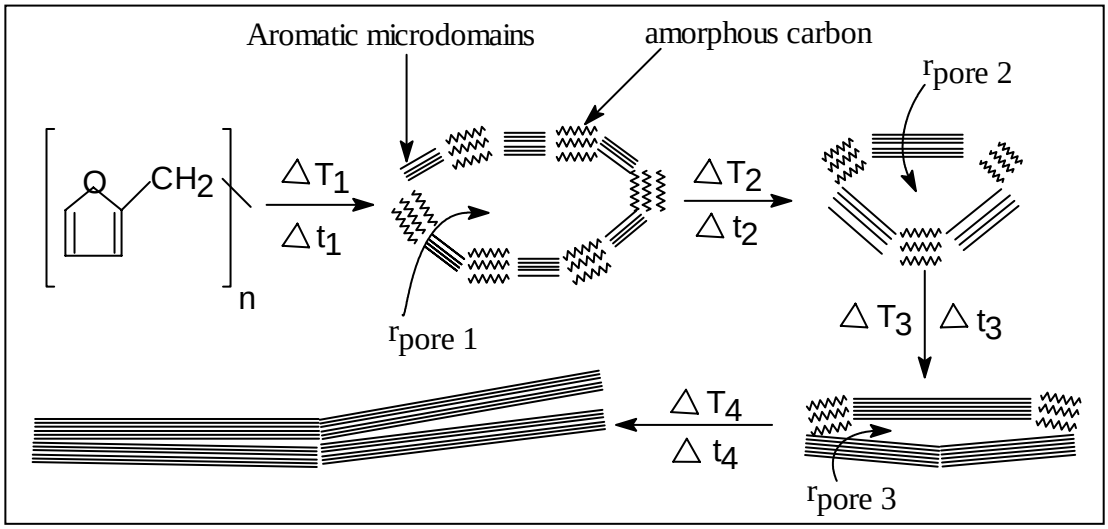

Figure 4.19: Conceptual model for adsorptive structure evolution in PFA-derived carbon molecular sieve [C72]

The size of the aromatic microdomains increases at the expense of the amorphous carbon regions with the increasing of soak times as well as temperatures. Despite a more ordered structure is formed in the short range; it is still highly disordered over the long range. As aromatic microdomains slowly grow with longer time at fixed temperatures or higher temperatures, it will adjust the orientation and improve the order of the structure, thus narrow the pores. Meanwhile, the misalignment between the aromatic microdomains begins to diminish and results in the reduction of average pore mouth dimensions [C72].

The researchers [C72] inferred that the misalignment of the aromatic microdomains would improve the ultramicroporosity in the carbon. At high degrees of misalignment, the pores are larger and numerous. As the degree of misalignment decreases, the pores become narrow and finally the overall porosity drops. Hence, r_{pore2} is on average, nominally less than r_{pore1}. As the material is heated to a high temperature, the internal growth of the aromatic microdomains continues and the amorphous carbon is consumed. With longer time or higher temperatures, the micropore structure will collapse, as the microdomains enlarge and more completely

align with one another. Therefore, the time and temperature effects can be considered as an annealing process, which in the limit leads to a nearly nonpermeable, microcrystalline graphite structure.

4.2.3 Effect of Purge Gas Flow Rate

It was observed that, as pyrolysis temperature increases, the carbon content will increase and the elemental ratio of hydrogen, oxygen and nitrogen to carbon decrease [C2]. This is because the heat will break the polymer chains of membrane during pyrolysis process and different volatile byproducts were produced. These evolved gases, which channeling their way out of the solid matrix during pyrolysis, develop the micropores of the carbon molecular sieve membranes [C4,C13]. Typical volatile products consisted of H_2, H_2O, CO and CO_2 as well as smaller amount of hydrogen cynide (HCN), CH_4 and NH_3 depending on the polymer. For a polyimide, typical less volatile byproducts include benzene, toluene, phenol and other heavier molecules that resemble portions of the polyimide chain [C44] while the noncarbon elements usually remove as volatiles from PAN membranes are hydrogen cynide (HCN), hydrogen (H_2), ammonia (NH_3), methane (CH_4), water (H_2O), carbon monoxide (CO), carbon dioxide (CO_2) and nitrogen (N_2) [B21-1.2,C67].

If the less volatile by products are not removed quickly enough during pyrolysis, they can presumably degrade further and leave carbon deposits on the surface of the carbon, which can be considered to be a form of chemical vapor deposition (CVD). Thus, at lower purge gas flow rates, the flow rate will determine whether the pores will blocked by carbon deposited by the polymer decomposition byproducts. Pore blocking via carbon deposition can occur either in the pores or on the fiber surface. Hence, the reduction in flow rate leads to an increase in the boundary layer thickness. This indicates that the permeability will decrease [C44,Th2]. The carbon deposit inside the pores will give additional resistance to the permeating gases.

The increasing of purge gas flowrate caused the increasing of the membrane's permeability without interfering its selectivity. The results in Figure 4.20 and Figure 4.21 showed that the permeabilities for oxygen and nitrogen were very low when the purge gas flow rate 20 cm^3/min was utilized. High permeability could be achieved if the high purge gas flow rates 150 – 200 cm^3/min were applied. It was observed that both oxygen and nitrogen permeability increased remarkably from 50 – 130 GPU at 20 cm^3/min flowrate to 150 – 730 GPU at 200 cm^3/min flowrate.

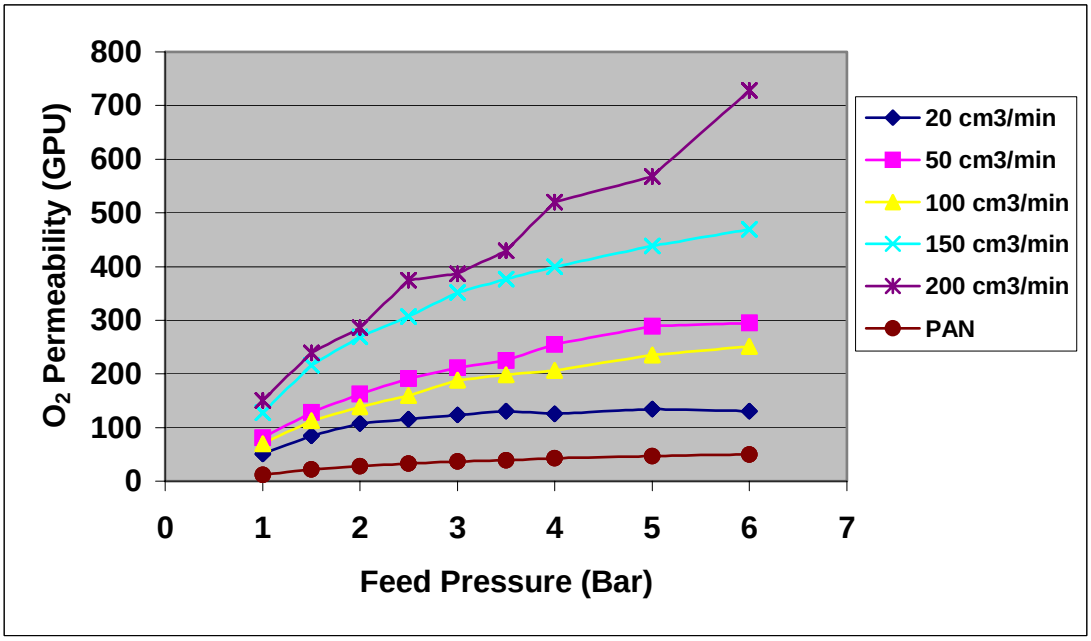

Figure 4.20: Influence of purge gas flowrates on the oxygen permeability at different feed pressure

However, the membrane carbonized at 20 cm^3/min purge gas flowrates still had higher permeability than original PAN membranes. This probably reflects that the pore system of membranes was not totally blocked by the volatile byproducts. The original PAN membranes have very low oxygen and nitrogen permeability with the range of 10 – 50 GPU. It is due to permeation of gases through the pore system is faster than the permeation through the polymer matrix of membranes. Thus, molecular sieving membranes tend to give higher productivity than conventional solution-diffusion membranes.

The membranes' selectivity achieved was in the range of 1.1 – 3.3. Figure 4.22 displays that the selectivity of the membrane did not affect much by the purge

gas flow rates. These finding is in agreement with the result of Geizler and Koros [C44] which observed the decrease of permeate flux by at least 2 orders of magnitude without increasing of selectivity when the purge gas flow rate 20 cm^3/min was applied.

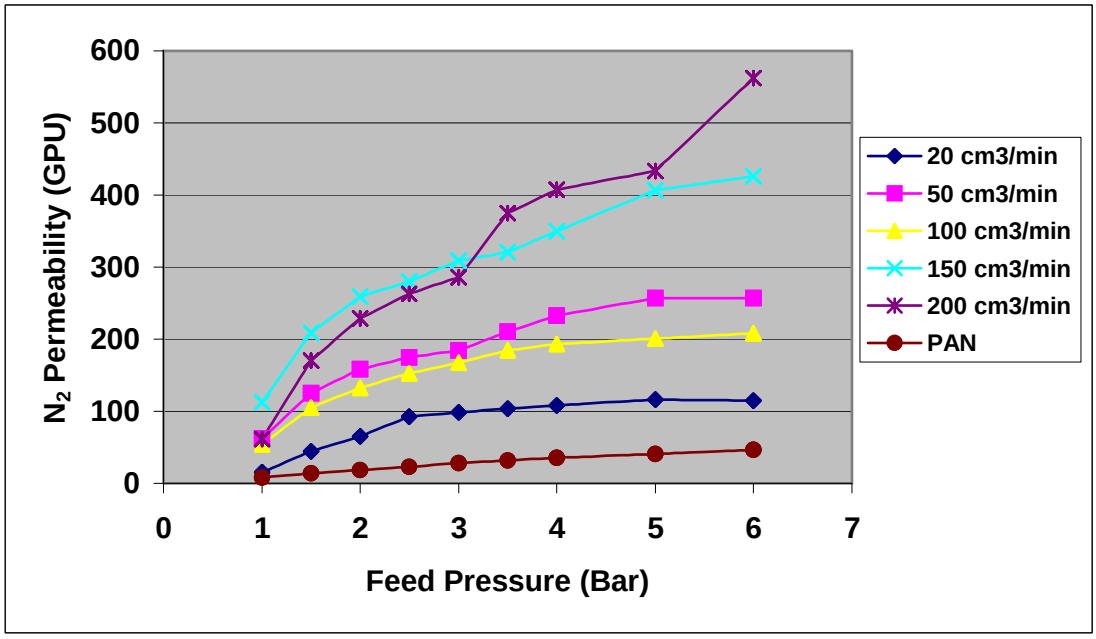

Figure 4.21: Influence of purge gas flowrate on the nitrogen permeability at different feed pressure

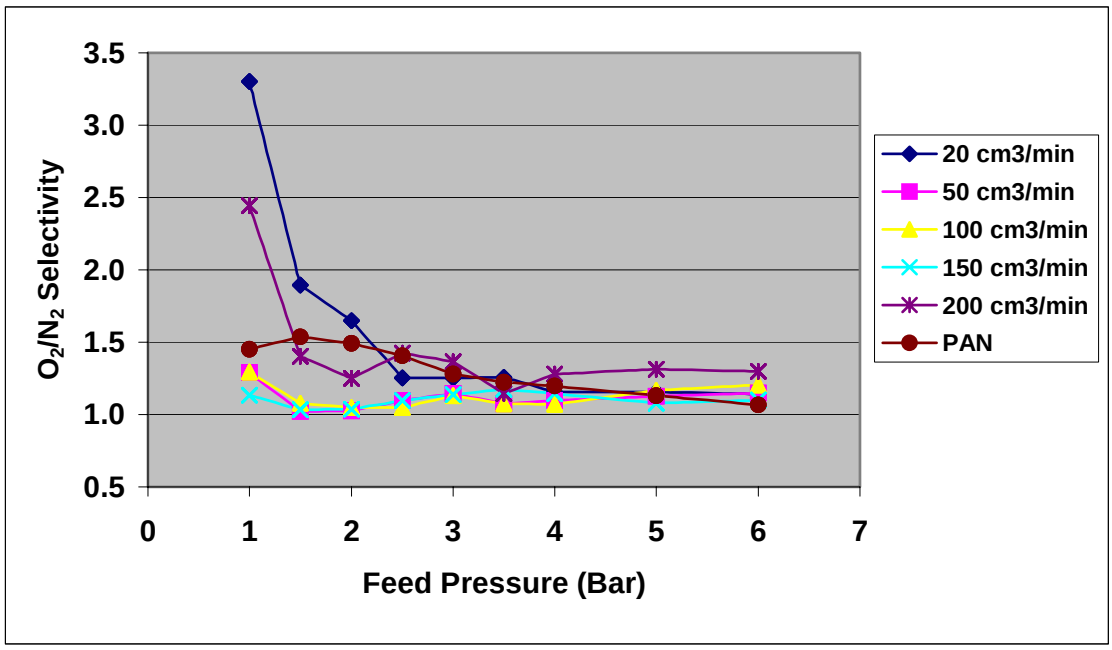

Figure 4.22: Influence of purge gas flowrate on the membrane selectivity at different feed pressure

This observation displays that purge gas flowrates is essentially importance to enhance the productivity of carbon membranes without sacrificing its separation ability. A suitable and optimum inert gas flow rate must be determined for different carbon membrane precursors.

SEM results in Figure 4.23 displayed the variation of membranes surface carbonized at different purge gas flowrates. Large amount of pores are evident on the surface on the membranes carbonized at high purge gas flowrates. In contrast, a lot of pores were blocked and coated by carbon deposit when low purge gas flowrates were applied. However, neither support layers nor skin layers of membranes were influenced by the purge gas flowrates as displayed in Figure 4.24 and 4.25. Therefore, there is no significant diversity between the membranes pyrolized at different purge gas flowrates.

In addition, the FTIR results support the preceding observation, which exhibited that only functional group nitril (C-N) owned by membranes fabricated using different purge gas flowrates at 500°C. Figure 4.26 shows the FTIR result for carbon membrane carbonized by using 20 cm^3/min purge gas flowrate. Other FTIR results were presented in Appendix D-11 to Appendix D-13. The results indicated the purge gas flowrates during pyrolysis would not affect the chemical structure of the membranes. Obviously, the purge gas flowrates will not manipulate the bulk structure of the membranes and affect the pore size distribution, but it is responsible in making alteration on the membranes surface properties.

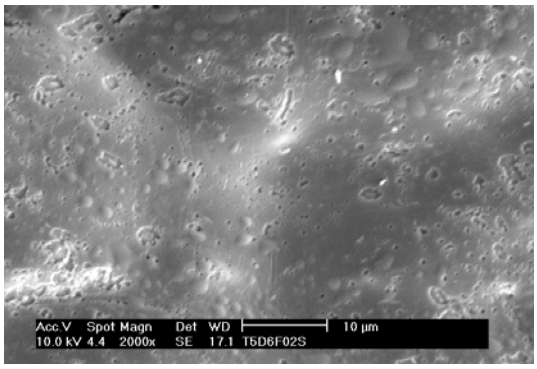

(a) 20 cm^3/min

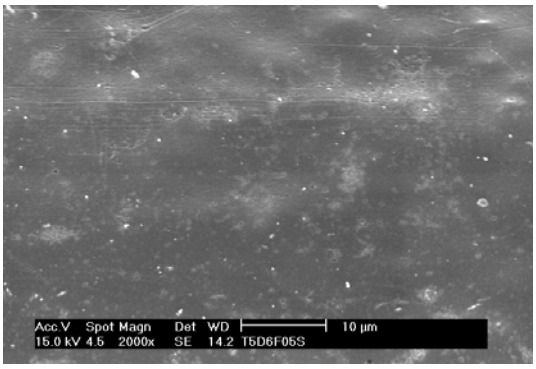

(b) 50 cm^3/min

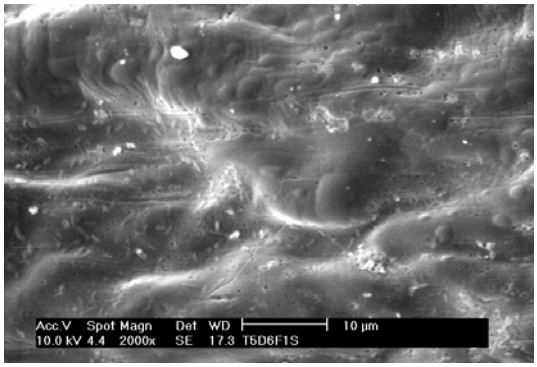

(c) 100 cm^3/min

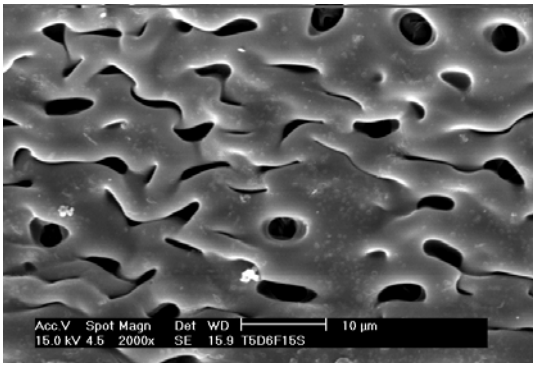

(d) 150 cm^3/min

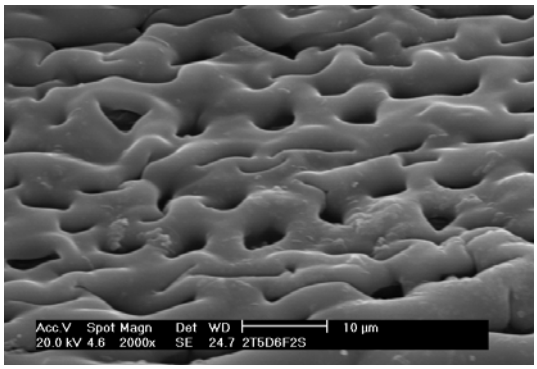

(e) 200 cm^3/min

Figure 4.23: Surface of PAN membranes carbonized at different purge gas flowrates

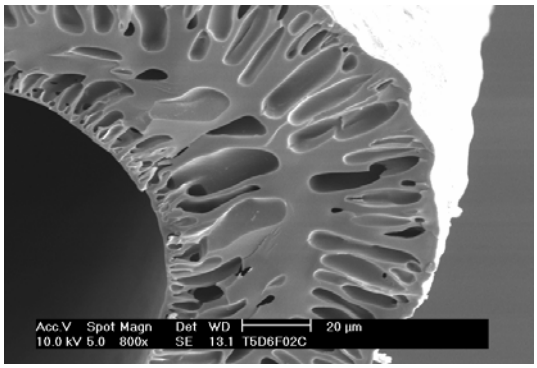

(a) 20 cm^3/min

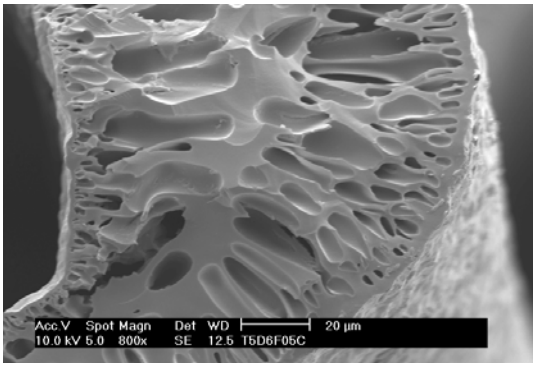

(b) 50 cm^3/min

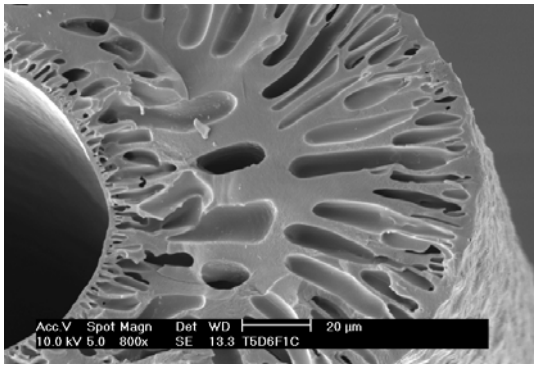

(c) 100 cm^3/min

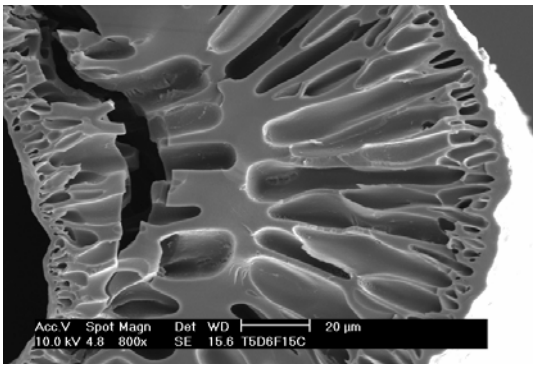

(d) 150 cm^3/min

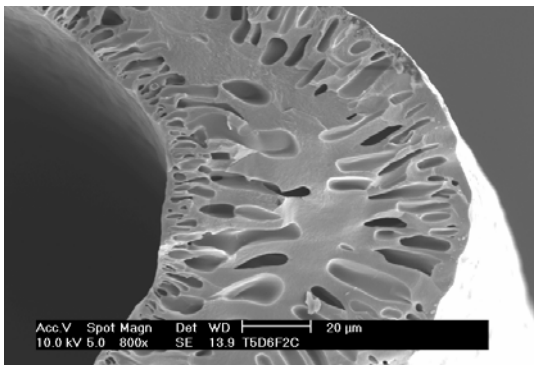

(e) 200 cm^3/min

Figure 4.24: Cross section of PAN membranes at different purge gas flowrates

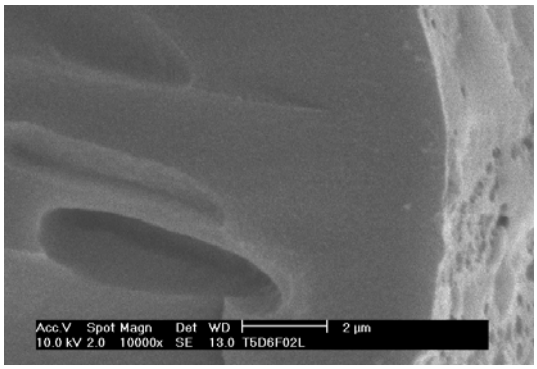

(a) 20 cm^3/min

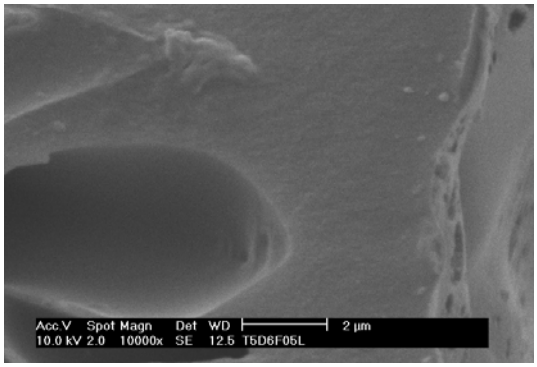

(b) 50 cm^3/min

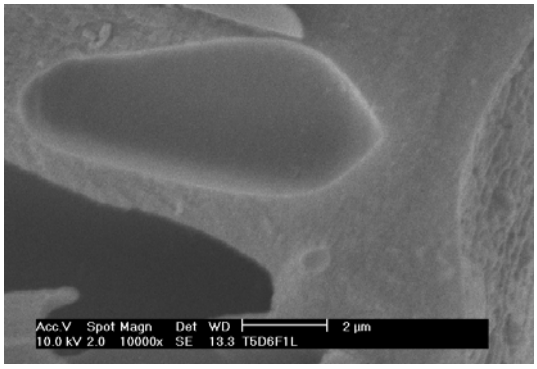

(c) 100 cm^3/min

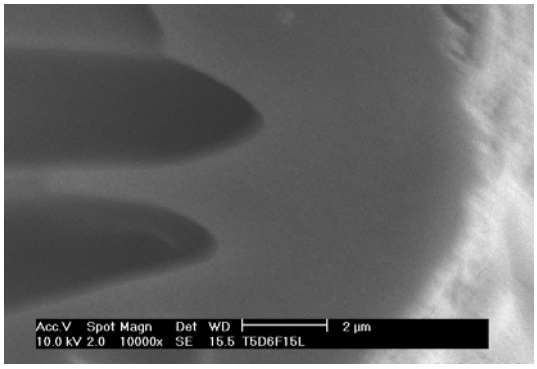

(d) 150 cm^3/min

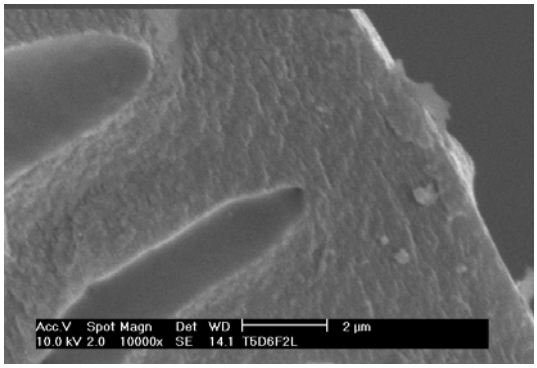

(e) 200 cm^3/min

Figure 4.25: Skin layer of PAN membranes at different purge gas flowrates

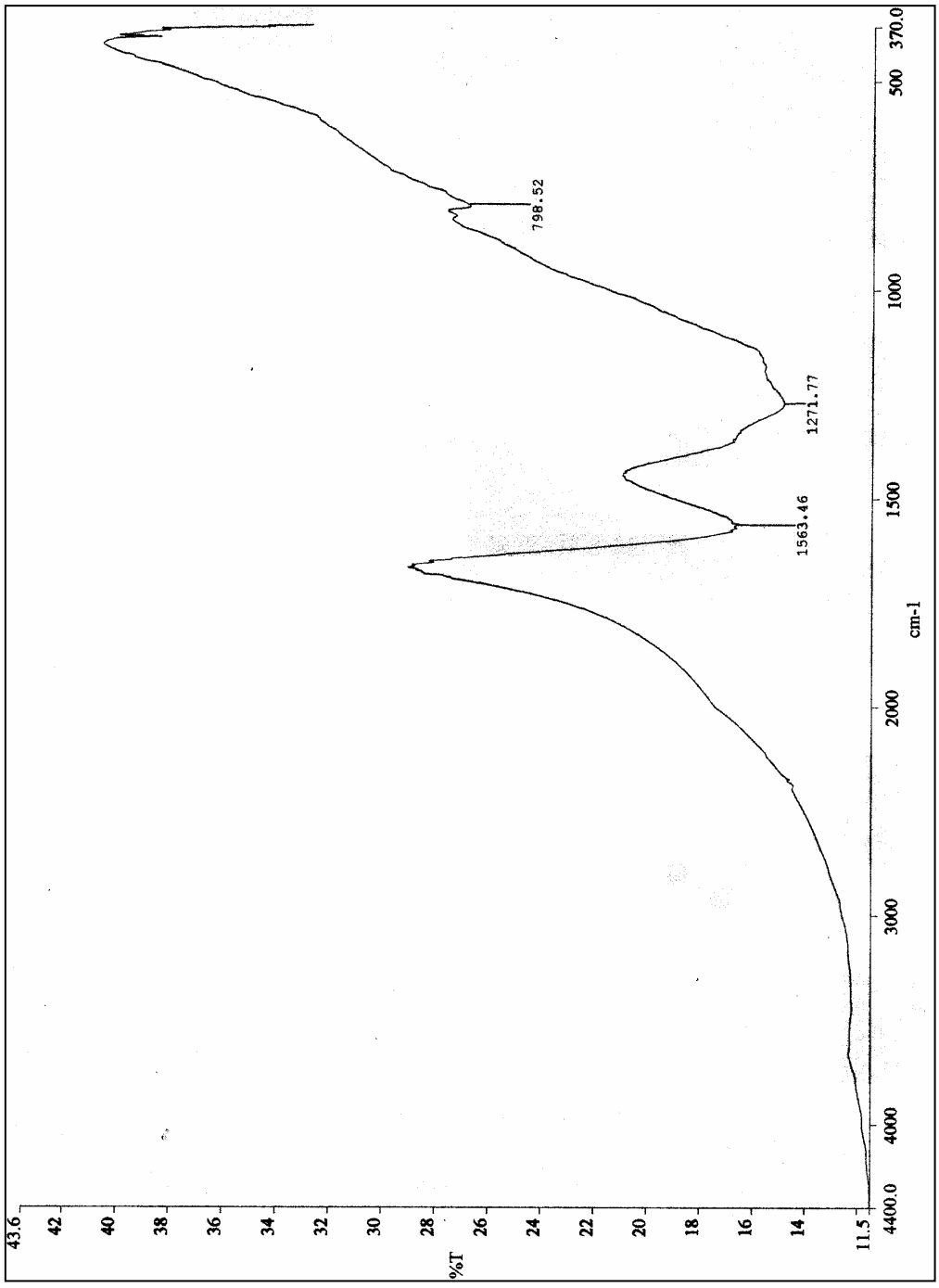

Figure 4.26: FTIR result for carbon membrane carbonized at 20 cm^3/min

4.3 Influence of Thermastabilization Process Atmosphere

During thermastabilization process, the purge gas chosen is critical for the resulting carbon membranes. It is because different atmosphere of thermastabilization process leading to different structure of the stabilized membranes. TGA results in Figure 4.27 and Figure 4.28 display that the weight loss was greater for the membrane pyrolyzed without oxidative thermastabilization treatment. The weight loss was significant especially at temperature 300°C – 350°C because the glassy temperature for PAN is 317°C. It means that the chemical stability of the oxidative thermastabilized membrane is higher than the membrane obtained from inert thermastabilization process.

However, if the membrane was exposed under oxygen purge only, the weight of the membrane was entirely loss at around 650°C due to the excessive oxidation process as shown in Figure 4.29. This indicated that the fibers were melting and removed as volatile gas. In addition, the PAN hollow fibers already broke even carbonized until 500°C only. Therefore, inert gas should be used for PAN heating treatment after thermastabilization process.

The polymerization reactions may occur from simple heating of PAN in inert or oxidizing atmosphere and give rise to a thermally stable cyclized structure, which is often referred as ladder polymer as shown in Figure 4.30. Two different chemical structures would form by inert stabilization and oxidative stabilization process. Cyclization and oxidation take place in the oxidative stabilization process while there is only cyclization process taking place in the former process. Previous researcher reported that the oxidative treatment produces more thermally stable structures [B21-1.2,B6-2.7,C67].

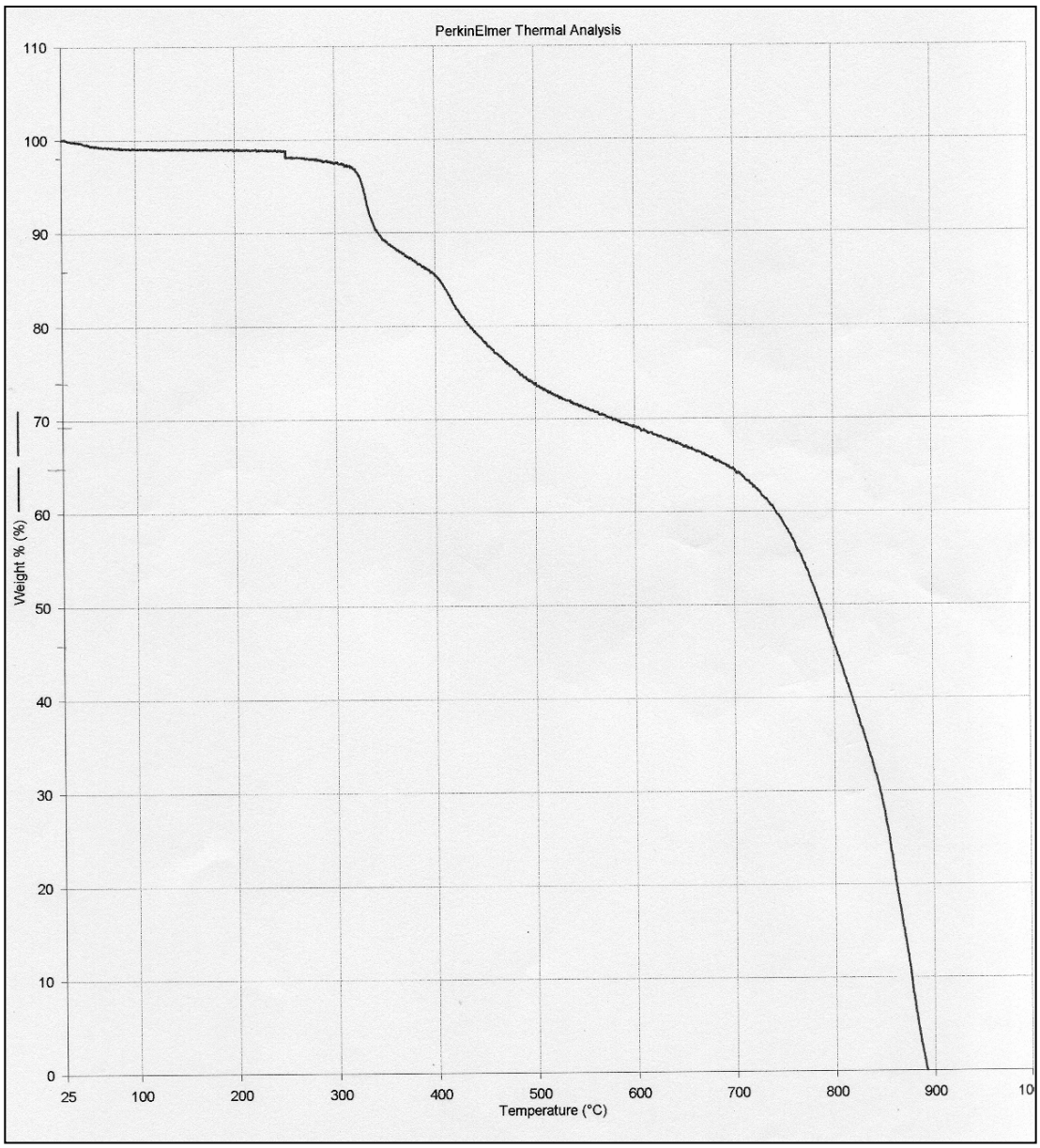

Figure 4.27: TGA result for the membrane stabilized under oxidative atmosphere

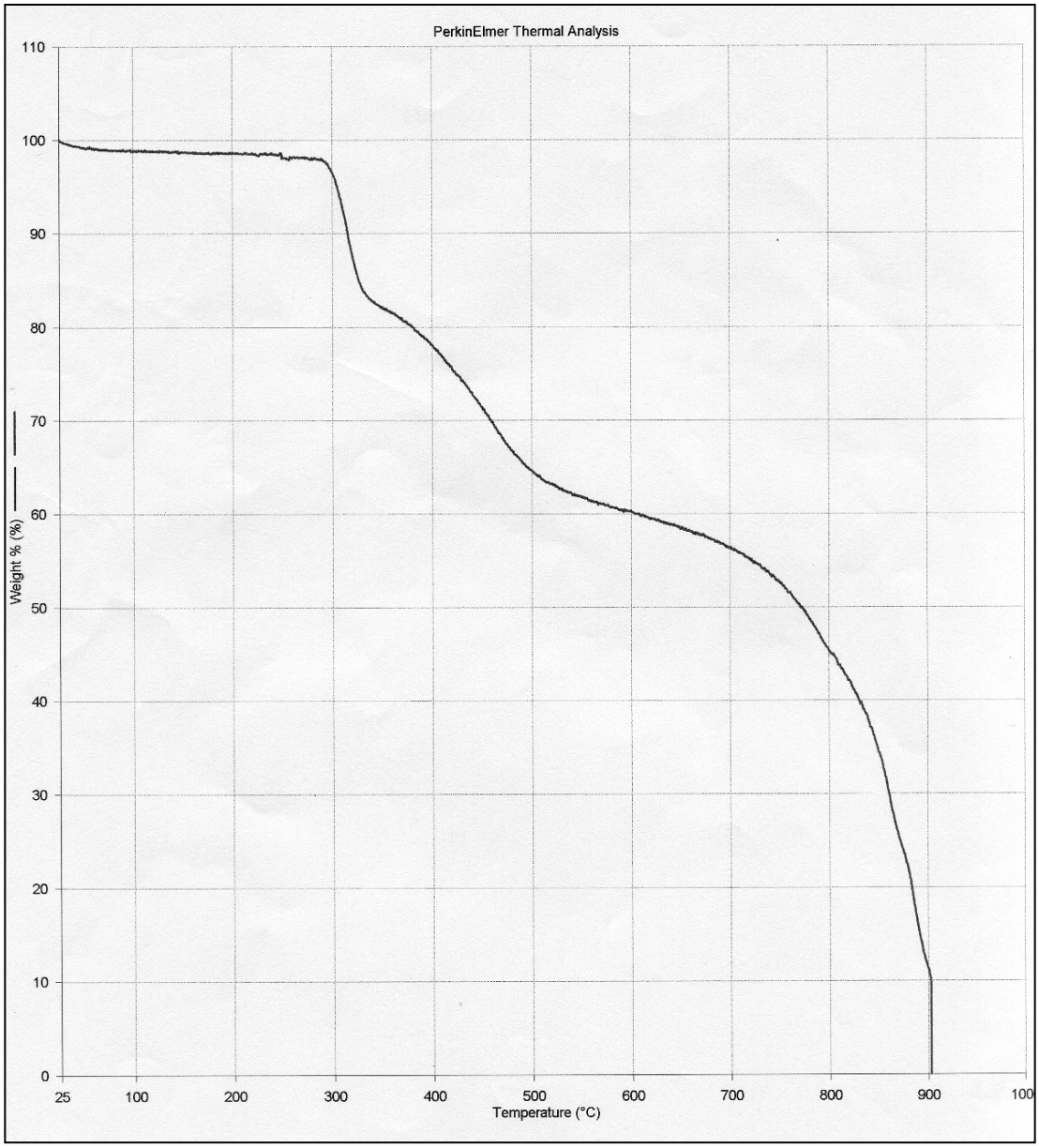

Figure 4.28: TGA result for the membrane stabilized under inert atmosphere

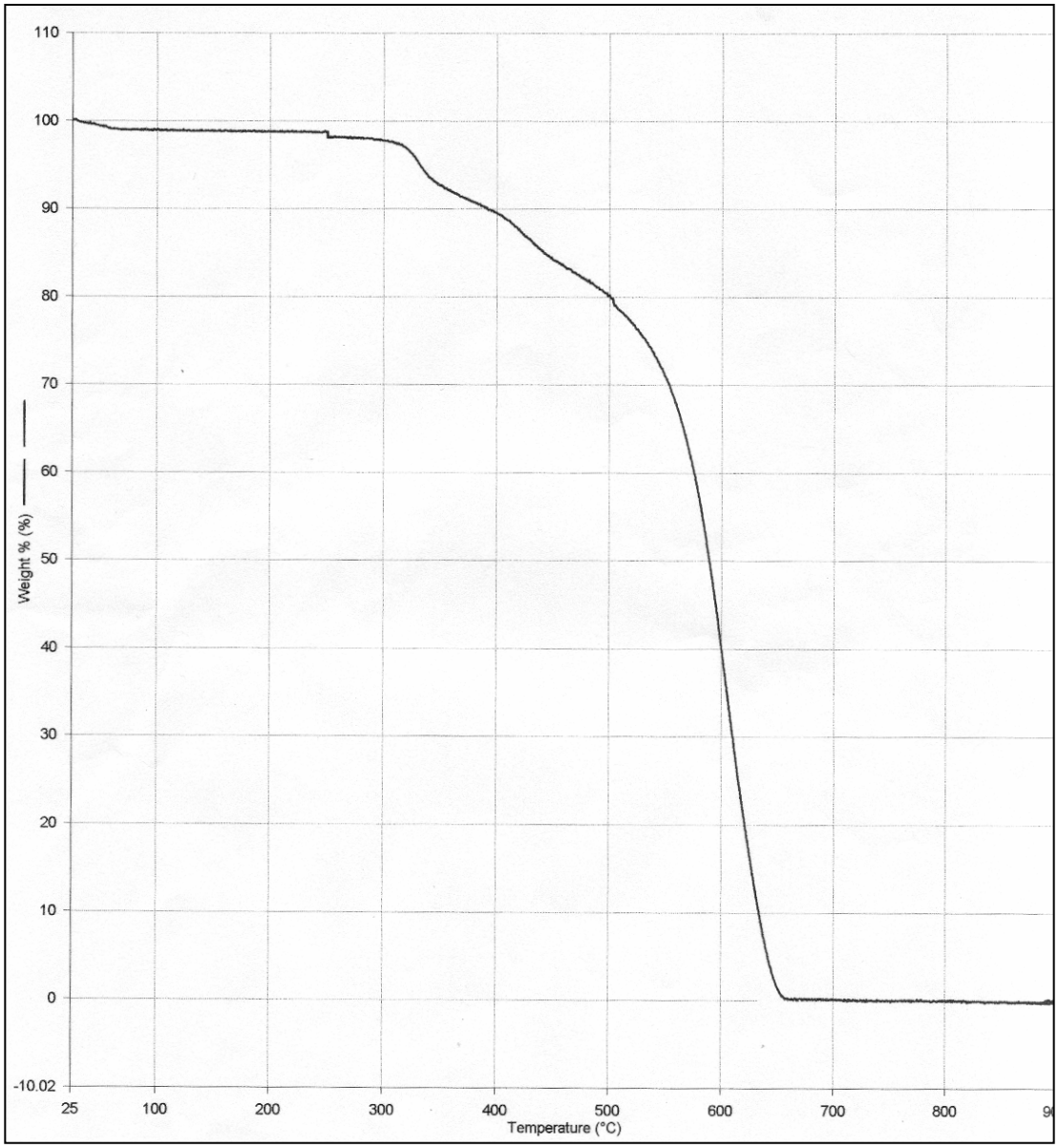

Figure 4.29: TGA result for the membrane stabilized and carbonized with oxygen atmosphere

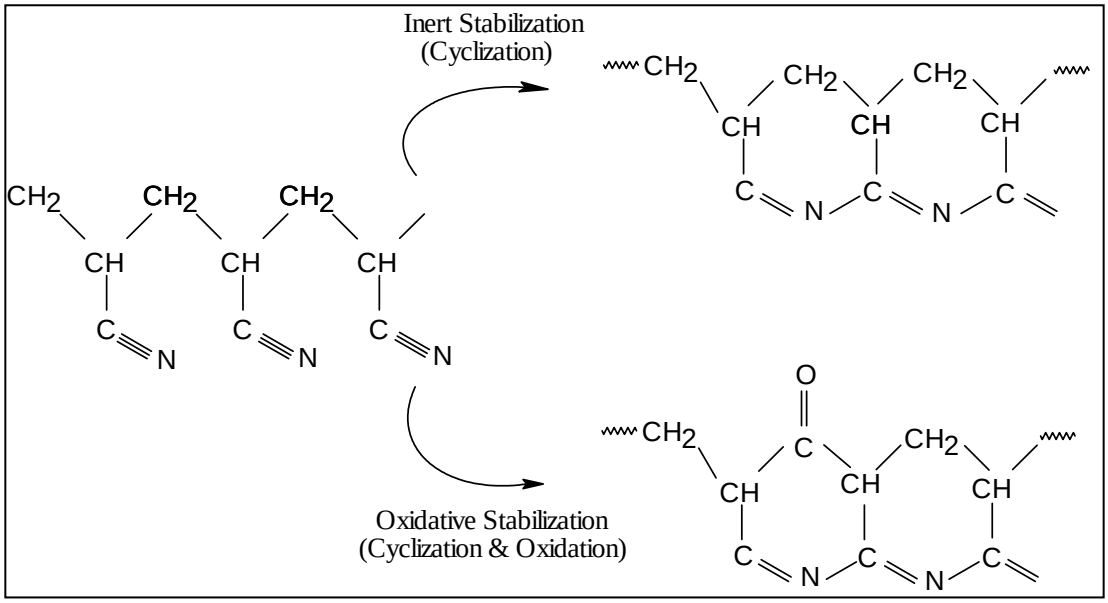

Figure 4.30: Formation of ladder polymer in inert stabilization and oxidative stabilization process

The rate of cyclization for the PAN fibers heated under an oxidizing atmosphere is faster than the membranes heated under inert atmosphere and the final carbon products have better yield with improved mechanical properties. It is due to oxidized PAN fibers have preferentially an aromatic character, which prevents the backbone carbon chain from extensive splitting. Conversely, aromatization does not readily occur at low temperatures for PAN fibers stabilized in inert atmosphere. Thereby, it has to be induced at higher temperatures, which causes considerable splitting of the main carbon chain and leads to the formation of a low yield and poor mechanical properties carbon fibers. It was reported that larger weight loss occurred for unoxidized carbon fibers [B21-1.2].

When PAN fibers are heated under controlled oxidizing atmosphere, would cause reorganization of the polymer chains and three-dimensional linking of the parallel molecular chains by oxygen bonding [B21-1.2]. In addition, previous researchers [C62] observed that when a PAN hollow fiber is heated at above 180°C in the presence of O_2, C≡N bonds will be converted into C=N bonds, the ladder polymer will be formed and the cohesive energy between the relative chains will drop appreciably. It was found that O_2 is introduced in the form of C=O groups and

bonded to the carbon backbone of the ladder polymer. The O_2 of C=O is released as water vapor during carbonization. The densities of stabilized hollow fiber are due to the structural rearrangements associated with the cyclization reactions and the incorporation of O_2

Oxidative stabilization reactions initiate in the amorphous part of PAN fiber. The reactions contribute to the major portion of the macroscopic shrinkage. Crystalline morphology is largely maintained during this stage, although considerable randomization of crystal lamellae takes place. Stabilization reactions are primarily intramolecular. Intermolecular cross-linking occurs above ~ 300°C in the presence of O_2. Macroscopic shrinkage observed during stabilization is proposed to be an “entropic” process, with “chemical” forces serving only to modify the observed response [C65].

Oxidation increased permeance without greatly damaging the selectivities. It is due to oxidation significantly increased the micropore volume but the pore size distribution was not broadened. Therefore, oxidation did not greatly affect the chemical structure of the membrane. Besides that, the changes in elemental compositions by the oxidation were much smaller than those by carbonization [C28].

BAB V

CONCLUSIONS

5.1 Conclusions

From the research conducted and the preceding discussion, the carbon molecular sieve membrane will definitely emerge as another alternative membrane for gas separation process and other separation processes. Despite carbon membranes consist of 4 major configurations: flat, capillary, tube and hollow fiber, carbon hollow fiber membranes are recognized to have enormous potential to applied broadly in the gas separation industry for instance air separation industry. Presently, hollow fibers are the most famous membrane geometry due to their high surface area per unit volume of membrane module and other enormous advantages [F3].

Carbon membrane with it unique characteristics and advantages will make it competitive with polymeric membrane even with other inorganic membrane. However, intensive research and development must be carried out to commercialize the carbon membrane in international market. It is important that the study regarding the influence of pyrolysis process on the carbon membrane performance plays a significant role as a starting stage to commercialize the production of carbon membrane in Malaysia and worldwide. From obtained results, there are a few conclusions reached.

1. Polyacrylonitrile membranes are a suitable precursor for carbon membranes as it can withstand high temperature heat treatment and is relatively economic polymer.

2. Oxidative thermastabilization process is required prior to carbonization of PAN membrane to carbon membranes. After this treatment, the membranes have higher thermal stability for heat treatment at high temperatures.

3. The inert gas pyrolysis is an appropriate process to fabricate and produce carbon hollow fiber membranes. This is because it can produce high productivity carbon membranes.

4. Pyrolysis temperature is one of the most important parameters, which influence the structure as well as the permeation properties of carbon membranes. Increasing of pyrolysis temperatures resulted in the increasing of permeability at initial stage of 250°C but the permeability decreased after 600°C. High selectivities were achieved at temperatures 700°C – 800°C.

5. Heating duration or soak time during pyrolysis process also give significant influence on the carbon membranes properties. As the heating duration increased, the permeability of the membranes increased at early stage but decreased after 120 min. It was found that high heating duration responsible for the formation of high selectivity carbon membranes. Sufficient soak time is important for the formation of complete carbon membranes.

6. Another significant factor, which has pronounced effect on the carbon membranes surface properties is purge gas flowrate. The high purge gas flowrate leaded to the production of high permeability membranes without sacrificing the membrane selectivity.

5.2 Recommendations

Although carbon membranes still require improvement before they can become dominant commercialized inorganic membranes, carbon membranes have great potential to replace other inorganic membranes in the market because they have many useful characteristics and are able to separate gas mixtures, which have similar size of gas molecules, efficiently. From this research, a few recommendations were proposed for future investigation.

1. Optimization of precursor preparation process

Besides pyrolysis process, the polymer solution preparation, spinning process, solvent exchange process and others are important steps to ensure the production of excellent carbon membranes.

2. Optimization of pyrolysis process

There are abundant parameters during process, which will determine the properties and performance of a carbon membrane. A wider coverage of study on the pyrolysis process condition including heating rate, types of purge gas and amount of heating steps should be conducted. All the experimental results obtained should be simulated using computer software to obtain an ideal and practical pyrolysis condition, which can be implemented in pilot-scale.

3. Composite precursor for carbon membranes

Combination utilization of low cost and high cost polymers to produce composite carbon membranes is an alternative way to get economical and high performance carbon membranes. The membranes consisted of skin layer with high yield carbon and substructure with low yield carbon. High yield carbon leads to the development of high selective skin layer while low yield carbon can results in open porous structure with minimum resistance for the gas permeation [Th2].

4. Polymer blend carbonization method

The polymer blend carbonization method will become an important tool for producing carbon membranes with mixed-matrix materials overcome the challenges and limitation of membrane technology in the gas separation industry. The concept of this method has illustrated in Figure 5.1. Mixed matrix materials comprising molecular sieve entities embedded in a polymer matrix offer the potential to combine the processability of polymers wit the superior gas separation properties of rigid molecular sieving materials [G1,G6].

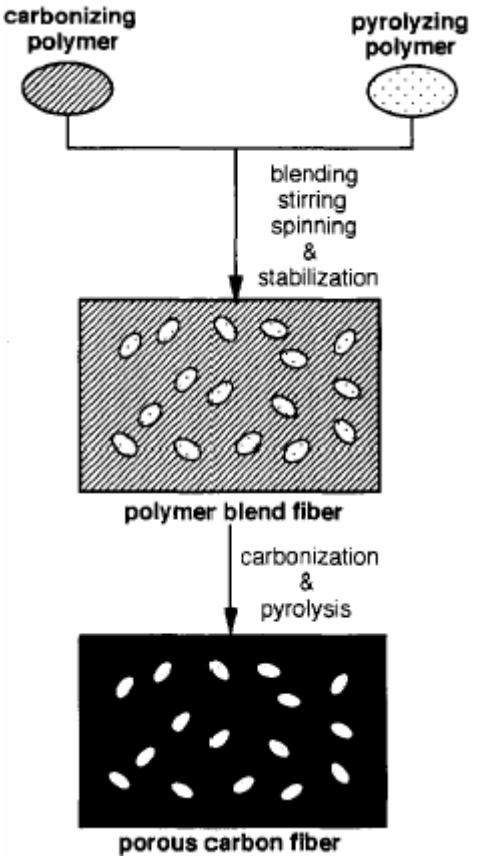

Fig 5.1: Schematic diagram of the polymer blend carbonization concept [C52]

The carbonization polymer blend will lead to the formation of porous structure. It is because of the thermally unstable polymer (pyrolyzing polymer) will decomposing and remaining pores on the carbon matrix obtained from the stable polymer (carbonizing polymer). Polymer blends of phenolic resin and poly(vinyl butyral) [C52] as well as poly(diphenylene pyromellitimide) (PP) and poly(ethylene

glycol) (PEG) [C51] were used by previous researchers. Although polymer blends have widely used as important industrial raw materials for highly functional materials, the implementation of this carbonization method just at the beginning stage [C51]. More study is needed to identify suitable pyrolyzing polymers and carbonizing polymer for blending.

REFERENCES

C1 Tanihaara, N., Shimazaki, H., Hirayama, Y., Nakanishi, S., Yoshinaga, T. and Kusuki, Y. (1999). “Gas Permeation Properties of Asymmetric Carbon Hollow Fiber Membranes Prepared from Asymmetric Hollow Fiber.” *J. Membr. Sci*. **160**. 179-186.

C2 Kusuki, Y., Shimazaki, H., Tanihara, N., Nakanishi, S. and Yoshinaga, T. (1997). “Gas Permeation Properties and Characterization of Asymmetric Carbon Membranes Prepared by Pyrolyzing Asymmetric Polyimide Hollow Fiber Membrane.” *J. Membr. Sci.* **134**. 245-253.

C3 Fuertes, A. B. and Centeno, T. A. (1999). “Preparation of Supported Carbon Molecular Sieve Membrane.” *Carbon*. **37**. 679-684.

C4 Suda, H. and Haraya, K. (1997). “Gas Permeation through Micropores of Carbon Molecular Sieve Membranes Derived from Kapton Polyimide, *J. Phys. Chem. B.* **101**. 3988-3994.

C5 Centeno, T. A. and Fuertes, A. B. (1999). “Supported Carbon Molecular Sieve Membranes based on Phenolic Resin.” *J. Membr. Sci.* **160**. 201-211.

C6 Fuertes, A. B. and Centeno, T. A. (1998). “Preparation of Supported Asymmetric Carbon Molecular Sieve Membranes.” *J. Membr. Sci.* **144**. 105-111.

C7 Fuertes, A. B. and Centeno, T. A. (1998). “Carbon Molecular Sieve Membranes from Polyetherimide.” *Microporous & Mesoporous Materials.* **26**. 23-26.

C8 Kusakabe, K., Gohgi, S. and Morooka, S. (1998). “Carbon Molecular Sieving Membranes Derived from Condensed Polynuclear Aromatic (COPNA) Resins for Gas Separation.” *Ind. Eng. Chem. Res.* **37**. 4262-4266.

C9 Hayashi, J., Yamamoto, M., Kusakabe, K. and Morooka, S. (1995). “Simultaneous Improvement of Permeance and Permselectivity of 3,3’4,4’-

Biphenyltetracarboxylic Dianhydride-4,4'-Oxydianiline Polyimide Membrane by Carbonization." *Ind. Eng. Chem. Res.* **34**. 4364-4370.

C10 Jones, C. W. and Koros, W. J. (1995). "Characterization of Ultramicroporous Carbon Membranes with Humidified Feeds." *Ind. Eng. Chem. Res.* **34**. 158-163.

C11 Jones, C. W. and Koros, W. J. (1995). "Carbon Composite Membranes: A Solution to Adverse Humidity Effects." *Ind. Eng. Chem. Res.* **34**. 164-167.

C12 Petersen, J., Matsuda, M. and Haraya, K. (1997). "Capillary Carbon Molecular Sieve Membranes Derived from Kapton for High Temperature Gas Separation." *J. Membr. Sci.* **131**. 85-94.

C13 Wang, Shu Sen, Zeng, Mei Yun and Wang, Zhi Zong (1996). "Asymmetric Molecular Sieve Carbon Membranes." *J. Membr. Sci.* **109**. 267-270.

C14 Linkov, V. M., Sanderson, R. D. and Jacobs, E. P. (1994). "Highly Asymmetrical Carbon Membranes." *J. Membr. Sci.* **95**. 93-99.

C15 Chen, Y. D. and Yang, R. T. (1994). "Preparation of Carbon Molecular Sieve Membrane and Diffusion of Binary Mixtures in the Membrane." *Ind. Eng. Chem. Res.* **33**. 3146-3153.

C16 Rao, M. B. and Sircar, S. (1996). "Performance and Pore Characterization of Nanoporous Carbon Membrane for Gas Separation." *J. Membr. Sci.* **110**. 109-118.

C17 Rao, M. B. and Sircar, S. (1993). "Nanoporous Carbon Membranes for Separation of Gas Mixtures by Selective Surface Flow." *J. Membr. Sci.* **85**. 253-264.

C18 Koresh, J. E. and Soffer, A. (1986). "Mechanism of Permeation through Molecular – Sieve Carbon Membrane. Part 1 – The Effect of Adsorption and the Dependence on Pressure." *J. Chem. Soc. Faraday Trans. I.* **82**. 2057-2063.

C19 Koresh, J. E. and Soffer, A. (1980). "Study of Molecular Sieve Carbons. Part 1 – Pore Structure, Gradual Pore Opening and Mechanism of Molecular Sieving." *J. Chem. Soc. Faraday Trans. I.* **76**. 2457-2471.

C19a Koresh, J. E. and Soffer, A. (1980). "Study of Molecular Sieve Carbons. Part 2 – Estimation of Cross-sectional Diameters of Non-spherical Molecules." *J. Chem. Soc. Faraday Trans. I.* **76**. 2472-2485.

C19 Koresh, J. E. and Soffer, A. (1980). "Molecular Sieving Range of Pore

b Diameters of Adsorbents." *J. Chem. Soc. Faraday Trans. I.* **76**. 2507-2509.

C19c Koresh, J. E. and Soffer, A. (1981). Molecular Sieve Carbons. Part 3 – Adsorption Kinetics According to a Surface-Barrier Model." *J. Chem. Soc. Faraday Trans. I.* **77**. 3005-3018.

C20 Hatori, H., Yamada, Y. and Shiraishi, M. (1992). "Preparation of Macroporous Carbon Films from Polyimide by Phase Inversion Method." *Carbon.* **30**. 303-304.

C21 Hatori, H., Shiraishi, M., Nakata, H. and Yoshitomi, S. (1992). "Carbon Molecular Sieve Films from Polyimide." *Carbon.* **30**. 305-306.

C22 Jones, C. W. and Koros, W. J. "Carbon Molecular Sieve Gas Separation Membranes – I Preparation and Characterization based on Polyimide Precursors." *Carbon.* **32**. 1419-1425.

C23 Katsaros, F. K., Steriotis, T. A., Stubos, A. K., Mitropoulos, A., Kanellopoulos, N. K. and Tennison, S. (1997). "High Pressure Gas Permeability of Microporous Carbon Membranes." *Microporous Materials.* **8**. 171-176.

C24 Ogawa, M. and Nakano, Y. (1999). "Gas Permeation through Carbonized Hollow Fiber Membranes Prepared by Gel Modification of Polyamic Acid." *J. Membr. Sci.* **162**. 189-198.

C25 Acharya, M. and Foley, H. C. (1999) "Spray-coating of Nanoporous Carbon Membranes for Air Separation." *J. Membr. Sci.* **161**. 1-5.

C26 Bird, A. J. and Trimm, D. L. (1983). "Carbon Molecular Sieves Used in Gas Separation Membranes." *Carbon.* **21**. 177-180.

C27 Linkov, V. M., Sanderson, R. D. and Rychkov, B. A. (1994). "Composite Carbon – Polyimide Membranes." *Material Letters.* **20**. 43-46.

C28 Kusakabe, K., Yamamoto, M. and Morooka, S. (1998). "Gas Permeation and Micropore Structure of Carbon Molecular Sieving Membranes Modified by Oxidation." *J. Membr. Sci.* **149**. 59-67.

C29 Yamamoto, M., Kusakabe, K., Hayashi, J. and Morooka, S. (1997). "Carbon Molecular Sieve Membrane Formed by Oxidative Carbonization of a Copolyimide Film Coated on a Porous Support Tube." *J. Membr. Sci.* **133**. 195-205.

C30 Hayashi, J., Mizuta, H., Yamamoto, M., Kusakabe, K. and Morooka, S. (1997). "Pore Size Control of Carbonized BPTA-pp'ODA Polyimide Membrane by

Chemical Vapor Deposition of Carbon." *J. Membr. Sci.* **124**. 243-251.

C31 Liang, Chang Hai, Sha, Guan Yan and Guo, Shu Cai (1999). "Carbon Membrane for Gas Separation Derived from Coal Tar Pitch." *Carbon.* **37**. 1391-1397.

C32 Keizer, K. and Verweij, H. (1996). "Progress in Inorganic Membranes." *Chemtech.* Jan. 37-41.

C33 Hsieh, H. P. (1990). "Inorganic Membranes." *Membrane Materials and Processes.* **84**. 1-18.

C34 Jones, C.W. and Koros, W. J. (1994). "Carbon Molecular Sieve Gas Separation Membranes – II Regeneration Following Organic Exposure." *Carbon.* **32**. 1427-1432.

C35 Koresh, J. E. and Soffer, A. (1983). "Molecular Sieve Carbon Permselective Membrane Part I: Presentation of a New Device for Gas Mixture Separation." *Sep. Sci. Tech.* **18**. 723-734.

C36 Koresh, J. E. and Soffer, A. (1987). "The Carbon Molecular Sieve Membranes. General Properties and the Permeability of CH_4/H_2 Mixture." *Sep. Sci. Tech.* **22**. 973-982.

C37 Wang, Shu Sen, Zeng, Mei Yun and Wang, Zhi Zhong (1996). "Carbon Membrane for Gas Separation." *Sep. Sci. Tech.* **31**. 2299-2306.

C38 Fuertes, A. B., Nevskaia, D. M. and Centeno, T. A. (1999). "Carbon Composite Membranes from Matrimid and Kapton Polyimide." *Microporous & Mesoporous Materials.* **33**. 115-125.

C39 Centeno, T. A. and Fuertes, A. B. (2000). "Carbon Molecular Sieve Gas Separation Membranes Based on Poly(vinylidene chloride-co-vinyl chloride)." Carbon. **38**. 1067-1073.

C40 Suda, H. and Haraya, K. (1995). "Molecular Sieving Effect of Carbonized Kapton Polyimide Membrane." *J. Chem. Soc. Chem. Commun.* 1179-1180.

C41 Haraya, K., Suda, H., Yanagishita, H. and Matsuda, S. "Asymmetric Capillary Membrane of a Carbon Molecular Sieve." *J. Chem. Soc. Chem. Commun.* 1781-1782.

C42 Soria, R. (1995). "Overview on Industrial Membranes." *Catalysis Today.* **25**. 285 – 290.

C43 Bauer, J. M. Elyassini, J., Moncorge, G., Nodari, T. and Totino, E. (1991).

"New Developments and Application of Carbon Membranes." *Key Eng. Materials.* **61 & 62**. 207-212.

C44 Geiszler, V. C. and Koros, W. J. (1996). "Effect of Polyimide Pyrolysis Conditions on Carbon Molecular Sieve Membrane Properties." *Ind. Eng. Chem.* Res. **35**. 2999-3003.

C45 Hayashi, J., Mizuta, H., Yamamoto, M., Kusakabe, K. and Morooka, S. (1996). "Separation of Ethane/Ethylene and Propane/Propylene System with a Carbonized BPDA-pp'ODA Polyimide." *Ind. Eng. Chem. Res.* **35**. 4176-4181.

C46 Rao, M. B. and Sircar, S. (1993). "Nanoporous Carbon Membrane for Gas Separation." *Gas Sep. Purif.* **7**. 279-284.

C47 Kita, H., Yoshino, M., Tanaka, K. and Okamoto, K. (1997). "Gas Permselecivity of Carbonized Polypyrrolone Membrane." *J. Chem. Soc. Chem. Commun.* 1051-1052.

C48 Suda, H. and Haraya, K. (1997). "Alkene/alkane Permselectivities of a Carbon Molecular Sieve Membrane." *J. Chem. Soc., Chem. Commun.* 93-94.

C49 Okamoto, K., Kawamura, S., Yoshino, M., Kita, H., Hirayama, Y., Tanihara, N. and Kusuki, Y. (1999). "Olefin/paraffin Separation through Carbonized Membranes Derived from an Asymmetric Polyimide Hollow Fiber Membrane." *Ind. Eng. Chem. Res.* **38**. 4424-4432.

C50 Inagaki, M., Harada, S., Sato, T., Nakajima, T., Horino, Y. and Morita, K. (1989). "Carbonization of Polyimide Film "Kapton"." *Carbon.* **27**. 253-257.

C51 Kyotani, T. (2000). "Control of Pore Structure in Carbon." *Carbon.* **38**. 269-286.

C52 Ozaki, J., Endo, N., Ohizumi, W., Igarashi, K., Nakahara, M., Oya, A., Yoshida, S. and Iizuka, T. (1997). "Novel Preparation Method for the Production of Mesoporous Carbon Fiber from a Polymer Blend." *Carbon.* **35**. 1031-1033.

C53 Ogawa, M. and Nakano, Y (2000). "Separation of CO_2/CH_4 Mixture through Carbonized Membrane Prepared by Gel Modification." *J. Membr. Sci.* **173**. 123-132.

C54 Anshu Singh-Ghosal and Koros, W. J. (2000). "Air Separation Properties of Flat Sheet Homogeneous Pyrolytic Carbon Membranes." *J. Membr. Sci.* **174**. 177-188.

C55 Shiflett, M. B. and Foley, H. C. (2000). “On the Preparation of Supported Nanoporous Carbon Membranes.” *J. Membr. Sci.* **179**. 275-282.

C56 Wang, Huang Ting, Zhang, Li Xiong and Gavalas, G. R. (2000). “Preparation of Supported Carbon Membranes from Furfuryl alcohol by Vapor Deposition Polymerization.” *J. Membr. Sci.* **177**. 25-31.

C57 Fuertes, A. B. (2000). “Adsorption-selective Carbon Membrane for Gas Separation.” *J. Membr. Sci.* **177**. 9-16.

C58 Anshu Singh and Koros, W. J. (1996). “Significance of Entropic Selectivity for a Advanced Gas Separation Membranes.” *Ind. Eng. Chem. Res.* **35**. 1231-1234.

C59 Fain, D. E. (1991). “Technical & Economic Aspects and Prospects for Gas Separation with Inorganic Membranes.” *Key Eng. Materials.* **61 & 62**. 327-336.

C60 Venkataraman, V. K., Rath, L. K. and Stern, S. A. (1991) “Potential Applications of Microporous Inorganic Membranes to the Separation of Industrial Gas Mixture.” *Key Eng. Materials* **61 & 62**. 347-352

C61 Lee, J. C., Lee, B. H., Kim, B. G., Park, M. J., Lee, D. Y., Kuk, I. H., Chung, H., Kang, H. S., Lee, H. S. and Ahn, D. H. (1997). “The Effect of Carbonization Temperature of PAN Fiber on the Properties of Activated Carbon Fiber Composites.” *Carbon.* **35**. 1479-1484.

C62 Ko, Tse Hao. (1991). “The Influence of Pyrolysis on Physical Properties and Microstructure of Modified PAN Fibers during Carbonization.” *J. Applied Polymer Sci.* **43**. 589-600.

C63 Ryu, Zhen Yu, Zheng, Jing Tang, Wang, Mao Zhang. (1998). “Porous Structure of PAN-based Activated Carbon Fibers.” *Carbon*. **36**. 427-432.

C64 Furukawa, S. and Nitta, T. (2000). “Non-equilibrium Molecular Dynamics Simulation Studies on Gas Permeation Across Carbon Membranes with Different Pore Shape Composed of Micro-graphite Crystallites.” *J. Membr. Sci.* **178**. 107-119.

C65 Gupta, A. and Harrison, I. R. (1996). “New Aspects in the Oxidative Stabilization of PAN-based Carbon Fibers.” *Carbon*. **34**. 1427-1445.

C66 Gupta, A. and Harrison, I. R. (1997). “New Aspects in the Oxidative Stabilization of PAN-based Carbon Fibers: II” *Carbon*. **35**. 809-818.

C67 Edie, D. D. (1998). “The Effect of Processing on the Structure and Properties

of Carbon Fibers." *Carbon*. **36**. 345-362.

C68 Fuertes, A. B. (2001). "Effect of Air Oxidation on Gas Separation Properties of Adsorption-selective Carbon Membranes." *Carbon.* **39**. 697-706.

C69 Sircar, S., Rao, M. B. and Thaeron, C. M. A. (1999). "Selective Surface Flow Membrane for Gas Separation." *Sep. Sci. Tech.* **34**.2081-2093.

C70 Shiflett, M. B. and Foley, H. C. (2001). "Reproducible Production of Nanoporous Carbon Membranes." *Carbon.* **39**. 1421-1446.

C71 Anand, M., Langsam, M., Rao, M. B. and Sircar, S. (1997). "Multicomponent Gas Separation by Selective Surface Flow (SSF) and Poly-trimethylsilylpropyne (PTMSP) Membranes." *J. Membr. Sci.* **123.** 17-25.

C72 Mariwala, R. K. and Foley, H. C. (1994). "Evolution of Ultramicroporous Adsorptive Structure in a Poly(furfuryl alcohol)-derived Carbongenic Molecular Sieves." *Ind. Eng. Chem. Res.* **33**. 607-615.

C73 Lafyatis, D. S., Tung, J. and Foley, H. C. (1991). "Poly(furfurylalcohol)-derived Carbon Molecular Sieves: Dependence of Adsorptive Properties on Carbonization Temperature, Time and Poly(ethylene glycol) Additives." *Ind. Eng. Chem. Res.* **30.** 865-873.

C74 Ruthven, D. M. (1992). "Diffusion of Oxygen and Nitrogen in Carbon Molecular Sieve." *Chem. Eng. Sci.* **47.** 4305-4308.

C75 Damle, A. S., Gangwal, S. K., Spivey, J. J., Longanbach, J., Venkataraman, V. K. (1991). "Carbon Membranes for Gas Separation." *Key Eng. Materials.* **61 & 62.** 273-278.

C76 Kapoor, A. and Yang, R. T. (1989). "Kinetic Separation of Methane-carbon Dioxide Mixture by Adsorption in Molecular Sieve Carbon." *Chem. Eng. Sci.* **44.** 1723-1733.

C77 Steriotis, T. H., Beltsios, K., Mitropoulos,A. CH., Kanellopoulos, N., Tennison, S., Wiedenman, A. and Keiderling, U. (1997). "On the Structure of an Asymmetric Carbon Membrane with a Novolac Resin Precursor." *J.Applied Polymer Sci.* **64.** 2323-2345.

C78 C.Gomez-de-Salazar, A.Sepulveda-Escribano and F.Rodriguez-Reinoso (2000). "Preparation of Carbon Molecular Sieves by Controlled Oxidation Treatments." *Carbon.* **38.** 1889-1892.

C79 Thaeron, C., Parrillo, D. J., Sircar, S., Clarke, P. F., Paranjape, M. and Pruden,

B. B. (1999). “Separation of Hydrogen Sulfide-methane Mixtures by Selective Surface Flow Membrane.” *Sep.Purif.Tech.* **15.** 121-129.

C80 Mochida, I., Yatsunami, S., Kawabuchi, Y. and Nakayama, Y. (1995). “Influence of Heat-treatment on the Selective Adsorption of CO_2 in a Model Natural Gas Over Molecular Sieve Carbons.” *Carbon.* **33.** 1611-1619.

C81 Ash, R., Barrer, R. M. and Purna Sharma (1976). “Sorption and Flow of Carbon Dioxide and Some Hydrocarbons in a Microporous Carbon Membrane.” *J. Membr. Sci.* **1.** 17-32.

F1 Pesek, S. C. and Koros, W. J. (1994). “Aqueous Quenched Asymmetric Polysulfone Hollow Fiber Prepared by Dry/wet Phase Separation.” *J. Membr. Sci.* **88**. 1-19.

F2 Pesek, S. C. and Koros, W. J. (1993). “Aqueous Quenched Asymmetric Polysulfone Membranes Prepared by Dry/wet Phase Separation.” *J. Membr. Sci.* **81**. 71-88.

F3 Sharpe, I. D., Ahmad Fauzi Ismail and Shilton, S. J. (1999). “A Study of Extrusion Shear and Forced Convection Residence Time in the Spinning of Polysulfone Hollow Fiber Membranes for Gas Separation.” *Sep. & Purif. Tech.* **17**.101-109.

F4 Cabasso, I., Klein, E. and Smith, J. K. (1976). “Polysulfone Hollow Fibers I Spinning & Properties.” *J. Appl. Poly. Sci.* **20**. 2377-2394.

F5 Rautenbach, R., Struck, A., Melin, T. and Roks, M. F. M. (1998). “Impact of Operating Pressure on the Permeance of Hollow Fiber Gas Separation Membranes.” *J. Membr. Sci.* **146**. 217-223.

F6 Clausi, D. T. and Koros, W. J. (2000). “Formation of Defect-free Polyimide Hollow Fiber Membranes for Gas Separations.” *J. Membr. Sci.* **167**. 79-89.

F7 Pinnau, I. and Koros, W. J. (1992). "Influence of Quench Medium on the Structures and Gas Permeation Properties of Polysulfone Membranes by Wet and Dry/wet Phase Inversion.” *J. Membr. Sci.* **71**. 81-96.

F8 Pinnau, I. and Koros, W. J. (1993). “A Qualitative Skin Layer Formation Mechanism for Membranes Made by Dry/wet Phase Inversion.” *J. Poly. Sci. Part B.* **31**. 419-427.

F9 Stern, S. A., Gareis, P. J., Sinclair, T. F. and Mohr, P. H. (1963). “Performance of a Versatile Variable-volume Permeability Cell. Comparison of Gas

Permeability Measurements by the Variable-volume and Variable-pressure Methods." *J. Appl. Poly. Sci.* **7**. 2035-2051.

F10 Pinnau, I., Wind, J. and Peinemann, K. (1990). "Ultrathin Multicomponent Poly(ether sulfone) Membranes for Gas Separation Made by Dry/wet Phase Inversion." *Ind. Eng. Chem.* **29**. 2028-2032.

F11 Puri, P. S. (1990). "Fabrication of Hollow Fiber Gas Separation Membranes." *Gas Sep. & Purif.* **4**. 29-36.

F12 Shilton, S. J., Ahamd Fauzi Ismail, Gough, P. J., Dunkin, I. R. and Gallivan, S. L. (1997). "Molecular Orientation and the Performance of Synthetic Polymeric Membranes for Gas Separation." *Polymer.* **38**. 2215-2220.

F13 Shilton, S. J. and Bell, G. (1994). "The Rheology of Fibre Spinning and the Properties of Hollow-Fibre Membranes for Gas Separation." *Polymer.* **35**.5327-5334.

F14 McKelvey, S., Clausi, D. T., Koros, W. J. (1997). "A Guide to Establishing Hollow Fiber Macroscopic Properties for Membrane Applications." *J. Membr. Sci.* **124.** 223-232.

F15 Van't Hof, J. A., Reuvers, A. J., Boom, R. M., Rolevink, H. H. M., Smolders, C. A. (1992). "Preparation of Asymmetric Gas Separation Membranes with High Selectivity by a Dual-bath Coagulation Method." *J. Membr. Sci.* **70.** 17-30.

F16 Brown, P. J., East, G. C., Mclntyre, J. E. (1990). "Effect of Residual Solvent on the Gas Transport Properties of Polysulfone Hollow Fiber Membranes." *Polymer Communications.* **31.** 156-159.

F17 Lui, A., Talbot, F. D. F., Matsuura, T., Sourirajan, S. (1988). "Studies on the Solvent Exchange Technique for Making Dry Cellulose Acetate Membranes." *J.Applied Polymer Sci.* **36.** 1809-1820.

F18 Yong, C., Fouda, A. E., Matsuura, T. "Effect of Drying Conditions on the Performance and Quality of Synthetic Membranes Used for Gas Separations." *AICHE Symposium.* **85.** 18-33.

F19 Manos, P. (1978). "Solvent Exchange Drying of Membranes for Gas Separation." (US Patent 4120,098).

F20 Pfromm, P. H., Pinnau, I., Koros, W. J. (1993). "Gas Transport Through Integral-asymmetric Membranes: a Comparison to Isotropic Film Transport

Properties." *J.Appl.Polymer.Sci.* **48.** 2161-2171.

F21 Koros, W. J. and Fleming, G. K. (1993). "Membrane-based Gas Separation." *J. Membr. Sci.* **83.** 1-80.

B1-4 Kesting, R. E. and Fritzsche, A. K. (1993). "Polymeric Gas Separation Membranes." New York: Wiley-Interscience Publication. 224-283.

B3-1 Mulder, M. (1991). "Basic Principles of Membrane Technology." Netherlands: Kluwer Academic Publishers. 1-16.

B3-3 Mulder, M. (1991). "Basic Principles of Membrane Technology." Netherlands: Kluwer Academic Publishers. 54-109.

B6-2.2 Burggraaf, A. J. and Keizer, K. (1991). "Synthesis of Inorganic Membranes." in. Bhave, R. R. "Inorganic Membranes Synthesis, Characteristics and Applications." New York: Van Nostrand Reinhold. 14-19.

B6-2.3 Burggraaf, A. J. and Keizer, K. (1991). "Synthesis of Inorganic Membranes." in. Bhave, R. R. "Inorganic Membranes Synthesis, Characteristics and Applications." New York: Van Nostrand Reinhold. 19-26.

B6-2.7 Burggraaf, A. J. and Keizer, K. (1991). "Synthesis of Inorganic Membranes." in. Bhave, R. R. "Inorganic Membranes Synthesis, Characteristics and Applications." New York: Van Nostrand Reinhold. 49-53.

B18 Moch, I. (1997). "Hollow-Fiber Membranes." in. Ruthven, D. M. "Encyclopedia of Separation Technology." Vol 2. Canada: Wiley-Interscience. 1001-1026.

B21-1.1 Donnet, J. B., Bansal, R. C. (1984). "Carbon Fiber." New York: Marcel Dekker. 2-12.

B21-1.2 Donnet, J. B., Bansal, R. C. (1984). "Carbon Fiber." New York: Marcel Dekker. 12-27.

B23 Billmeyer, F. W. (1971). "Textbook of Polymer Science." New York: Wiley Interscience. 521.

D1 Ahmad Fauzi Ismail, Shilton, S. J., Dunkin, I. R. and Gallivan, S. L. (1997). "Direct Measurement of Rheologically Induced Molecular Orientation in Gas Separation Hollow Fiber Membranes and Effects on Selectivity." *J. Membr. Sci.* **126**. 133-137.

G1 Koros, W. J. and Rajiv Mahajan (2000). "Pushing the Limits on Possibilities for Large Scale Gas Separation: Which Strategies?" *J. Membr. Sci.* **175**. 181-

196.

G2 Koros. W. J. (1995). “Membranes: Learning a Lesson from Nature.” *Chem. Eng. Prog.* Oct. 68-81.

G3 Roman, I. C., Ubersax, R. W. and Fleming, G. K. (2001). “New Directions in Membranes for Gas Separation.” *Chimica & Industria-Giug.* 1-3.

G4 Robeson, L. M. (1999). “Polymer Membranes for Gas Separation.” *Current Opinion in Solid State & Materials Science.* **4.** 549-552.

G5 Franken, T. (1998). “Membrane Selection-more than Material Properties Alone.” *Membr. Tech.* **97.** 7-10.

G6 Rajiv Mahajan, Koros, W. J., Thundyil, M. (1999). “Mixed Matrix Membranes:Important and Challenging!” *Membr. Tech.* **105.** 6-8.

G7 Strathmann, H. (1999). “Membrane Processes for Sustainable Industrial Growth.” *Membr. Tech.* **113.** 9-11.

G8 Stern, S. A. (1994). “Review: Polymers for Gas Separations: The Next Decade.” *J. Membr. Sci.* **94.** 1-65.

G9 Robeson, L. M. (1991). “Correlation of Separation Factor Versus Permeability for Polymeric Membranes.” *J. Membr. Sci.* **62.** 165-185.

G10 Meares, P. (1989). “What is a Membrane? Part II.” *J. Membr. Sci.* **43.** 1-3.

G11 Baker, R. (2001). “Future Directions of Membrane Gas-separation Technology.” *Membr. Tech.* **138.** 5-10.

Th1 Ahmad Fauzi bin Ismail (1997). “Novel Studies of Molecular Orientation in Synthetic Polymeric Membranes for Gas Separation.” University of Strathclyde: Ph.D. Thesis.

Th2 Geiszler, V. C. (1997). “Polyimide Precursors for Carbon Membranes.” University of Texas: Ph.D. Thesis.

Th3 Shu, Guang Li (1994). “Preparation of Hollow Fiber Membranes for Gas Separation.” University of Twente: Ph.D. Thesis.

T1 Ash, R., Barrer, R. M. and Lowson, R. T. (1973). *J. Chem. Soc. Faraday Trans. I.* **69.** 2166.

T2 Graham, A. (1866). “On the Law of the Diffusion of Gases.” *Philos. Mag.* **32**. 401-420.

T3 Hatori, H. et al. (1992). “Carbon Molecular Sieve Films from Polyimide.” *Carbon.* **30**. 719.

T4 Henis, J. M. S. and Tripodi, M. K. (1980). “A Novel Approach to Gas Separation using Composite Hollow Fiber Membranes.” *Sep. Sci. & Tech.* **15**. 1059.

T5 Hayashi, J., Yamamoto, M., Kusakabe, K. and Morooka, S. (1997). “Effect of Oxidation on Gas Permeation of Carbon Molecular Sieve Membranes based on BPDA-pp’ODA Polyimide.” *Ind. Eng. Chem. Res.* **36**. 2134-2140.

T6 Loeb, S. and Sourirajan, S. (1962). *Adv. Chem. Ser.* **38**. 117.

T7 Mitchell, J. K. (1830). *Am. J. Med.* **7**. 36-67.

T8 Mitchell, J. K. (1831). *Royal Inst. J.* **2**. 101, 307.

T9 Moaddeb, M. and Koros, W. J. (1997). “Gas Transport Properties of Thin Polymeric Membranes in the Presence of Silicon Dioxide Particles.” *J. Membr. Sci.* **125**. 143-163.

P1 Ismail, A. F., David, L. I. B. (2001). “ A Review on the Latest Development of Carbon Membranes for Gas Separation.” *J. Membr. Sci.* **193**. 1-18.

Reference Convertor:

Number	David's Ref.
C1	C1
C2	C2
C3	C3
C4	C4
C5	C5
C6	C6
C7	C7
C8	C8
C9	C9
C10	C10
C11	C11
C12	C12
C13	C13
C14	C14
C15	C15
C16	C16
C17	C17
C18	C18
C19	C19
C19a	C19a
C19b	C19b
C19c	C19c
C20	C20
C21	C21
C22	C22
C23	C23
C24	C24
C25	C25
C26	C26
C27	C27
C28	C28
C29	C29
C30	C30
C31	C31
C32	C32
C33	C33
C34	C34
C35	C35
C36	C36
C37	C37
C38	C38
C39	C39

C40	C40
C41	C41
C42	C42
C43	C43
C44	C44
C45	C45
C46	C46
C47	C47
C48	C48
C49	C49
C50	C50
C51	C51
C52	C52
C53	C53
C54	C54
C55	C55
C56	C56
C57	C57
C58	C58
C59	C59
C60	C60
C61	C61
C62	C62
C63	C63
C64	C64
C65	C65
C66	C66
C67	C67
C68	C68
C69	C69
C70	C70
C71	C71
C72	C72
C73	C73
C74	C74
C75	C75
C76	C76
C77	C77
C78	C78
C79	C79
C80	C80
C81	C81
F1	F1
F2	F2
F3	F3
F4	F4
F5	F5
F6	F6

F7	F7
F8	F8
F9	F9
F10	F10
F11	F11
F12	F12
F13	F13
F14	F14
F15	F15
F16	F16
F17	F17
F18	F18
F19	F19
F20	F20
F21	F21
B1-4	B1-4
B3-1	B3-1
B3-3	B3-3
B6-2.2	B6-2.2
B6-2.3	B6-2.3
B6-2.7	B6-2.7
B18	B18
B21-1.1	B21-1.1
B21-1.2	B21-1.2
B23	B23
D1	D1
G1	G1
G2	G2
G3	G3
G4	G4
G5	G5
G6	G6
G7	G7
G8	G8
G9	G9
G10	G10
G11	G11
Th1	Th1
Th2	Th2
Th3	Th3
T1	T1
T2	T2
T3	T3
T4	T4
T5	T5
T6	T6
T7	T7
T8	T8

T9	T9
P1	P1

APPENDIX A: Fiber Spinning Techniques

APPENDIX A: Different fiber spinning techniques [138]

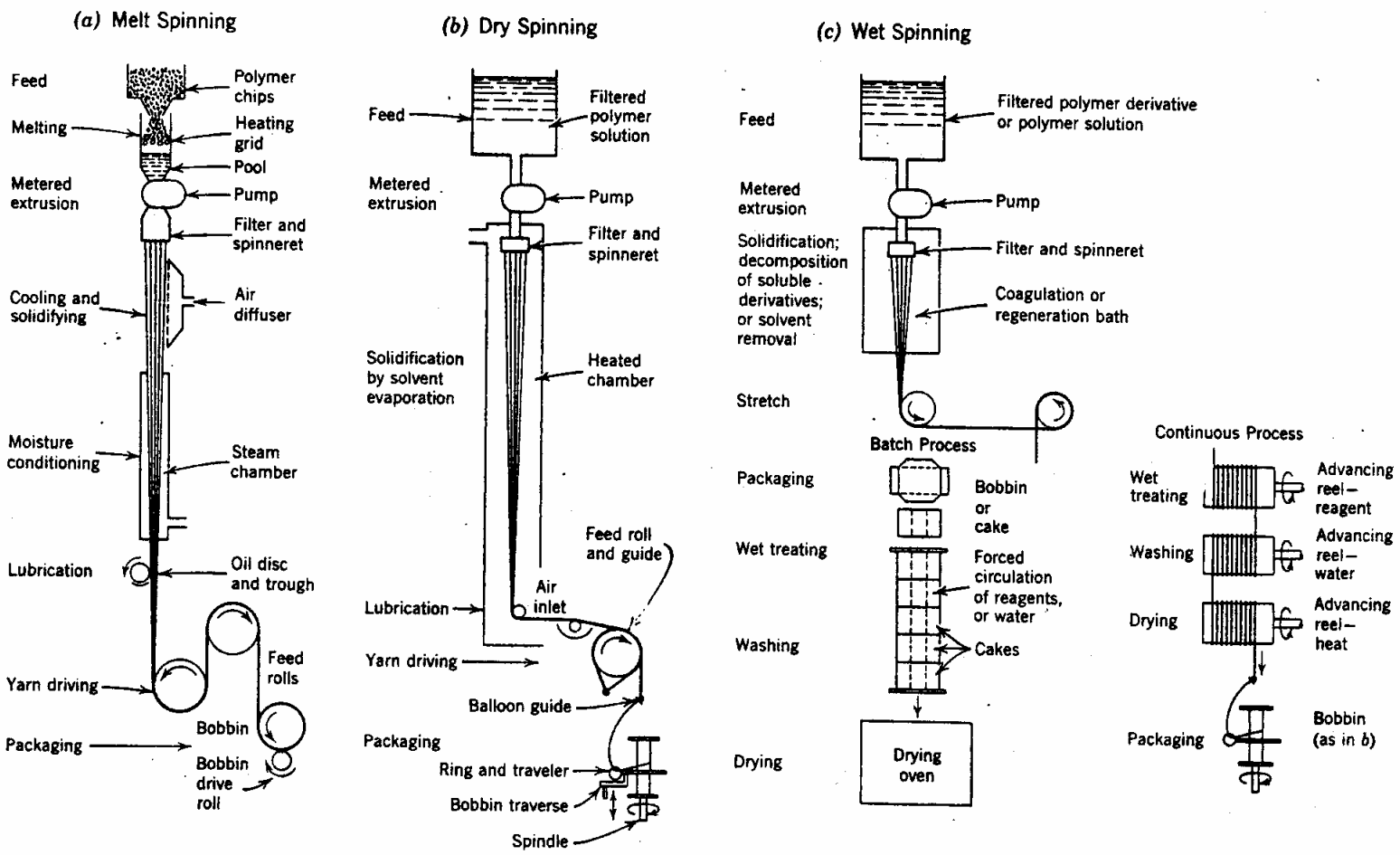

APPENDIX B: Tables of Permeation Results for Pure Oxygen and Nitrogen

APPENDIX B-1: Sample PAN

Feed Pressure (Bar)	OXYGEN (GPU) Permeability	Average Permeability	NITROGEN (GPU) Permeability	Average Permeability	Selectivity O_2/N_2	Average Selectivity O_2/N_2
	11.8117		8.0181		1.4731	
1	11.8166	11.7140	8.0372	8.0626	1.4702	1.4531
	11.5137		8.1324		1.4158	
	21.5680		13.8782		1.5541	
1.5	21.5071	21.4206	13.9227	13.9230	1.5447	1.5385
	21.1865		13.9681		1.5168	
	27.7219		18.4521		1.5024	
2	27.5712	27.5498	18.4671	18.4671	1.4930	1.4918
	27.3563		18.4820		1.4802	
	32.7902		23.0600		1.4220	
2.5	32.6729	32.6365	23.1478	23.1976	1.4115	1.4070
	32.4464		23.3850		1.3875	
	36.6024		28.2960		1.2936	
3	36.3400	36.4449	28.5081	28.4553	1.2747	1.2808
	36.3922		28.5617		1.2742	
	39.0852		31.7555		1.2308	
3.5	39.2853	39.0742	32.0521	31.9585	1.2257	1.2227
	38.8522		32.0679		1.2116	
	42.7943		35.0398		1.2213	
4	42.3181	42.4507	35.5863	35.4786	1.1892	1.1967
	42.2398		35.8097		1.1796	
	46.5672		40.4573		1.1510	
5	46.5197	46.5040	41.3743	41.1062	1.1244	1.1315
	46.4251		41.4871		1.1190	
	50.1713		45.9298		1.0923	
6	49.5180	49.6290	46.6624	46.4565	1.0612	1.0684
	49.1977		46.7772		1.0517	

T ≡ Pyrolysis temperature (°C)

D ≡ Heating duration (min)

F ≡ Flowrate (cm^3/min)

APPENDIX B-2: Sample T250D60F100

Feed Pressure (Bar)	OXYGEN (GPU) Permeability	Average Permeability	NITROGEN (GPU) Permeability	Average Permeability	Selectivity O_2/N_2	Average Selectivity O_2/N_2
1	0.0401 0.0370 0.0315	0.0362	0.0128 0.0117 0.0100	0.0115	3.1403 3.1492 3.1573	3.1489
1.5	0.0289 0.0305 0.0301	0.0298	0.0121 0.0137 0.0164	0.0140	2.3887 2.2322 1.8405	2.1538
2	0.0229 0.0239 0.0237	0.0235	0.0173 0.0183 0.0186	0.0181	1.3208 1.3078 1.2748	1.3011
2.5	0.0193 0.0221 0.0210	0.0208	0.0144 0.0153 0.0157	0.0151	1.3379 1.4447 1.3351	1.3726
3	0.0229 0.0227 0.0216	0.0224	0.0139 0.0130 0.0134	0.0134	1.6497 1.7411 1.6070	1.6660
3.5	0.0236 0.0220 0.0218	0.0225	0.0141 0.0136 0.0129	0.0135	1.6710 1.6226 1.6917	1.6618
4	0.0273 0.0264 0.0246	0.0261	0.0139 0.0148 0.0153	0.0147	1.9603 1.7878 1.6068	1.7850
5	0.0238 0.0236 0.0212	0.0229	0.0114 0.0122 0.0110	0.0115	2.0991 1.9305 1.9363	1.9886
6	0.0270 0.0239 0.0238	0.0249	0.0096 0.0097 0.0100	0.0098	2.8247 2.4586 2.3781	2.5538

APPENDIX B-3: Sample T500D60F100

Feed Pressure (Bar)	OXYGEN (GPU) Permeability	OXYGEN (GPU) Average Permeability	NITROGEN (GPU) Permeability	NITROGEN (GPU) Average Permeability	Selectivity O_2/N_2	Average Selectivity O_2/N_2
1	69.8089 69.6451 69.4820	69.6453	51.5578 54.9463 55.1121	53.8721	1.3540 1.2675 1.2607	1.2941
1.5	113.9428 112.6454 112.4853	113.0245	104.0555 105.2316 105.4418	104.9096	1.0950 1.0705 1.0668	1.0774
2	140.1286 138.8178 137.5312	138.8259	130.8609 132.8525 133.2102	132.3079	1.0708 1.0449 1.0324	1.0494
2.5	159.0314 160.1038 160.0498	159.7284	151.1355 152.8873 153.6789	152.5673	1.0522 1.0472 1.0415	1.0470
3	189.7043 188.4396 187.9028	188.6823	164.4735 167.2541 169.4021	167.0432	1.1534 1.1267 1.1092	1.1298
3.5	199.9949 198.2416 196.5187	198.2517	184.3431 184.4434 185.2492	184.6786	1.0849 1.0748 1.0608	1.0735
4	208.1293 206.6800 205.2506	206.6867	193.2242 191.9744 194.4905	193.2297	1.0771 1.0766 1.0553	1.0697
5	232.7784 240.5612 231.4171	234.9189	200.0286 200.1973 202.5887	200.9382	1.1637 1.2016 1.1423	1.1692
6	256.6299 251.7323 245.4859	251.2827	204.8257 206.9682 213.6735	208.4891	1.2529 1.2163 1.1489	1.2060

APPENDIX B-4: Sample T600D60F100

Feed Pressure (Bar)	OXYGEN (GPU) Permeability	OXYGEN (GPU) Average Permeability	NITROGEN (GPU) Permeability	NITROGEN (GPU) Average Permeability	Selectivity O_2/N_2	Average Selectivity O_2/N_2
	139.5468		113.5603		1.2288	
1	138.7838	134.2228	115.0399	114.8489	1.2064	1.1692
	124.3378		115.9464		1.0724	
	218.3532		201.6970		1.0826	
1.5	217.5113	217.2370	203.8227	203.6294	1.0672	1.0669
	215.8466		205.3686		1.0510	
	269.1788		258.2255		1.0424	
2	272.0639	269.1990	263.5884	261.9836	1.0322	1.0277
	266.3543		264.1370		1.0084	
	306.0565		294.9434		1.0377	
2.5	310.9778	308.5497	301.7363	300.2248	1.0306	1.0278
	308.6148		303.9948		1.0152	
	350.3597		329.8709		1.0621	
3	343.2531	345.5060	336.4289	336.1706	1.0203	1.0281
	342.9053		342.2118		1.0020	
	380.7059		334.9860		1.1365	
3.5	378.7178	377.7537	341.6936	341.2289	1.1084	1.1074
	373.8375		347.0070		1.0773	
	418.8707		364.7064		1.1485	
4	410.0737	411.4775	375.4965	375.7158	1.0921	1.0962
	405.4882		386.9446		1.0479	
	488.1455		393.5436		1.2404	
5	465.7535	471.4572	401.3212	403.3793	1.1606	1.1699
	460.4728		415.2730		1.1088	
	486.2752		388.1279		1.2529	
6	482.1190	481.2473	397.2389	397.3849	1.2137	1.2117
	475.3476		406.7879		1.1685	

APPENDIX B-5: Sample T700D60F100

Feed Pressure (Bar)	OXYGEN (GPU) Permeability	Average Permeability	NITROGEN (GPU) Permeability	Average Permeability	Selectivity O_2/N_2	Average Selectivity O_2/N_2
	105.4822		73.7102		1.4310	
1	104.8521	104.9529	73.8071	73.7877	1.4206	1.4224
	104.5243		73.8459		1.4154	
	172.2074		126.2467		1.3641	
1.5	171.7020	171.0428	128.7205	127.9402	1.3339	1.3371
	169.2190		128.8533		1.3133	
	208.2116		158.1283		1.3167	
2	206.6185	206.8669	160.6612	160.0632	1.2861	1.2926
	205.7707		161.3999		1.2749	
	240.8541		183.2534		1.3143	
2.5	240.0306	239.2257	179.4478	182.1848	1.3376	1.3133
	236.7925		183.8533		1.2879	
	264.1421		197.9111		1.3347	
3	258.3111	259.3148	199.8121	199.9696	1.2928	1.2970
	255.4911		202.1856		1.2636	
	288.2141		212.2720		1.3578	
3.5	280.1635	281.5607	209.5008	213.2710	1.3373	1.3208
	276.3045		218.0403		1.2672	
	333.6928		224.3098		1.4876	
4	321.4696	324.3793	231.7127	231.6095	1.3874	1.4022
	317.9754		238.8060		1.3315	
	405.8322		222.0046		1.8280	
5	373.4519	383.9151	241.0608	236.4709	1.5492	1.6297
	372.4613		246.3472		1.5119	
	475.6705		230.5713		2.0630	
6	414.9466	432.7782	241.8913	240.4769	1.7154	1.8054
	407.7176		248.9680		1.6376	

APPENDIX B-6: Sample T800D60F100

Feed Pressure (Bar)	OXYGEN (GPU) Permeability	Average Permeability	NITROGEN (GPU) Permeability	Average Permeability	Selectivity O_2/N_2	Average Selectivity O_2/N_2
	43.4395		23.1787		1.8741	
1	42.7705	42.9301	23.1867	23.1876	1.8446	1.8514
	42.5805		23.1975		1.8356	
	54.9577		31.6469		1.7366	
1.5	54.7624	54.7800	31.8585	31.8421	1.7189	1.7204
	54.6197		32.0208		1.7058	
	61.6480		35.6278		1.7303	
2	61.5852	61.5676	35.6413	35.6774	1.7279	1.7257
	61.4696		35.7629		1.7188	
	63.0905		37.7030		1.6734	
2.5	63.0652	63.0505	37.6278	37.6279	1.6760	1.6756
	62.9957		37.5529		1.6775	
	64.3615		38.2179		1.6841	
3	64.3220	64.2304	38.2411	38.2567	1.6820	1.6789
	64.0077		38.3110		1.6707	
	65.9396		39.2468		1.6801	
3.5	65.6984	65.7404	39.2697	39.2735	1.6730	1.6739
	65.5833		39.3041		1.6686	
	66.2020		38.8699		1.7032	
4	65.8691	65.9067	39.0373	39.0117	1.6873	1.6894
	65.6490		39.1280		1.6778	
	67.5215		39.5779		1.7060	
5	66.9036	67.0764	39.8286	39.7731	1.6798	1.6865
	66.8041		39.9128		1.6737	
	69.0157		40.4504		1.7062	
6	68.4745	68.5598	40.6596	40.6074	1.6841	1.6884
	68.1893		40.7123		1.6749	

APPENDIX B-7: Sample T500D10F100

Feed Pressure (Bar)	OXYGEN (GPU) Permeability	Average Permeability	NITROGEN (GPU) Permeability	Average Permeability	Selectivity O_2/N_2	Average Selectivity O_2/N_2
1	6.8833 6.7717 6.6395	6.7648	1.7618 1.7947 1.8790	1.8118	3.9069 3.7731 3.5335	3.7379
1.5	13.1705 13.1479 12.9587	13.0924	6.7552 6.9154 7.6306	7.1004	1.9497 1.9012 1.6983	1.8497
2	18.8773 18.7846 18.6020	18.7546	12.8116 12.8259 13.1145	12.9173	1.4735 1.4646 1.4184	1.4522
2.5	23.0931 22.5545 22.3896	22.6790	18.0729 18.2887 18.4819	18.2812	1.2778 1.2332 1.2114	1.2408
3	24.4737 24.3569 24.1266	24.3190	18.6990 18.7954 18.8881	18.7942	1.3088 1.2959 1.2773	1.2940
3.5	25.4036 25.1890 25.1793	25.2573	20.0726 20.0788 20.1311	20.0942	1.2656 1.2545 1.2508	1.2570
4	26.2950 26.1811 26.0623	26.1795	20.7425 21.0659 21.0853	20.9646	1.2677 1.2428 1.2360	1.2488
5	27.9563 27.7034 26.8924	27.5173	22.3677 22.2593 22.1467	22.2579	1.2498 1.2446 1.2143	1.2362
6	28.5648 28.1862 27.7771	28.1760	23.0861 23.2969 23.3680	23.2503	1.2373 1.2099 1.1887	1.2120

APPENDIX B-8: Sample T500D30F100

Feed Pressure (Bar)	OXYGEN (GPU) Permeability	OXYGEN (GPU) Average Permeability	NITROGEN (GPU) Permeability	NITROGEN (GPU) Average Permeability	Selectivity O_2/N_2	Average Selectivity O_2/N_2
	46.1783		35.9027		1.2862	
1	46.0992	46.0731	36.0615	36.0571	1.2783	1.2778
	45.9418		36.2070		1.2689	
	74.8198		70.2223		1.0655	
1.5	74.1243	74.3002	70.3876	70.3601	1.0531	1.0560
	73.9563		70.4705		1.0495	
	120.3609		88.6452		1.3578	
2	95.9112	103.6118	88.9382	89.0179	1.0784	1.1644
	94.5632		89.4704		1.0569	
	114.1578		99.4005		1.1485	
2.5	113.2570	113.4582	101.6532	100.9986	1.1142	1.1236
	112.9599		101.9420		1.1081	
	110.3431		103.9501		1.0615	
3	108.3442	108.9887	104.5559	104.5378	1.0362	1.0426
	108.2788		105.1072		1.0302	
	121.8596		113.4121		1.0745	
3.5	120.5226	120.6249	114.0006	113.8891	1.0572	1.0592
	119.4925		114.2547		1.0458	
	126.2321		113.4599		1.1126	
4	125.7603	125.2999	115.3072	114.7244	1.0907	1.0923
	123.9074		115.4061		1.0737	
	141.2740		111.0947		1.2717	
5	133.5618	135.5869	111.4397	112.5153	1.1985	1.2057
	131.9250		115.0115		1.1471	
	148.0346		115.6044		1.2805	
6	142.1695	143.7520	125.2919	122.6543	1.1347	1.1751
	141.0519		127.0665		1.1101	

APPENDIX B-9: Sample T500D60F100

Feed Pressure (Bar)	OXYGEN (GPU) Permeability	OXYGEN (GPU) Average Permeability	NITROGEN (GPU) Permeability	NITROGEN (GPU) Average Permeability	Selectivity O_2/N_2	Average Selectivity O_2/N_2
	53.0218		37.1143		1.4286	
1	51.8489	51.9582	37.4366	37.3970	1.3850	1.3895
	51.0038		37.6401		1.3550	
	91.6082		88.9512		1.0299	
1.5	90.7986	91.0017	89.2215	89.1702	1.0177	1.0206
	90.5984		89.3379		1.0141	
	109.8417		95.4229		1.1511	
2	108.6798	109.0288	96.0773	96.0803	1.1312	1.1348
	108.5649		96.7407		1.1222	
	130.7384		108.8141		1.2015	
2.5	129.3666	129.7335	111.5713	111.4077	1.1595	1.1650
	129.0956		113.8378		1.1340	
	145.1110		117.0144		1.2401	
3	141.1245	142.5829	117.6845	117.6191	1.1992	1.2123
	141.5132		118.1583		1.1977	
	150.9197		116.9478		1.2905	
3.5	147.8785	148.2792	121.8004	120.4656	1.2141	1.2318
	146.0392		122.6486		1.1907	
	166.4232		123.6821		1.3456	
4	161.2007	161.3067	124.0804	124.6590	1.2992	1.2944
	156.2961		126.2145		1.2383	
	190.8457		136.0776		1.4025	
5	187.9365	184.0602	139.1494	136.1219	1.3506	1.3518
	173.3985		133.1386		1.3024	
	201.0540		143.4897		1.4012	
6	198.3371	197.0225	149.7647	148.4115	1.3243	1.3289
	191.6765		151.9802		1.2612	

APPENDIX B-10: Sample T500D120F100

Feed Pressure (Bar)	OXYGEN (GPU) Permeability	Average Permeability	NITROGEN (GPU) Permeability	Average Permeability	Selectivity O_2/N_2	Average Selectivity O_2/N_2
	72.0512		45.7569		1.5747	
1	71.5262	71.6632	45.3752	45.6592	1.5763	1.5695
	71.4120		45.8456		1.5577	
	136.4795		81.4074		1.6765	
1.5	137.1773	133.4872	82.6614	82.3799	1.6595	1.6208
	126.8047		83.0708		1.5265	
	169.8220		103.4116		1.6422	
2	167.5596	165.6984	105.5819	105.2317	1.5870	1.5753
	159.7135		106.7015		1.4968	
	181.7057		116.1553		1.5643	
2.5	188.9569	186.2455	122.3338	119.3358	1.5446	1.5608
	188.0739		119.5184		1.5736	
	240.8606		125.8531		1.9138	
3	236.6127	235.4714	132.9627	130.7250	1.7795	1.8034
	228.9409		133.3592		1.7167	
	225.9209		133.5584		1.6916	
3.5	222.4250	223.7340	135.9264	137.6825	1.6364	1.6267
	222.8561		143.5627		1.5523	
	247.8314		136.5258		1.8153	
4	241.8739	243.4739	138.5944	138.2252	1.7452	1.7618
	240.7166		139.5555		1.7249	
	254.7330		169.1085		1.5063	
5	239.5703	239.0943	165.6289	170.4209	1.4464	1.4053
	222.9796		176.5255		1.2632	
	325.6295		240.4290		1.3544	
6	302.1608	295.2630	272.6817	268.2538	1.1081	1.1157
	257.9988		291.6508		0.8846	

APPENDIX B-11: Sample T500D180F100

Feed Pressure (Bar)	OXYGEN (GPU) Permeability	OXYGEN (GPU) Average Permeability	NITROGEN (GPU) Permeability	NITROGEN (GPU) Average Permeability	Selectivity O_2/N_2	Average Selectivity O_2/N_2
1	33.1485 33.0093 32.5535	32.9037	25.3383 25.3997 25.5372	25.4250	1.3082 1.2996 1.2747	1.2942
1.5	70.5521 69.3078 68.8524	69.5708	55.0385 56.2800 57.1600	56.1595	1.2819 1.2315 1.2046	1.2393
2	91.1775 90.7215 95.3823	92.4271	71.1053 70.8915 72.4156	71.4708	1.2823 1.2797 1.3172	1.2931
2.5	91.5670 94.8833 99.2779	95.2428	75.8761 77.7527 77.9777	77.2022	1.2068 1.2203 1.2732	1.2334
3	103.6874 102.0715 101.0219	102.2602	83.3457 84.2390 85.1517	84.2455	1.2441 1.2117 1.1864	1.2140
3.5	111.7200 111.3507 110.5286	111.1998	86.0373 88.8749 89.3464	88.0862	1.2985 1.2529 1.2371	1.2628
4	121.6641 127.8661 125.4176	124.9826	93.4913 93.1221 95.3823	93.9986	1.3013 1.3731 1.3149	1.3298
5	179.3043 160.9455 155.6337	165.2945	101.8510 103.7558 105.7332	103.7800	1.7605 1.5512 1.4719	1.5945
6	160.3980 192.6349 176.2220	176.4183	100.8922 102.0715 102.6045	101.8561	1.5898 1.8873 1.7175	1.7315

APPENDIX B-12: Sample T500D60F20

	OXYGEN (GPU)		NITROGEN (GPU)			
Feed Pressure (Bar)	Permeability	Average Permeability	Permeability	Average Permeability	Selectivity O_2/N_2	Average Selectivity O_2/N_2
1	51.8785 50.6118 50.5296	51.0067	15.3598 15.3706 15.6202	15.4502	3.3776 3.2928 3.2349	3.3017
1.5	84.9291 84.7670 84.2388	84.6450	44.4883 44.5087 44.9013	44.6328	1.9090 1.9045 1.8761	1.8965
2	107.3143 107.1664 107.0680	107.1829	65.0083 64.3357 65.5961	64.9800	1.6508 1.6657 1.6322	1.6496
2.5	116.3788 115.8009 115.6573	115.9457	92.2236 92.4685 92.9622	92.5515	1.2619 1.2523 1.2441	1.2528
3	124.0724 123.5793 123.4811	123.7109	98.4720 98.5054 99.4848	98.8207	1.2600 1.2545 1.2412	1.2519
3.5	130.6409 130.8976 130.2578	130.5988	103.2975 103.8148 104.2499	103.7874	1.2647 1.2609 1.2495	1.2584
4	126.3240 124.9700 124.9031	125.3990	107.4273 108.4984 109.5910	108.5056	1.1759 1.1518 1.1397	1.1558
5	137.5776 133.6356 132.5908	134.6013	115.6164 116.8579 117.0149	116.4964	1.1899 1.1436 1.1331	1.1555
6	132.7606 130.4217 129.3367	130.8397	113.7136 114.6118 115.5243	114.6166	1.1675 1.1379 1.1196	1.1417

APPENDIX B-13: Sample T500D60F50

Feed Pressure (Bar)	OXYGEN (GPU) Permeability	OXYGEN (GPU) Average Permeability	NITROGEN (GPU) Permeability	NITROGEN (GPU) Average Permeability	Selectivity O_2/N_2	Average Selectivity O_2/N_2
	90.5508		61.6287		1.4693	
1	76.9182	80.6720	62.4348	62.5269	1.2320	1.2916
	74.5471		63.5171		1.1737	
	131.7162		124.9126		1.0545	
1.5	127.3464	128.4264	125.5612	125.4540	1.0142	1.0238
	126.2165		125.8880		1.0026	
	163.9902		155.5516		1.0542	
2	162.5207	162.7689	158.8206	158.4832	1.0233	1.0273
	161.7959		161.0774		1.0045	
	202.6516		171.5113		1.1816	
2.5	189.4237	191.4533	177.5992	174.9248	1.0666	1.0953
	182.2846		175.6641		1.0377	
	213.6315		184.3223		1.1590	
3	209.9226	211.0377	187.1756	184.3509	1.1215	1.1449
	209.5588		181.5547		1.1542	
	227.2847		204.8257		1.1096	
3.5	224.3329	225.6419	212.8168	210.2991	1.0541	1.0734
	225.3083		213.2547		1.0565	
	262.0999		229.0065		1.1445	
4	254.7376	254.8717	234.3322	232.7594	1.0871	1.0954
	247.7775		234.9393		1.0546	
	291.3625		245.9297		1.1847	
5	289.0409	289.0531	260.9686	257.2255	1.1076	1.1251
	286.7560		264.7783		1.0830	
	300.7847		248.7972		1.2090	
6	294.9157	294.9906	259.4752	257.0440	1.1366	1.1487
	289.2714		262.8596		1.1005	

APPENDIX B-14: Sample T500D60F150

Feed Pressure (Bar)	OXYGEN (GPU) Permeability	Average Permeability	NITROGEN (GPU) Permeability	Average Permeability	Selectivity O_2/N_2	Average Selectivity O_2/N_2
	128.2922		112.2474		1.1429	
1	127.1679	127.4007	112.5376	112.4846	1.1300	1.1326
	126.7421		112.6687		1.1249	
	217.7022		208.3252		1.0450	
1.5	216.8887	216.3583	209.0757	209.0775	1.0374	1.0349
	214.4841		209.8316		1.0222	
	271.0433		258.1824		1.0498	
2	268.5352	269.0960	259.7229	259.4685	1.0339	1.0371
	267.7095				1.0277	
	308.9942				1.1065	
2.5	306.5462	306.8253	279.4835	280.1625	1.0968	1.0952
	304.9356		281.7447		1.0823	
	357.3855		300.4110		1.1897	
3	351.3281	351.5327	310.0396	309.0865	1.1332	1.1382
	345.8844		316.8090		1.0918	
	396.0833		316.4635		1.2516	
3.5	367.9591	376.7919	320.5417	320.5772	1.1479	1.1759
	366.3333		324.7263		1.1281	
	406.0593		346.5729		1.1716	
4	398.6223	399.6570	349.3544	349.3694	1.1410	1.1441
	394.2895		352.1809		1.1196	
	443.0489		402.1206		1.1018	
5	439.6925	438.2655	406.8183	406.5317	1.0808	1.0782
	432.0552		410.6562		1.0521	
	483.6617		423.0278		1.1433	
6	468.0598	468.8586	429.2856	425.9407	1.0903	1.1009
	454.8543		425.5089		1.0690	

APPENDIX B-15: Sample T500D60F200

Feed Pressure (Bar)	OXYGEN (GPU) Permeability	Average Permeability	NITROGEN (GPU) Permeability	Average Permeability	Selectivity O_2/N_2	Average Selectivity O_2/N_2
	151.8321		60.6603		2.5030	
1	149.1954	149.9418	61.5461	61.3885	2.4241	2.4429
	148.7979		61.9592		2.4015	
	241.2782		163.7529		1.4734	
1.5	238.9552	239.2216	172.9179	170.6361	1.3819	1.4034
	237.4313		175.2376		1.3549	
	287.8548		228.3068		1.2608	
2	284.0480	285.6068	228.6808	228.5873	1.2421	1.2494
	284.9175		228.7744		1.2454	
	376.6869		260.3442		1.4469	
2.5	375.7365	374.2878	261.8703	262.9241	1.4348	1.4238
	370.4401		266.5577		1.3897	
	389.4271		250.5332		1.5544	
3	385.3957	386.6066	303.6642	285.7067	1.2692	1.3648
	384.9972		302.9229		1.2709	
	439.5422		376.3062		1.1680	
3.5	425.4769	429.7881	377.1958	374.8525	1.1280	1.1466
	424.3453		371.0554		1.1436	
	551.8166		401.1770		1.3755	
4	505.8319	519.9471	407.0251	407.0827	1.2428	1.2780
	502.1928		413.0462		1.2158	
	578.6926		424.6680		1.3627	
5	564.0792	568.0055	432.8980	433.0064	1.3030	1.3124
	561.2446		441.4533		1.2714	
	756.6916		537.9946		1.4065	
6	727.1333	727.8741	571.0004	562.3629	1.2734	1.2968
	699.7975		578.0936		1.2105	

APPENDIX C: Simplified Correlation Chart for FTIR

APPENDIX C: Simplified Correlation Chart for FTIR

Functional Group	**Type of Vibration**	**Frequency (cm^{-1})**
C-H	Alkanes (stretch)	3000 – 2850
	$-CH_3$ (bend)	1450 and 1375
	$-CH_2-$ (bend)	1465
C=C	Alkene	1680 – 1600
	Aromatic	1600 and 1475
C-N	Amines	1350 – 1000
C=N	Imines and Oximes	1690-1640
C≡N	Nitriles	2260 – 2240

APPENDIX D: FTIR Results of Carbon Membranes at Different Pyrolysis Conditions

APPENDIX D-1: Sample T250D60F100

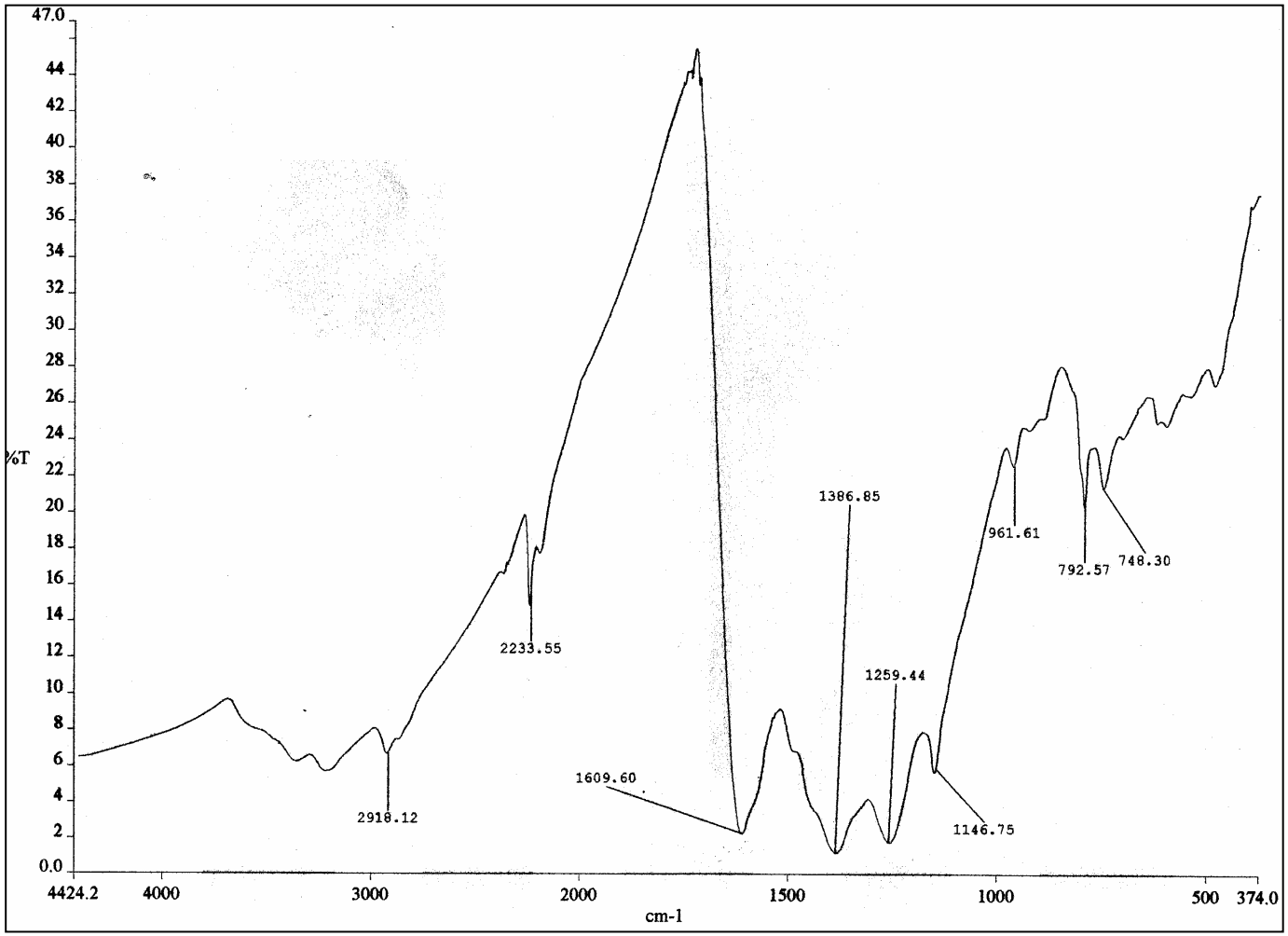

APPENDIX D-2: Sample T400D60F100

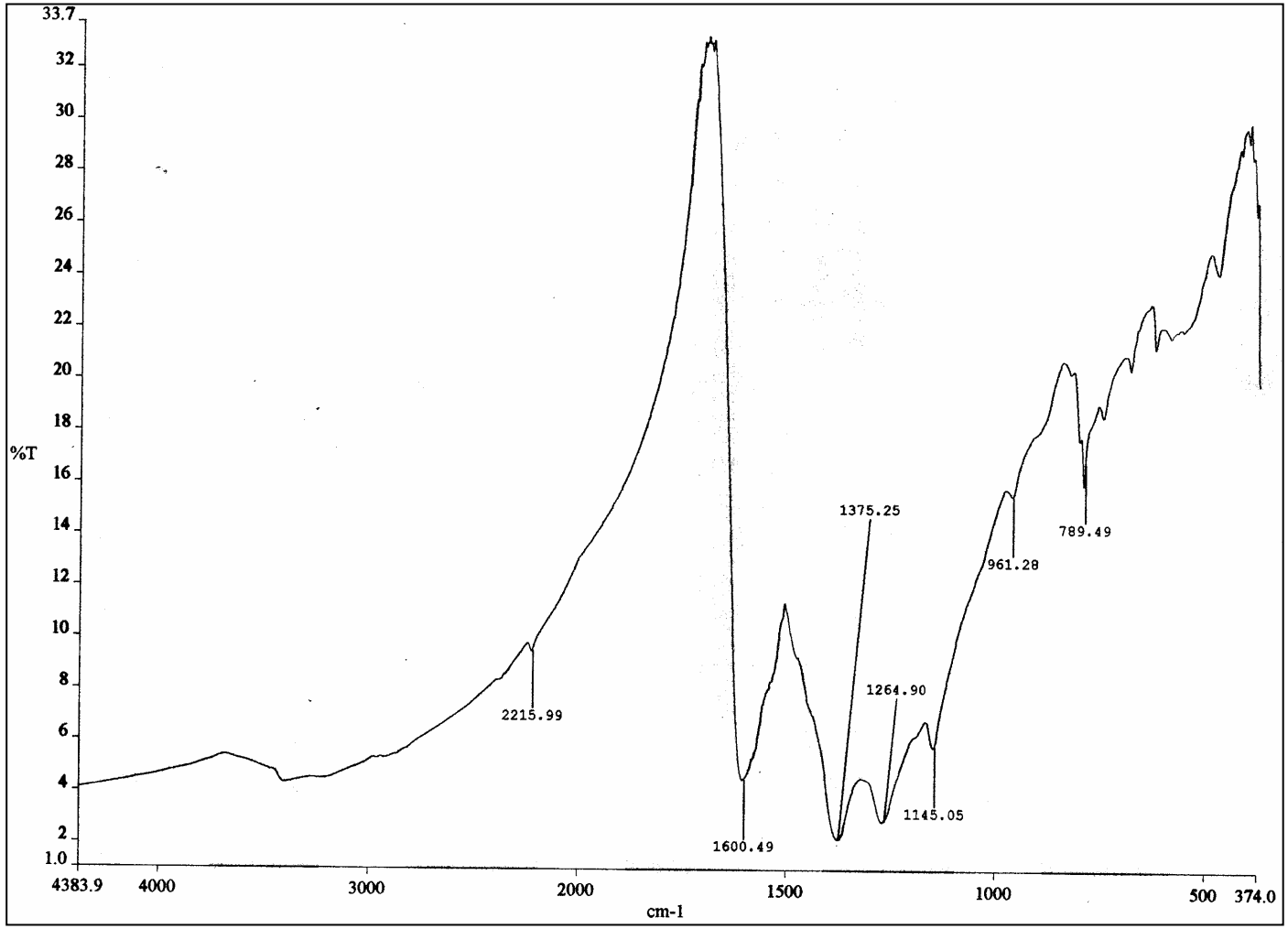

APPENDIX D-3: Sample T500D60F100

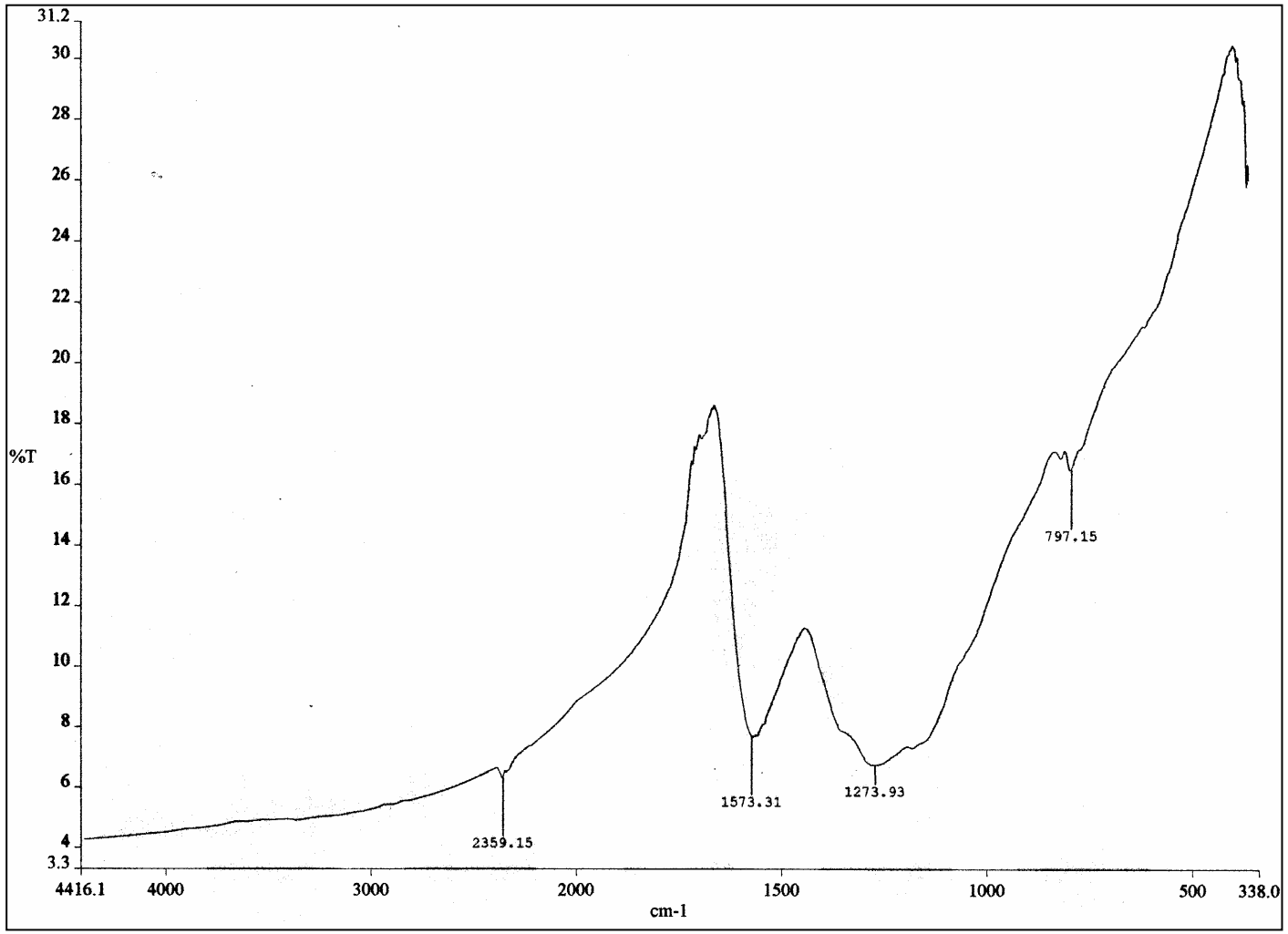

APPENDIX D-4: Sample T600D60F100

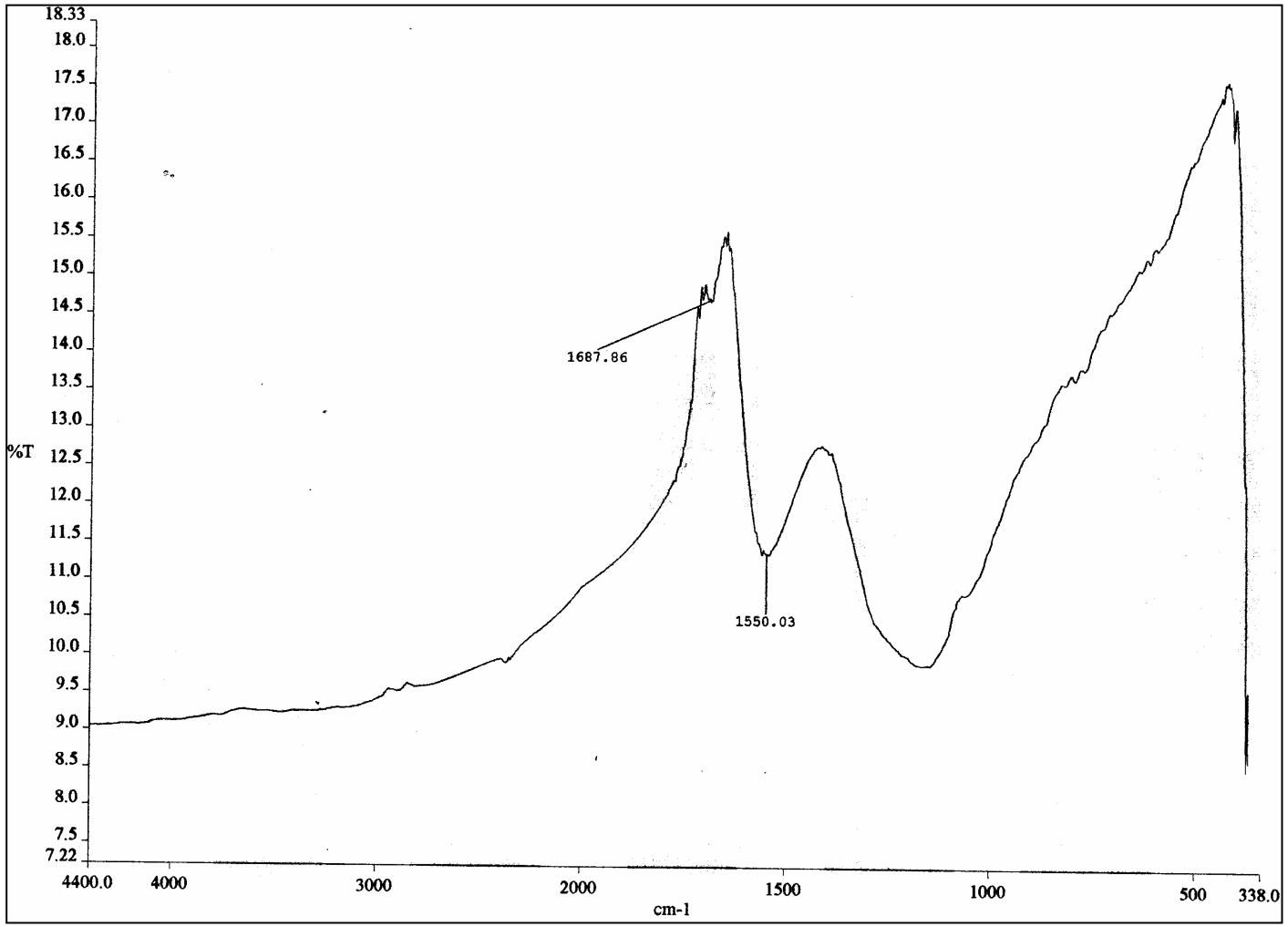

APPENDIX D-5: Sample T700D60F100

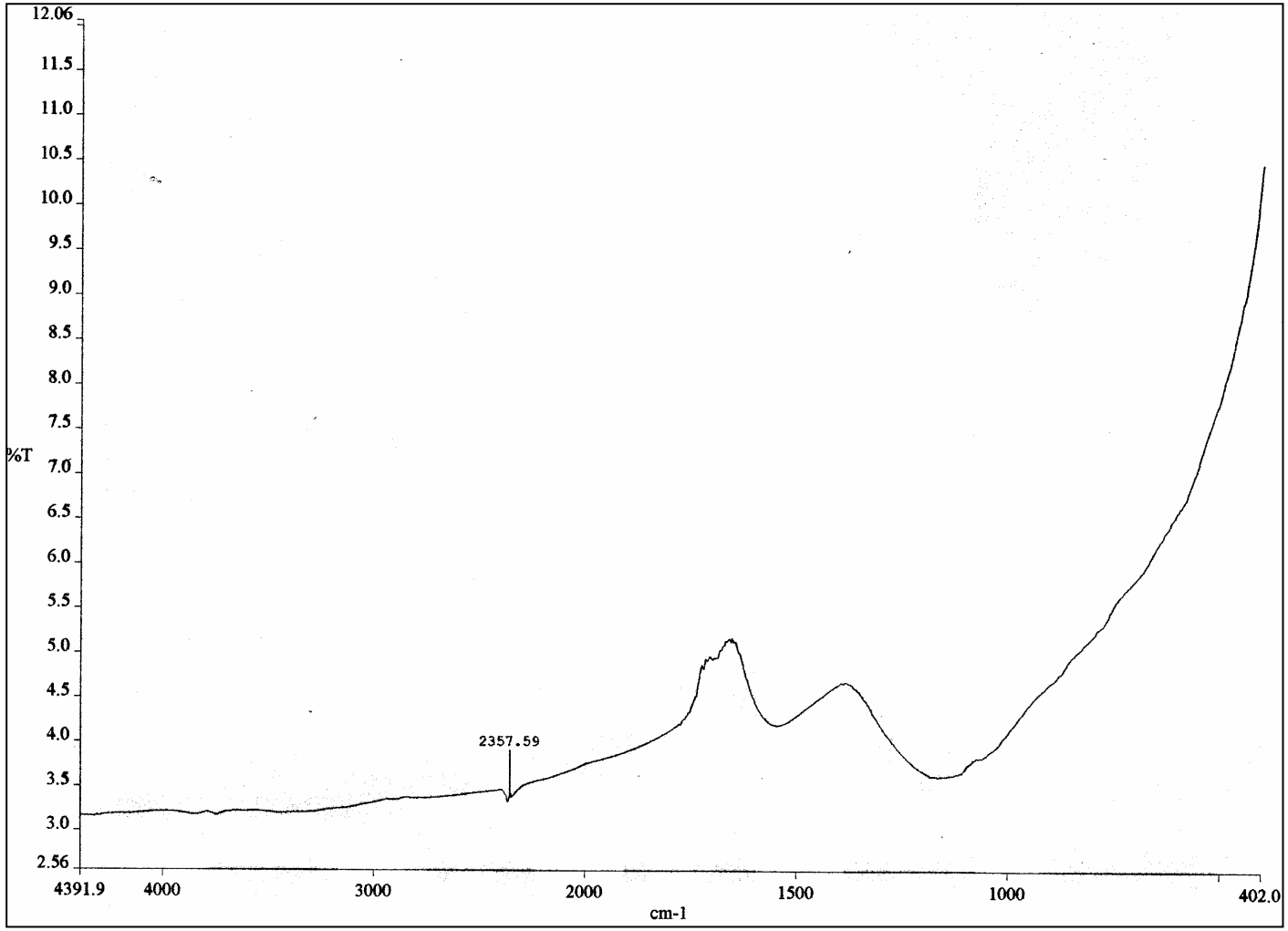

APPENDIX D-6: Sample T800D60F100

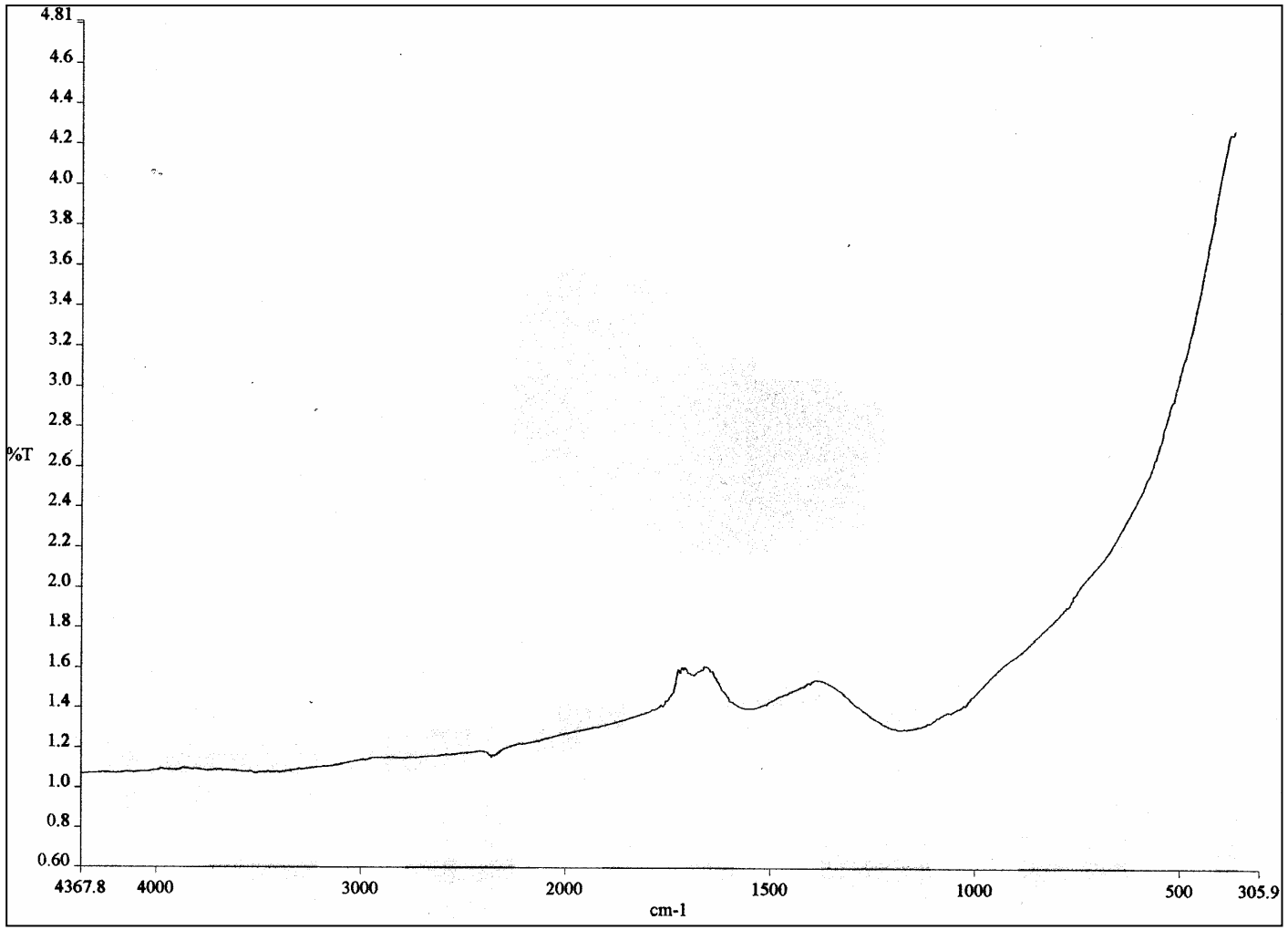

APPENDIX D-7: Sample T500D30F100

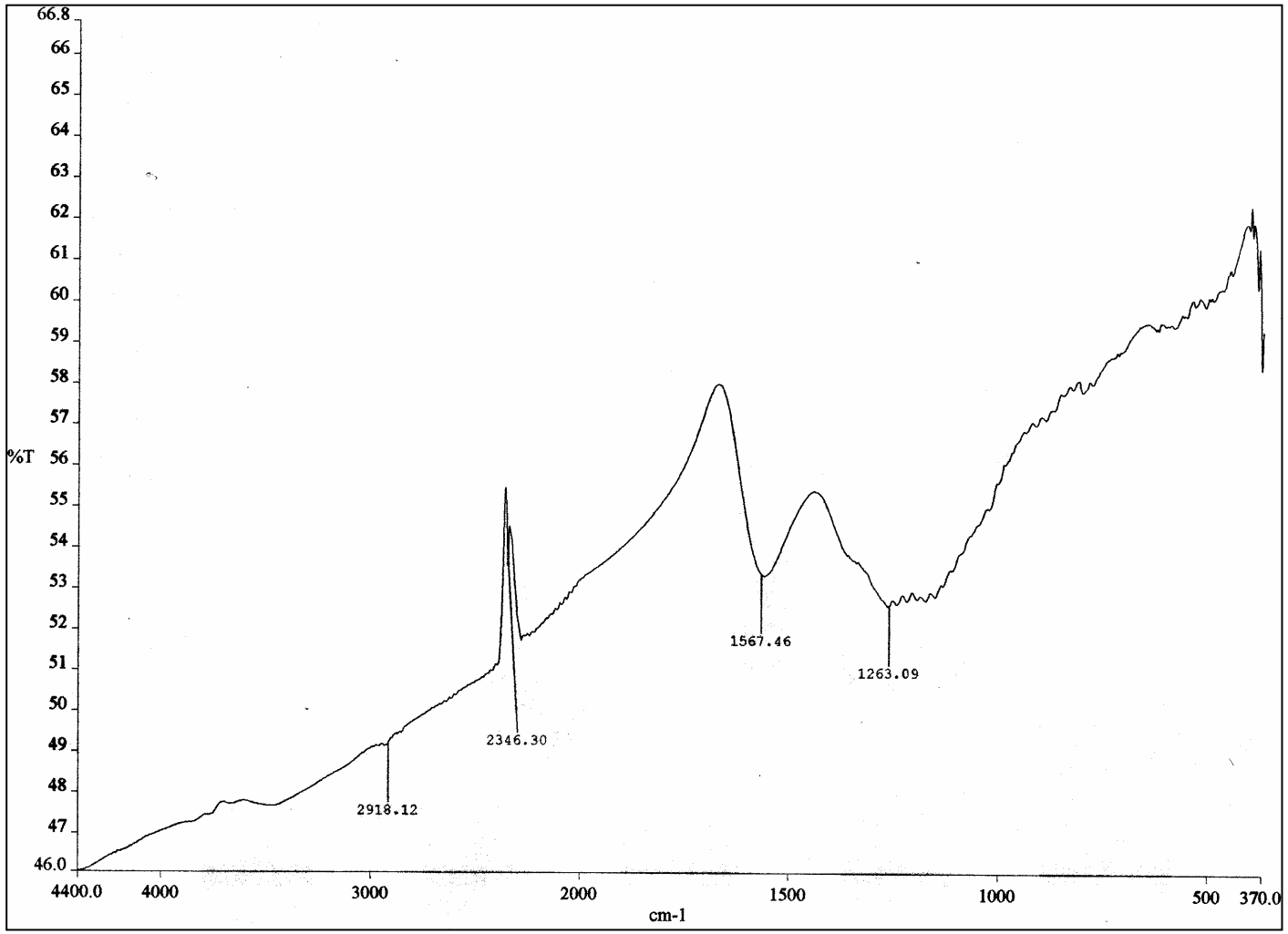

APPENDIX D-8: Sample T500D60F100

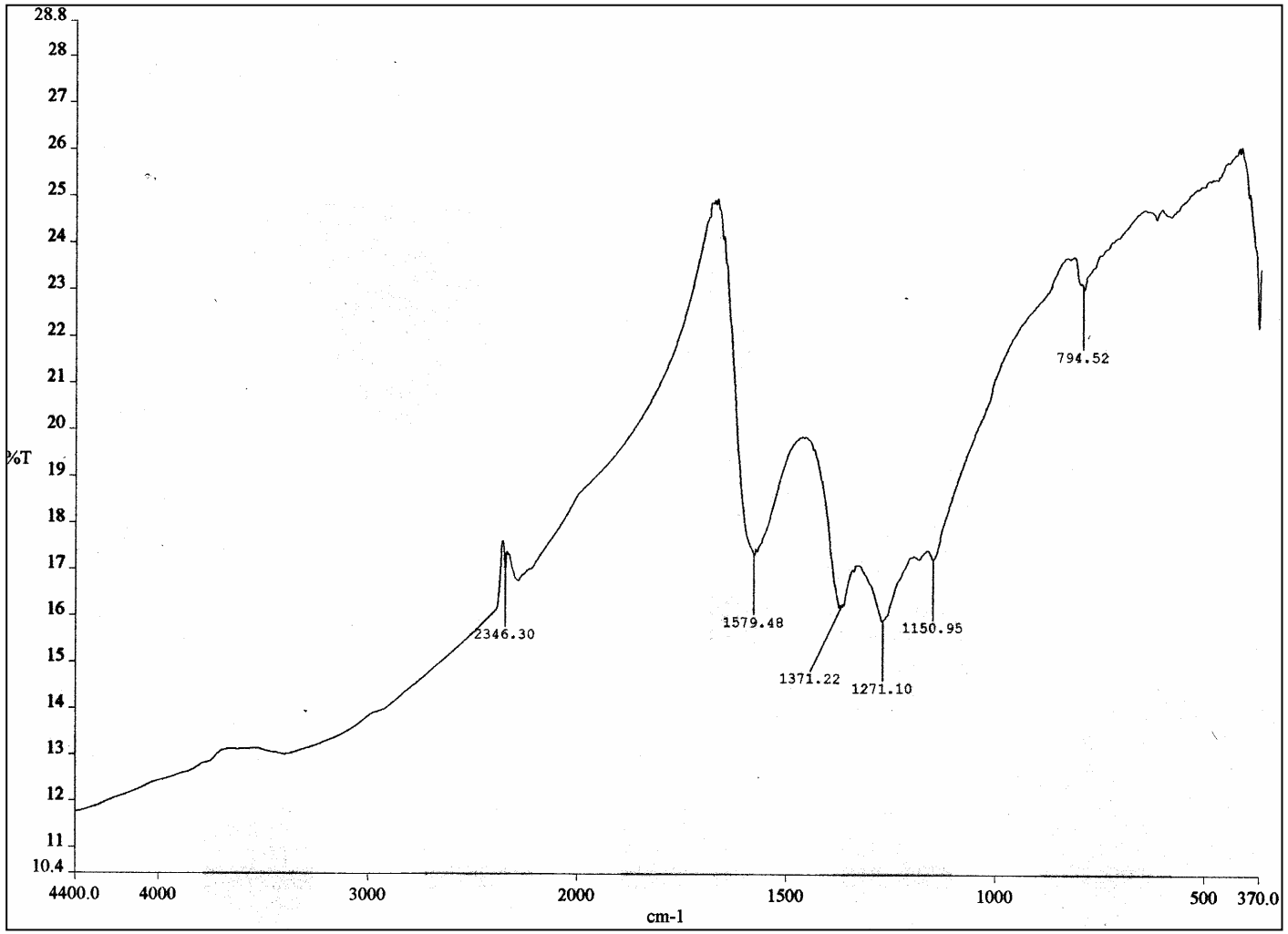

APPENDIX D-9: Sample T500D120F100

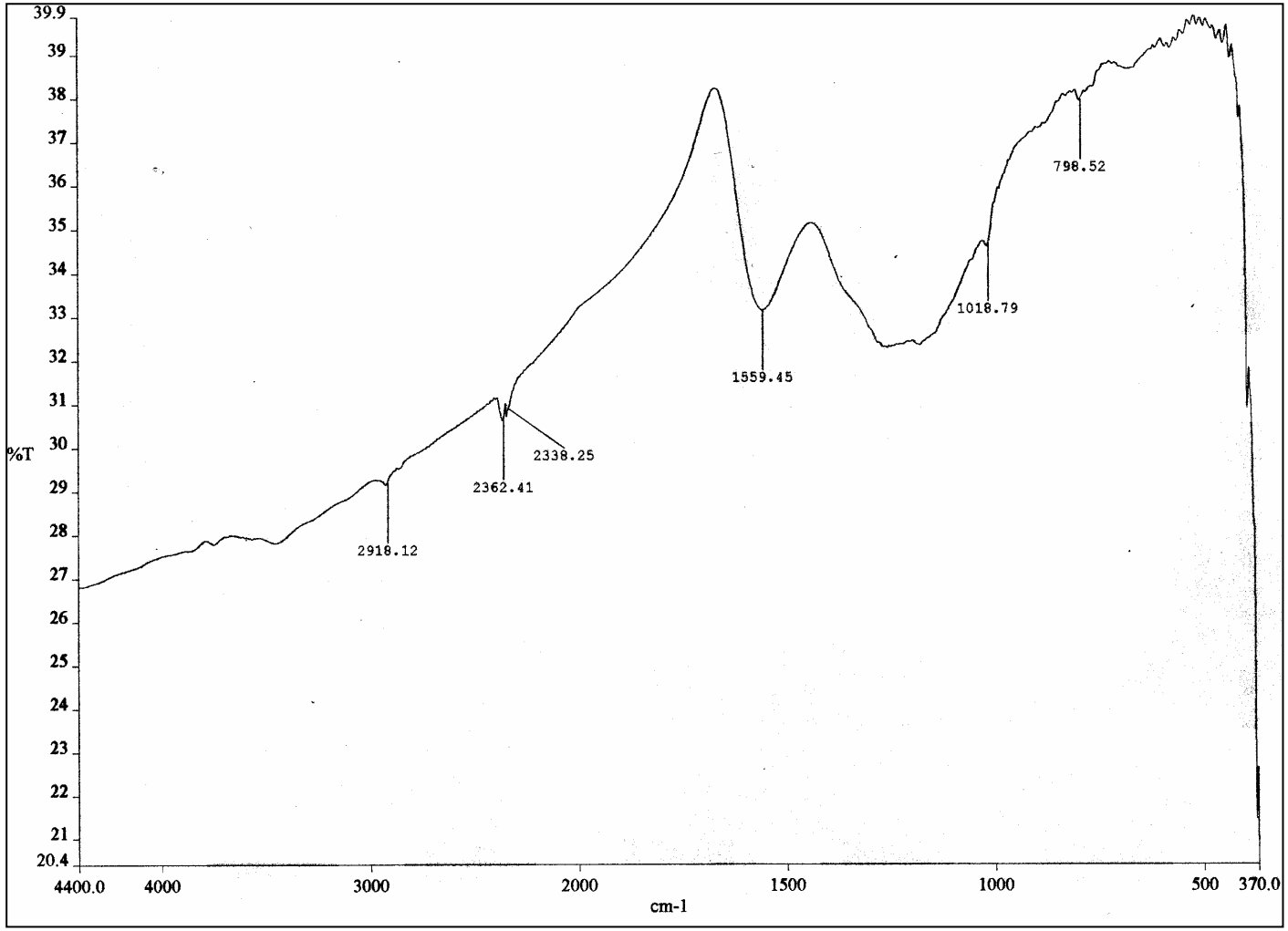

APPENDIX D-10: Sample T500D180F100

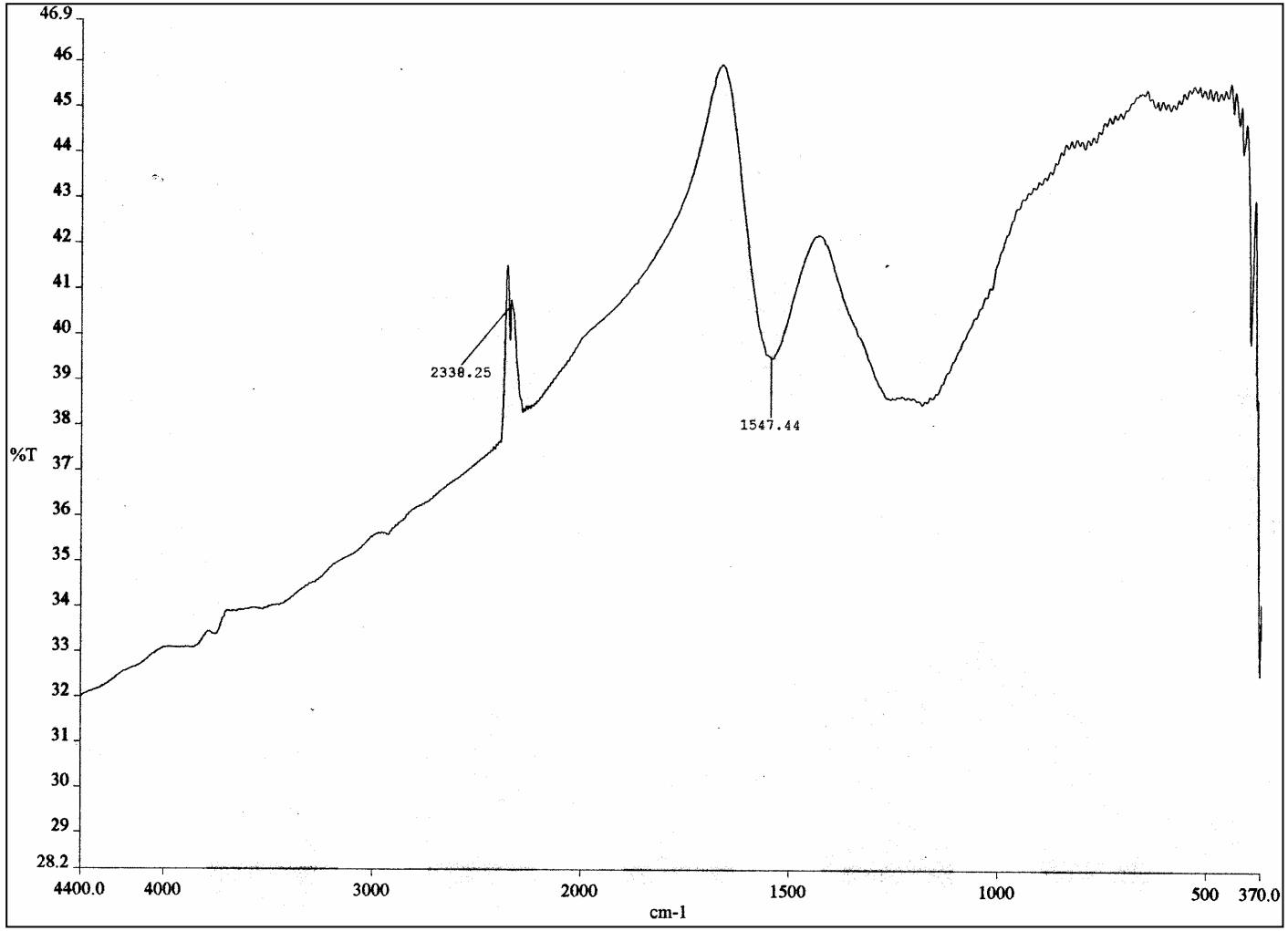

APPENDIX D-11: Sample T500D60F50

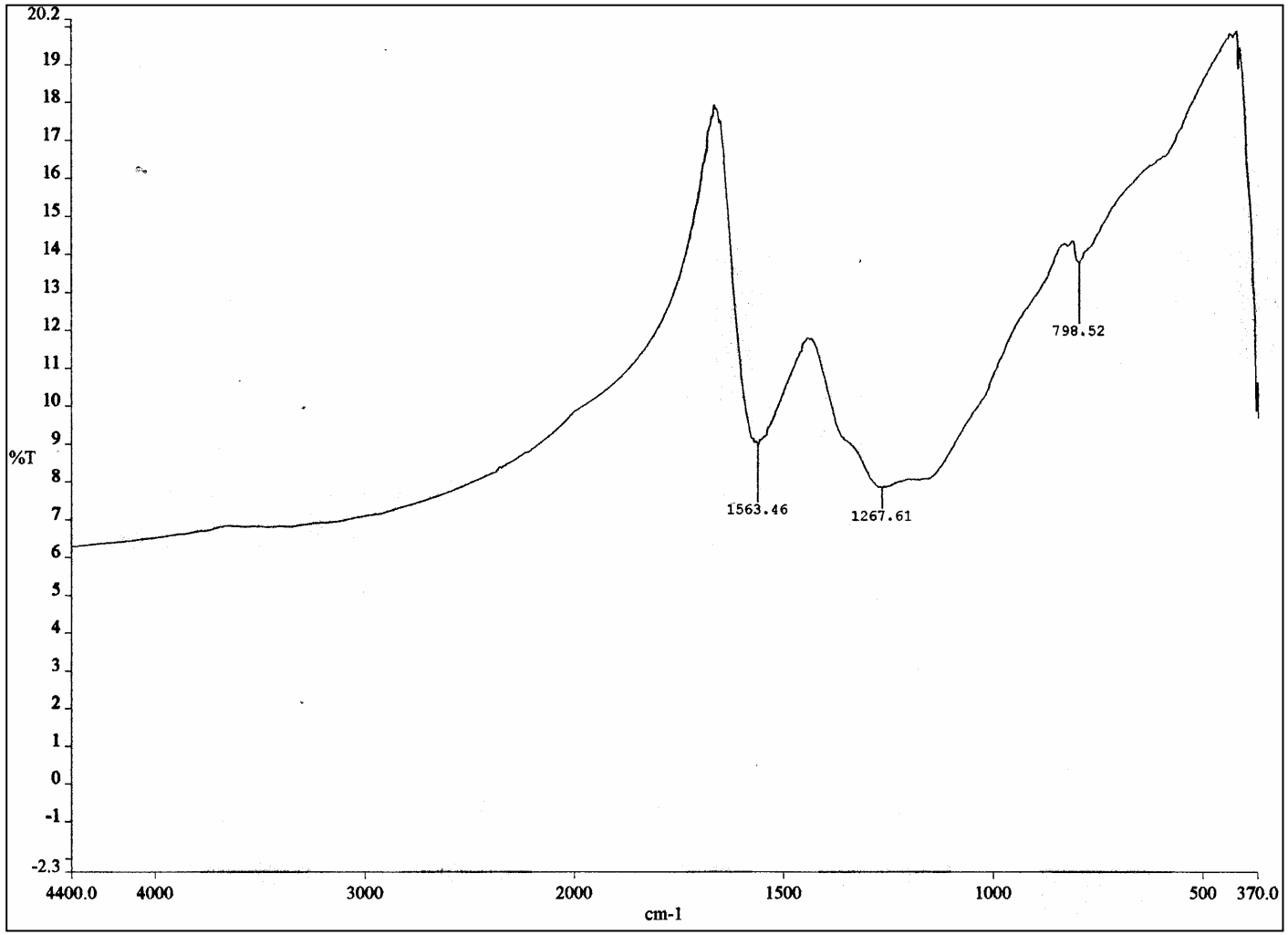

APPENDIX D-12: Sample T500D60F150

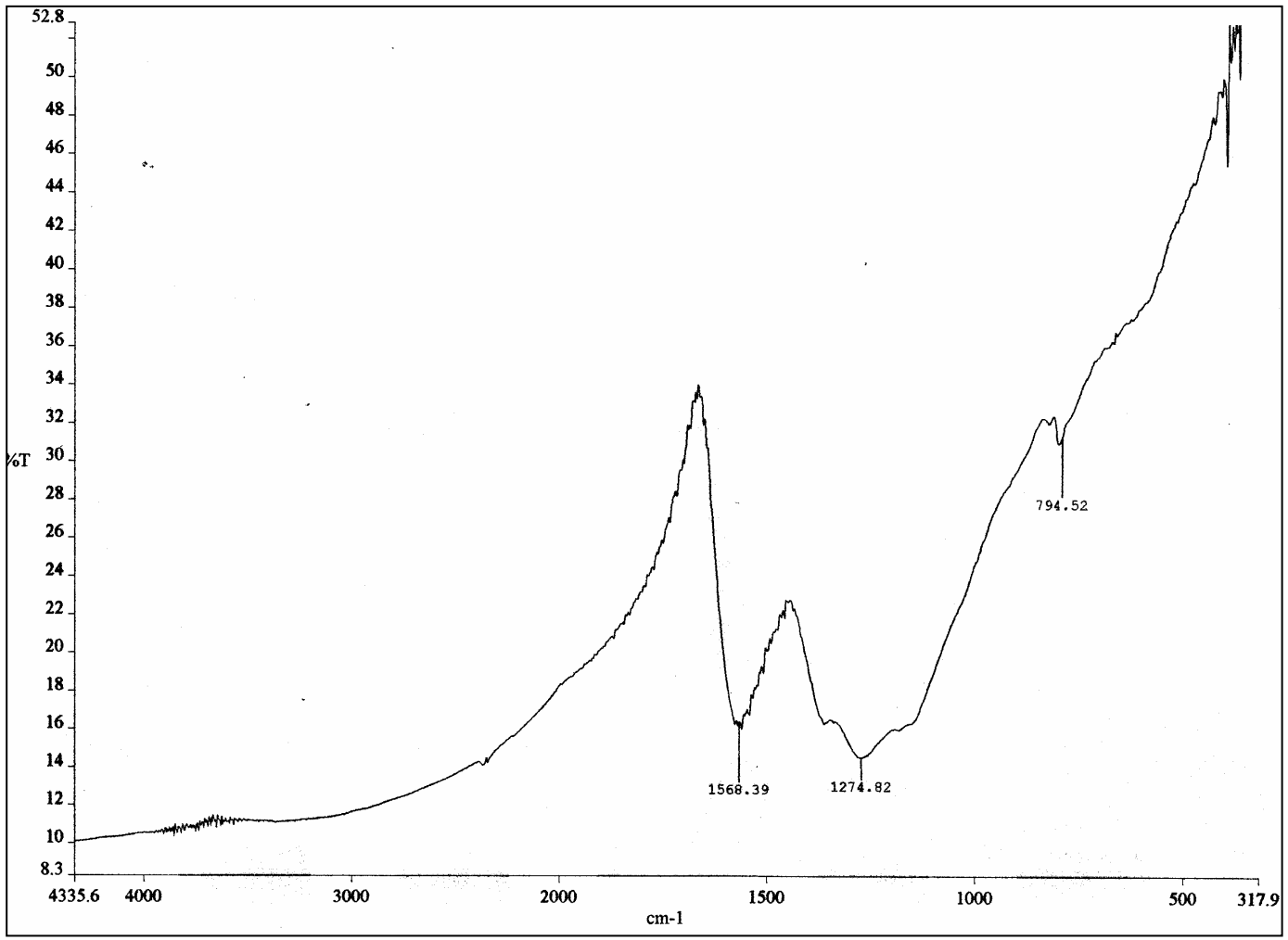

APPENDIX D-13: Sample T500D60F200

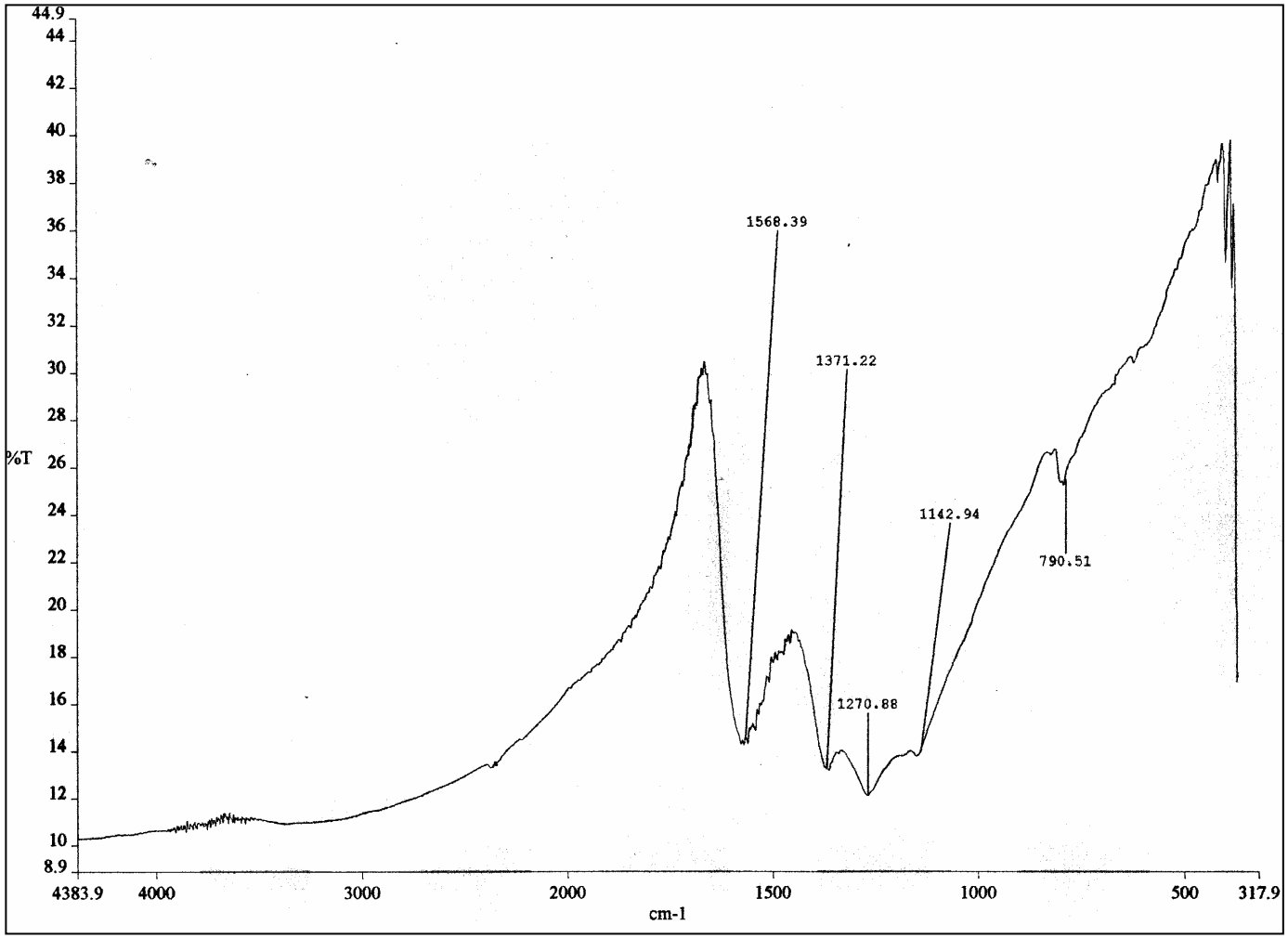

APPENDIX E: List of Publications